

# MReadings: MR in RT

Contributions from our MAGNETOM users

[www.siemens.com/magnetom-world-rt](http://www.siemens.com/magnetom-world-rt)

Not for distribution in the US





Gregor Thörmer, Ph.D.  
Global Segment Manager  
Men's and Women's Health

# Dear Reader,

## Advancing Radiation Therapy with Modern MRI

With the advent of high-precision treatment techniques, such as intensity modulated radiotherapy (IMRT) and volumetric modulated arc therapy (VMAT), it is possible to deliver high doses of radiation to irregular target volumes with sub-millimeter accuracy while sparing normal tissues at risk. Almost naturally, this development relies on excellent images on which to base treatment planning as well as treatment monitoring. Or, to quote from the article "Critical Role of Imaging in the Neurosurgical and Radiotherapeutic Management of Brain Tumors": "Ultimately, outcomes of radiation therapy [...] are only as good as the imaging they are based on." [1]

With its excellent soft-tissue differentiation and the ability to probe functional tissue properties, MRI is a perfect means to support target structure delineation, to help identify structures and organs at risk, and thus to contribute substantially to accurate treatment planning, delivery and monitoring.

## Practical implementation of MR in RT

In the past, institutions such as the Liverpool Cancer Therapy Centre in Sydney, Australia, already heavily relied on local radiology scanners to get access to MR images for RT planning. However, this often meant a compromise in image quality, since the requirements for RT planning are somewhat different from those for diagnostic imaging. In the first article of this issue, Gary Liney et al. describe their initial experience with a dedicated installation of a 3T MAGNETOM Skyra for exclusive use in radiotherapy, and how they implemented MR-based planning into clinical practice in Australia.

A prerequisite for the proper integration of MR into RT workflows is the ability to generate MR scans in the treatment position. In the second article, Thomas Koch et al. give hands-on guidance on how to set up radiotherapy patients with support devices, such as an MR compatible flat indexed tabletop and coils suitable for imaging in the treatment position.

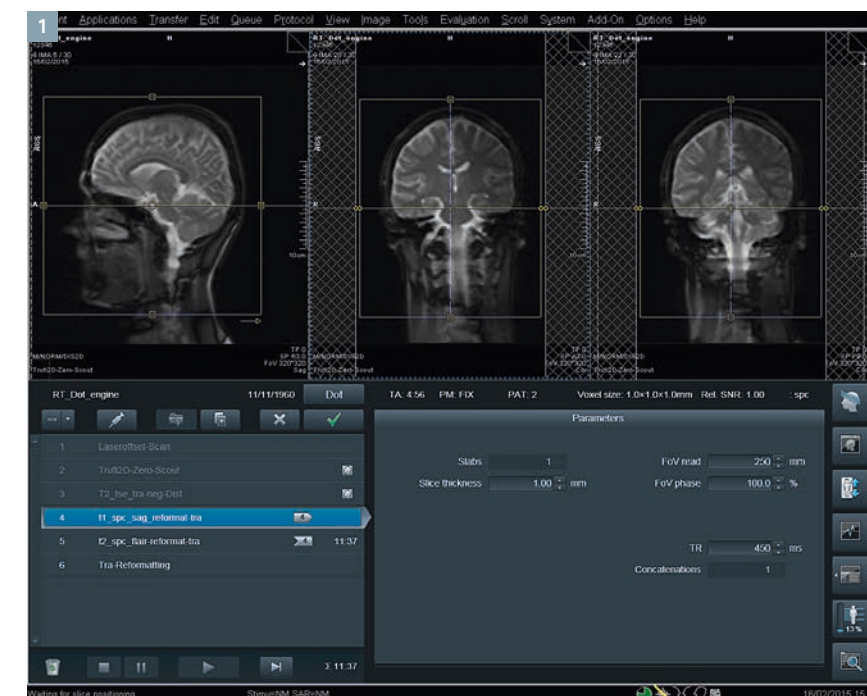
Besides these hardware components, Siemens recently introduced a dedicated imaging workflow for

Radiation Therapy (RT), the RT Dot Engine (Fig. 1), which is described in the third article. Both the accessories for patient positioning and this software are included in our dedicated MAGNETOM RT Pro edition.

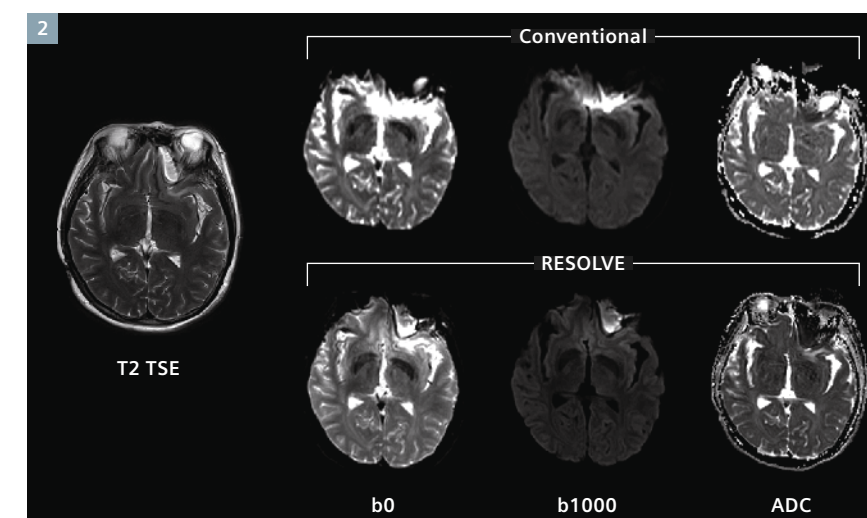
## Advanced clinical applications

In RT planning and therapy monitoring, functional techniques such as diffusion-weighted imaging (DWI) can provide valuable information. Maria Schmidt et al. from The Royal Marsden, London, elegantly summarize that "the ultimate aim of functional imaging techniques is to identify radio-resistant disease and thus provide a biological target volume for dose boosting." However, standard DWI techniques "in regions adjacent to air-tissue interfaces are known to suffer from poor geometric integrity". They further describe how applications like the Siemens-unique RESOLVE technique (Fig. 2) help "to ensure that the MRI examinations undertaken for RT planning purposes achieve the required geometric accuracy."

Another advanced imaging technique is Diffusion Tensor Imaging (DTI). Histopathological examinations have revealed that tumor cell dissemination in glioblastoma predominantly



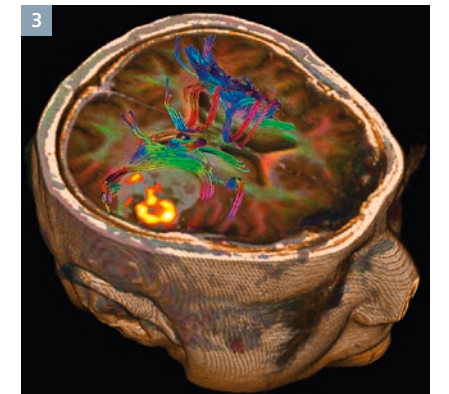
1 RT Dot Engine.



2 While spatial integrity of the conventionally acquired DWI scans often is compromised by susceptibility artifacts (caused by dental metal implants in the case shown here), images acquired with the readout segmented DWI technique result in significantly reduced artifacts and superior spatial integrity. Images courtesy of Tongji Hospital, Wuhan, China.

occurs along white matter tracts and brain vessels [2]. These routes of spread can be depicted with DTI since water will diffuse more rapidly in the direction aligned with the internal structure of axon fibers, and more slowly as it moves perpendicular to this preferred direction. Based on the information about the

principal diffusion direction in each voxel, tractography maps can be calculated and fused with morphological brain scans (Fig. 3). The group of Jatta Berberat employs the technique with the ultimate aim "to derive a biologically targeted volume to ensure coverage of the regions at greatest risk of micro-



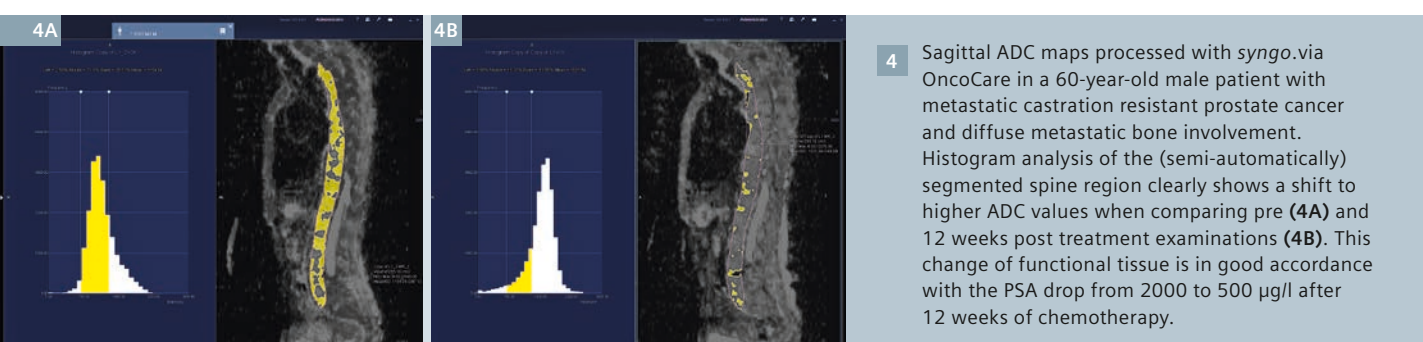
3 Visualization of white matter tracts with DTI with respect to the tumor location in a glioblastoma patient. This image has been acquired on a MAGNETOM Skyra 3T. Image courtesy of Fakultni Nemocnice, Plzen, Czech Republic.

scopic infiltration whilst excluding uninvolved brain."

When considering the additional opportunities of MRI in the treatment process, however, the potential advantages in terms of outcome are still under clinical evaluation in many cases. It is all the more worth mentioning that in the treatment of cervical cancers with brachytherapy, the significance of 3D volumetric imaging in the planning process, namely with MRI, has been attested by the GEC-ESTRO (Groupe Européen de Curiethérapie – European Society for Radiotherapy & Oncology). The still ongoing EMBRACE study shows that "with the MR image based brachytherapy approach [...] it is possible to obtain local control in over 90 percent of patients [...]". [3] In their article, Joann Prisciandaro et al. comprehensively describe the commissioning of devices and workflows and the clinical implementation of MR-guided brachytherapy services in their institution.

The practical integration of the acquired MR data into existing RT workflows is often compromised by limited capabilities of RT planning software solutions to visualize





(or even to load non-axial) image data. This missing link is closed with the new *syngo.via* RT Image Suite. As described in the article by Elena Nioutsikou, this software enables advanced multimodality image visualization and contouring on the images providing the best clinical information.

## Therapy and therapy response monitoring

MRI information is not only able to positively impact treatment planning; it also has the potential to transform the entire care continuum in cancer patients.

The case selection presented in the article by Anwar Padhani and Heminder Sokhi shows the ability to *positively* assess therapy efficiency in patients with metastatic disease with whole-body diffusion-weighted MRI when morphological imaging is unhelpful.

The next article by Susanne Bonekamp and Ihab Kamel highlights how postprocessing of functional image data, such as diffusion-weighted images, can help to assess therapy response at very early stages.

The works-in-progress software OncoTreat<sup>1</sup> described therein has since become the product known as OncoCare and is a very sensitive tool in assessing the change of tissue properties like cellular density in tumors undergoing therapy (Fig. 4).

## Research activities in the field of MR-only<sup>2</sup> RT planning and 4D motion management

In the “MR based” – or rather “MR enriched” – workflow it is common practice to perform both (1) CT, to provide the electron density information needed for dose calculation and the geometric accuracy that is expected for planning a precise treatment, and (2) MRI, as the preferred modality for tumor and definition of organs at risk [4].

The related additional cost and workload as well as patient compliance issues have motivated some clinicians and researchers to focus their efforts on establishing MR-only workflows for radiation therapy. One prerequisite is the spatial integrity of the acquired MR data. For the head, James Balter et al. have investigated the geometric distortions of the acquired MR data and

found that “86.9% of the volume of the head was displaced less than 0.5 mm”. In another article in this issue, Tufve Nyholm et al. discuss the technical aspects of MR-only radiotherapy more generally. Going one step further, Peter Greer et al. describe the implementation of an MR-only workflow for the prostate at their institution.

Another forward-looking contribution to this issue by Kinga Barbara Bernatowicz et al. is thought-provokingly entitled “4D-MRI: Future of Radiotherapy of Moving Targets? This article, in my opinion, is a fitting conclusion to this edition.

I would like to thank all the authors published in this issue for sharing their expertise and enthusiasm with other MAGNETOM users.

I wish you an enjoyable read.

Gregor Thörmer, Ph.D.

Global Segment Manager  
Men’s and Women’s Health

## References

- 1 Wang LL, Leach JL, Breneman JC, et al. Critical role of imaging in the neurosurgical and radiotherapeutic management of brain tumors. *Radiographics*. 2014;34:702-721.
- 2 Giese A, Westphal M. Glioma invasion in the central nervous system. *Neurosurgery* 1996 39(2):235-50.
- 3 EMBRACE: intErnational study on MRI guided BRachytherapy in locally Advanced CErvical cancer: Small canges, big improvements. *European Journal of Cancer*. 2013;49:5.
- 4 Chung, Na Na, Lai Lei Ting, Wei Chung Hsu, et al. Impact of Magnetic Resonance Imaging versus CT on Nasopharyngeal Carcinoma: Primary Tumor Target Delineation for Radiotherapy.” *Head & Neck* 2004;26: 241-246.

<sup>1</sup> WIP: The product is still under development and not commercially available yet. Its future availability cannot be ensured.

<sup>2</sup> Radiotherapy Planning where MR data is the only imaging information is ongoing research. The concepts and information presented in this article are based on research and are not commercially available. Its future availability cannot be ensured.

# Content

6 A Dedicated MRI Scanner for RT Planning  
*Gary Liney, et al.,  
Liverpool Cancer Therapy Centre,  
Sydney, Australia*

12 Evaluation of the CIVCO IPPS MRI-overlay for Positioning and Immobilization of RT Patients  
*Thomas Koch, et al.,  
Klinik und Praxis für Strahlentherapie und Radioonkologie,  
Sozialstiftung Bamberg, Germany*

18 RT Dot Engine  
*Gregor Thörmer, Martin Requardt,  
Siemens Healthcare, MRI,  
Erlangen, Germany*

22 Anatomical and Functional MRI for RT Planning of Head and Neck Cancers  
*Maria Schmid, et al.,  
Royal Marsden NHS Foundation  
Trust and Institute of Cancer  
Research, Sutton, UK*

28 Clinical Application of DTI in RT Planning  
*Jatta Berberat, et al.,  
Canton Hospital, Aarau,  
Switzerland*

32 MR Guided Gynecological HDR Brachytherapy  
*Joann Prisciandaro, et al.,  
University of Michigan,  
Ann Arbor, MI, USA*

38 *syngo.via* RT Image Suite  
*Elena Nioutsikou,  
Siemens Healthcare, Imaging &  
Therapy Division, Forchheim,  
Germany*

42 Whole Body DWI for Bone Marrow Tumor Detection  
*Anwar Padhani, Heminder Sokhi,  
Paul Strickland Scanner Centre,  
Mount Vernon Cancer Centre,  
Northwood, Middlesex, UK*

50 Case Report: Functional, Volumetric, Treatment Response Assessment Using MR OncoTreat  
*Ihab Kamel, Susanne Bonekamp  
The Johns Hopkins Hospital,  
Baltimore, MD, USA*

55 Optimizing MRI for Radiation Oncology  
*James Balter, et al.,  
University of Michigan,  
Ann Arbor, MI, USA*

60 Development of MR-only<sup>1</sup> Planning for Prostate RT Using Synthetic CT  
*Peter Greer, et al.,  
Calvary Mater Newcastle,  
Newcastle, New South Wales,  
Australia*

64 Technical Aspects of MR-only<sup>1</sup> RT  
*Tufve Nyholm, Joakim Jonsson  
Umeå University, Sweden*

70 4D-MRI: Future of RT of Moving Targets?  
*Kinga Bernatowicz, et al.,  
Center for Proton Therapy (CPT),  
Paul Scherrer Institut, Villigen  
PSI, Switzerland*

The information presented in MAGNETOM Flash is for illustration only and is not intended to be relied upon by the reader for instruction as to the practice of medicine. Any health care practitioner reading this information is reminded that they must use their own learning, training and expertise in dealing with their individual patients. This material does not substitute for that duty and is not intended by Siemens Medical Solutions to be used for any purpose in that regard. The treating physician bears the sole responsibility for the diagnosis and treatment of patients, including drugs and doses prescribed in connection with such use. The Operating Instructions must always be strictly followed when operating the MR System. The source for the technical data is the corresponding data sheets.

<sup>1</sup> Radiotherapy Planning where MR data is the only imaging information is ongoing research. The concepts and information presented in this article are based on research and are not commercially available. Its future availability cannot be ensured.



# A Dedicated MRI Scanner for Radiotherapy Planning: Early Experiences

Gary Liney<sup>1,2</sup>; Robba Rai<sup>1</sup>; Lois Holloway<sup>1</sup>; Shalini Vinod<sup>1</sup>

<sup>1</sup>Liverpool Cancer Therapy Centre, Sydney, Australia

<sup>2</sup>Ingham Institute for Applied Medical Research, Sydney, Australia

## Introduction

The last decade has seen a dramatic increase in the use of MRI for radiotherapy planning. MRI has a number of advantages for the simulation of treatment plans, over the current gold standard of computed tomography (CT); Its excellent and variable soft-tissue contrast has been shown to improve the delineation accuracy

of both the tumor and surrounding organs-at-risk; a range of functional techniques are able to measure and display tumor physiology in the same examination, potentially revealing sub-regions that could receive a boost in radiation dose; and finally, the absence of ionising radiation means the patient may be scanned

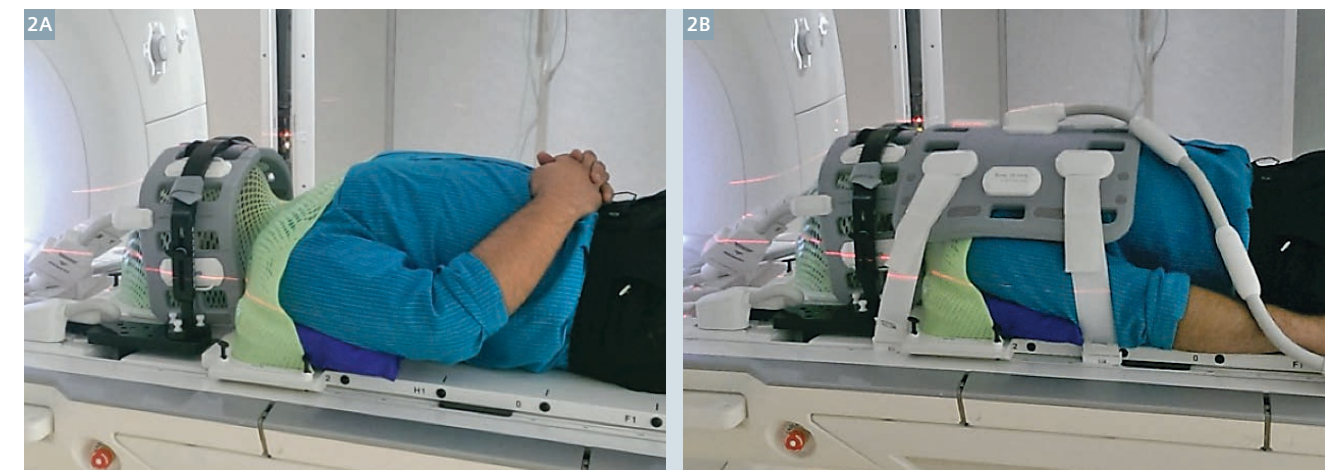
any number of times before, during and after treatment, giving the clinician the ability to assess and adapt plans on an individual basis.

## MR-simulator

In common with most radiotherapy centres, our department at Liverpool Cancer Therapy Centre (LCTC), located



**1** The 3 Tesla MAGNETOM Skyra MR-Simulator at Liverpool CTC, in south western Sydney, Australia. The 30 Gauss line can be seen marked on the floor which serves to emphasise this inner controlled area for the majority of our staff who have not previously worked in MRI. The object on the bed is our 3D volumetric distortion test phantom.



**2** Photographs showing the RF coil set-up used in head and neck planning scans. **(2A)** Two small flexible coils are placed laterally around the fixation shell using two coil supports. **(2B)** The 18-channel body array is connected to one of the available ports at the bottom of the table using a long cable.

in south western Sydney, relied heavily on local radiology scanners to provide MR images. This often meant a compromise in image protocol and the limited availability of these busy scanners restricted our patient throughput and any opportunity for further development. However, in August 2013, as part of a wider investment in MRI, which will also see the Australian MR-Linac program on site, we installed our own dedicated system for the exclusive use of radiotherapy patients to provide MR-based treatment simulation scans. This scanner is a wide-bore 3 Tesla MAGNETOM Skyra with XQ gradients and 64-channel RF architecture and was purchased with the latest suite of functional imaging sequences. Our MR-Simulator (MR-sim), shown in Figure 1, is configured with a number of radiotherapy-specific features in mind including in-room lasers (as on a CT-simulator), flat indexed table top and a range of RF coils suitable for optimum imaging with the patients in the treatment position. The field strength was chosen with aspirations of incorporating functional studies into future clinical practice.

Over the last 12 months or so, our small but dedicated team has climbed a steep learning curve and implemented MR-based planning successfully into clinical practice for a variety

of tumor sites. This process began even before the installation and acceptance testing of the system, with in-house safety and educational training being implemented for all radiotherapy and physics staff connected with MRI. Under normal operation, scanning is performed by our lead MR radiographer and one of a small number of specialist radiotherapists who are rotated through MR-Sim. Additional support is provided by the lead MR physicist and a radiologist. By preserving a significant portion of scan time during the week for research – one of the many advantages of having our own system – we have also been able to develop a number of studies that are beginning to explore the use of functional information and motion evaluation in treatment planning. This article serves as a brief illustration of how we are using this system in practice.

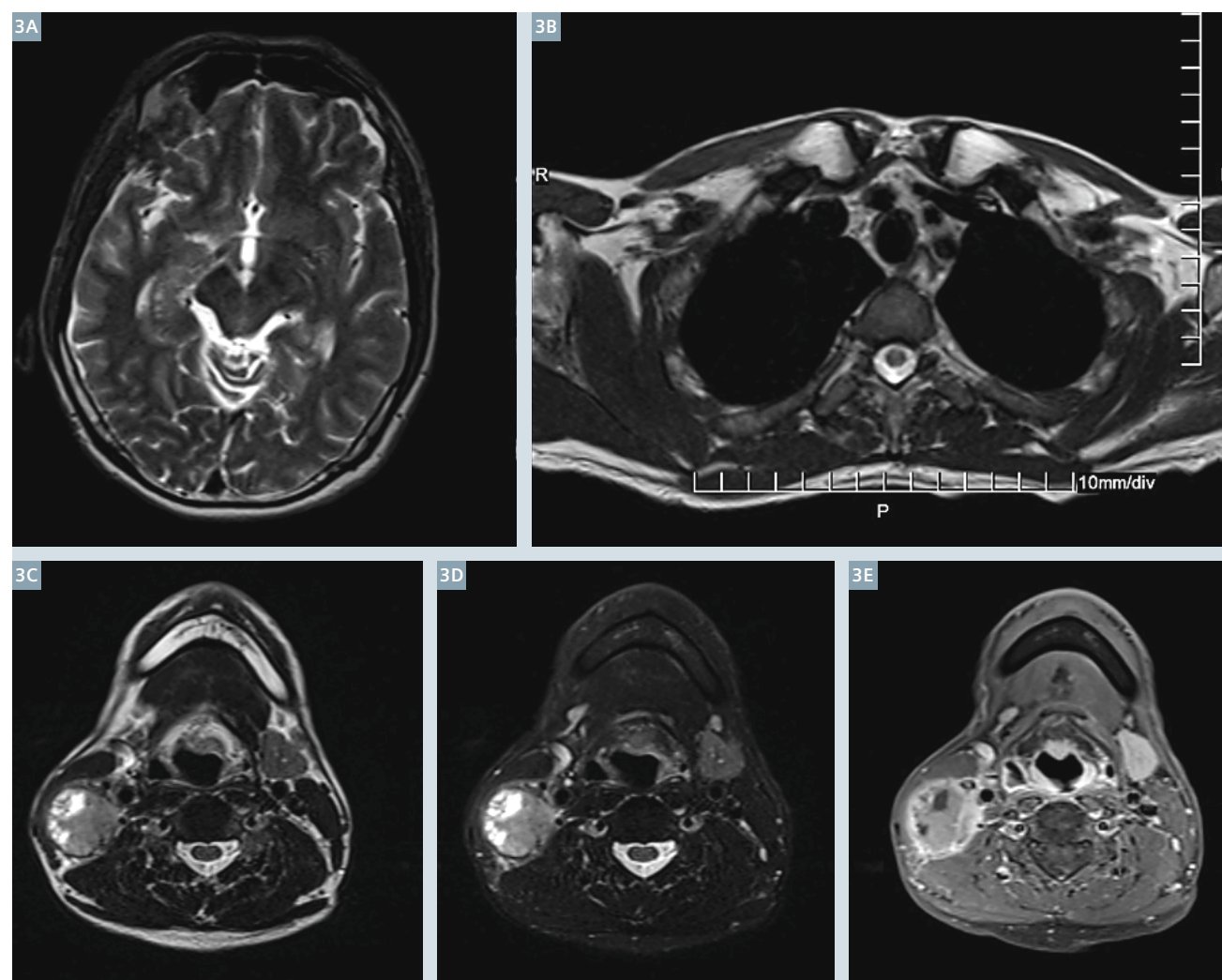
The vast majority of our workload requires MRI to be registered to CT for the electron density information needed in the dose calculation. To facilitate this, we image our patients in the treatment position and take advantage of the RF coils we have available. A good example of this is in head and neck tumors where patients lie on a flat table top and are imaged

in a fixation shell placed over their head and shoulders which is attached to the table. Previous attempts to cater for this equipment on other scanners were compromised either due to a narrower 60 cm bore or unsuitable RF coils. On the MR-Sim we take advantage of the in-built 32-channel RF coil under the flat table-top and use this in conjunction with two laterally positioned 4-channel flexible coils attached to a supporting bridge. More recently we have been able to add an 18-channel body array connected at the foot of the table by a long cable (Fig. 2). This gives us vastly improved signal-to-noise ratio (SNR) and greater coverage compared to what had previously been possible as shown in Figure 3.

## Imaging details

In working up our protocols, we have had to consider the specific requirements of MR-simulation, which is often quite different from standard diagnostic procedure [1]. Geometric distortion is something we have to be especially mindful of. For radial distances less than 15 cm from isocentre (i.e. up to 30 cm FOV), system distortions caused by non uniformity in  $B_0$  and non linearity of the gradients are within our tolerance, and the dominant contribution is instead



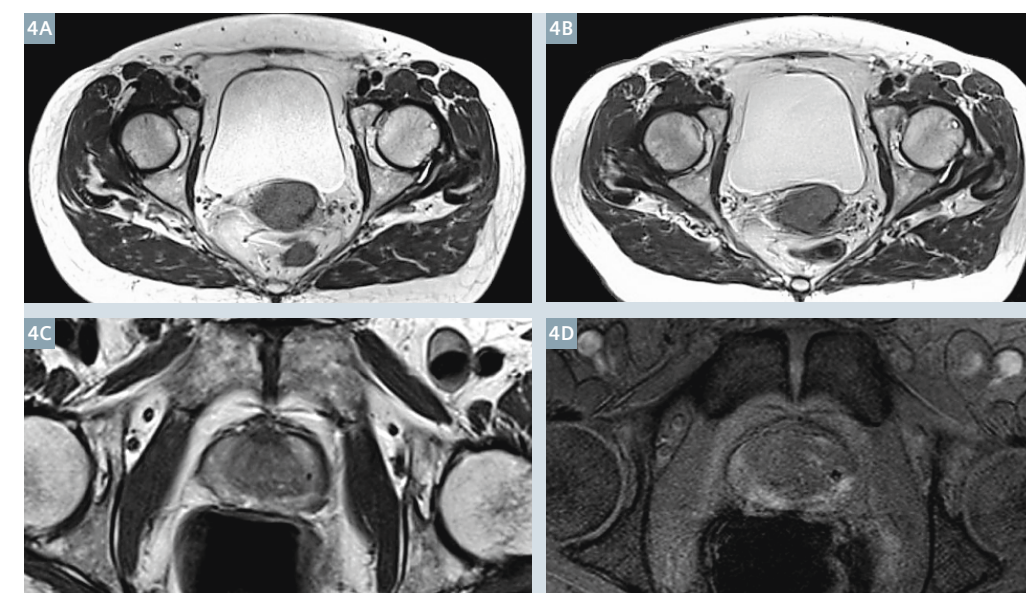


**3** Example images acquired in a head and neck tumor patient. Figures **3A** and **B** serve to illustrate the image quality and coverage obtained using dedicated RF coils which extend from midbrain down to sternal notch. The bottom images show a slice taken through the tumor using **(3C)** Dixon T2w in-phase, **(3D)** water-only and **(3E)** Dixon T1w water-only post-contrast.

from chemical shift and magnetic susceptibility within the patient. These effects can be mitigated by use of high receiver bandwidths which we set to 440 Hz/pixel or greater. The large coverage that is required for planning creates long scan times compared to diagnostic practice and we rely heavily on iPAT technology to keep these down to an acceptable level. Nevertheless, these scan times inevitably result in some organ motion and we have found BLADE to be useful in reducing artifacts for example from bladder filling. One of our current studies is comparing the image quality of this radial *k*-space technique against the administration of anti-peristaltic agents and normal cartesian acquisition as

shown in Figure 4A. Another particular interest for us is the development of a single planning scan for prostate patients with fiducial gold seeds. These exams would normally require two separate scans, a gradient-echo based sequence to identify the seed position and a second T2-weighted TSE for contouring the gland. The susceptibility artefact from the seed, while making them clearly visible, reduces positional accuracy, even with high bandwidths, and the requirement for two scans is less than ideal. However, we have begun looking at sequences such as turbo gradient spin-echo (TGSE) which offer the potential of combining both types of contrast into a single image (Fig. 4B).

To fully map out the geometric integrity of our system over large volumes, we have designed and built our own 3D phantom which covers 50 cm in each orientation (pictured in the magnet in Fig. 1). This test object has proved particularly useful in demonstrating the role of TimCT in cases when we have needed to exceed our 30 cm rule. By moving the patient through the bore while acquiring thin isocentric sections the distortion limit along the z-axis may be avoided altogether, thereby extending planning coverage. Figure 5 shows an example of this in a particularly difficult sarcoma case where more than 60 cm coverage was requested by the Oncologist and a total of 50 coil elements were used.



**4** Developing body protocols for RT simulation; A comparison of BLADE **(4A)** versus anti-peristaltic agent **(4B)** as an effective control of organ motion artefacts. Use of the TGSE **(4C)** to provide a prostate planning scan that combines T2w contrast and gold seed visualization. **(4D)** Standard gradient-echo image used for seed localisation, which exaggerates the dimension of the marker.

### Therapy response

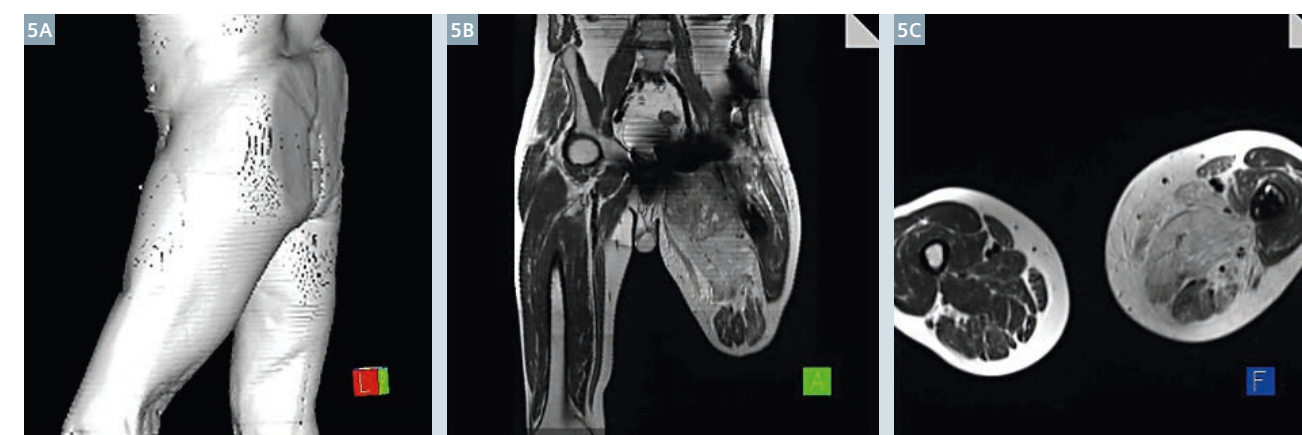
For most examinations we are using MRI at the commencement of treatment for its soft-tissue contrast and the improvement in planning contours. Alongside this routine work, we have begun several research studies that are using MRI to assess response over the course of treatment. These studies use both diffusion-weighted imaging (DWI) and dynamic contrast enhancement (DCE) to look at changes in tumor cellularity and vascularity respectively. In the case of diffusion, the commonly-used EPI sequence produces significant distortions and artifacts that has made its application in radiotherapy plan-

ning problematic. We have recently concluded a study that compared EPI with RESOLVE, which uses multi-segmentation in the frequency encoding direction combined with navigator self-correction, and showed improvements in ADC repeatability and geometric integrity compared to a T2-weighted gold standard [2]. Figure 6 shows a DWI example in a prostate patient acquired with  $b = 800 \text{ s/mm}^2$  together with the corresponding ADC map and we have now also adopted this sequence for rectum and cervix. As part of our DCE protocol we acquire pre-contrast

sequences at 2 and 15 degree flip angles to measure the native T1 prior to using dynamically acquired TWIST images. These scans are then analysed using the two compartment model which is available with the Tissue4D software.

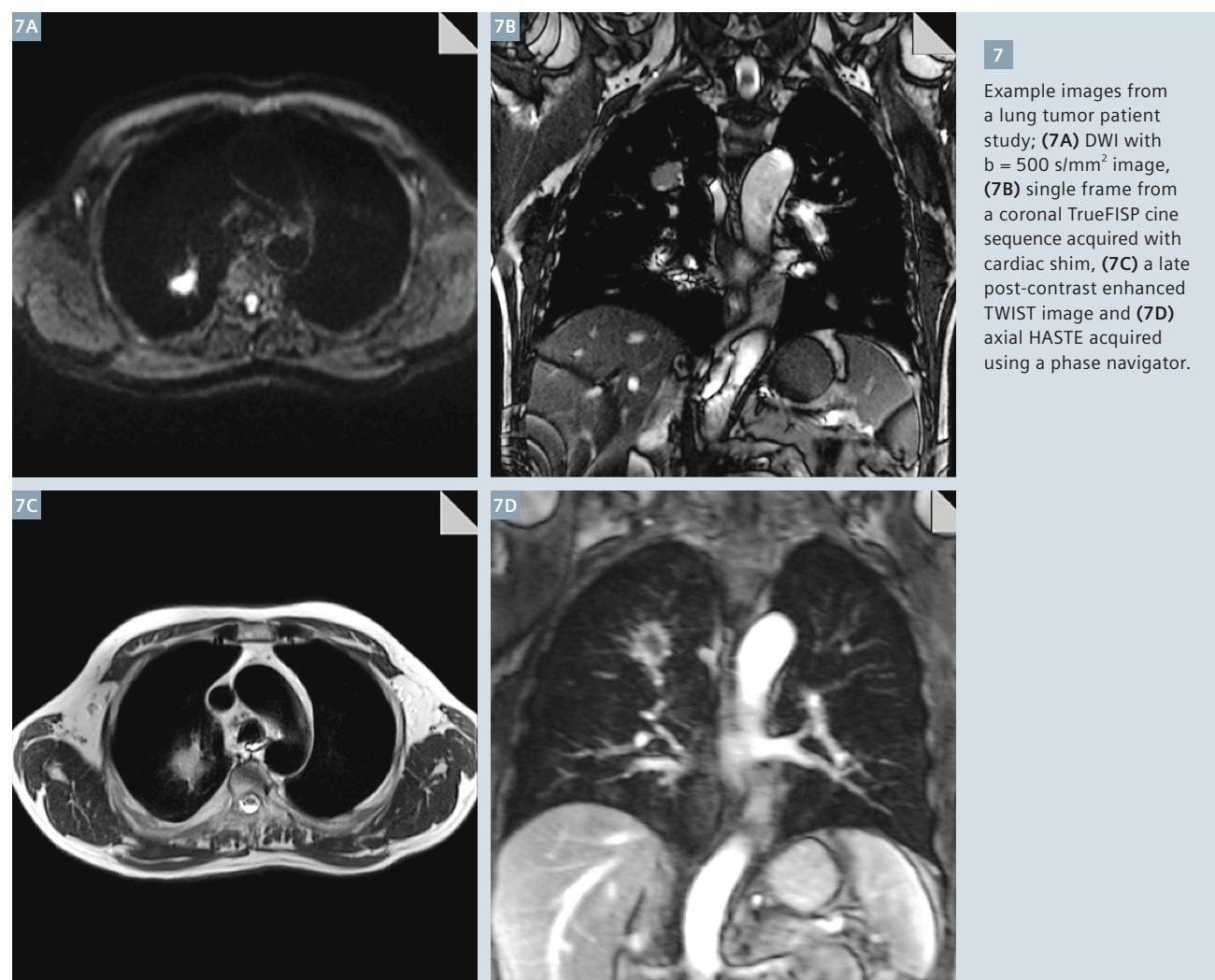
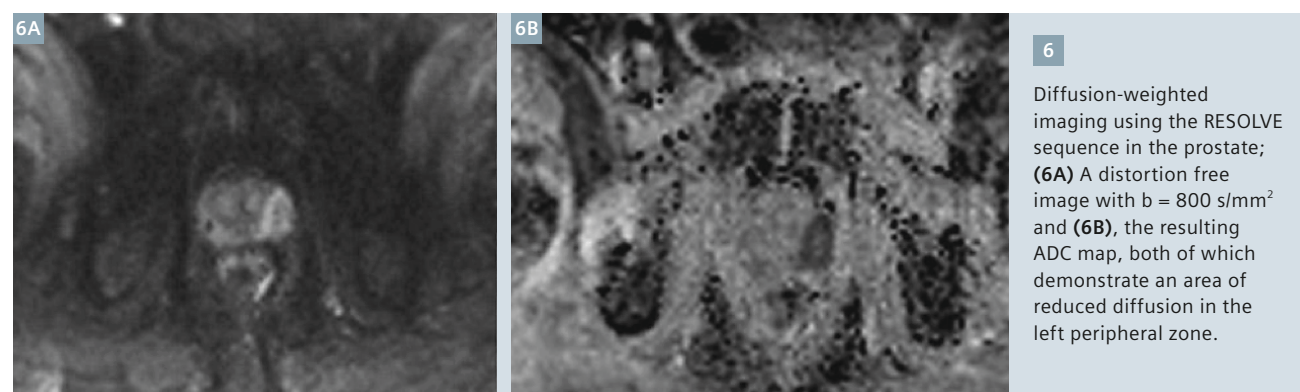
### Lung imaging

For our lung patients, we have developed an advanced imaging protocol providing a comprehensive assessment of anatomy, function and motion throughout their treatment (Fig. 7). For tumor contouring a T2-weighted HASTE sequence with a phase



**5** TimCT was used in this patient with a leg sarcoma and prosthesis *in situ* who could not straighten the effected leg. A full treatment simulation coverage of 61 cm in the head to foot direction was obtained by using the continuously moving table technique.



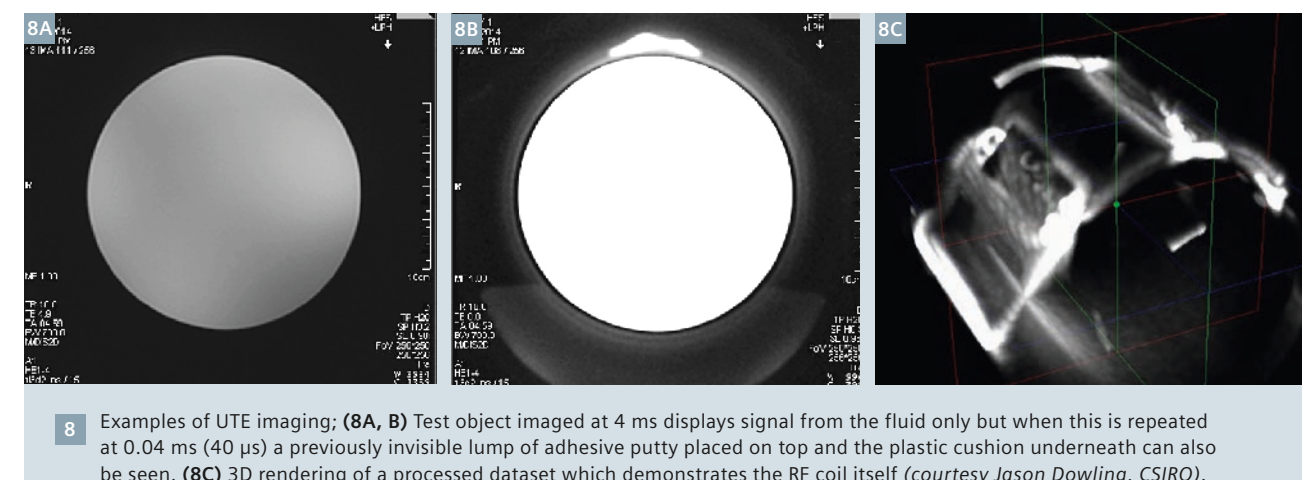


navigator placed in the liver dome is used to provide artefact free images. We then acquire a diffusion-weighted sequence to measure ADC, and cine TrueFISP scans during free breathing to assess tumor motion. The protocol is completed with a DCE TWIST sequence which is modified to acquire

a total of six separate short breath-hold windows from early first pass to 5 minutes post contrast. The incorporation of all this data is still in its infancy but we have already begun to use our own analysis to look at the tumor excursion and how it correlates with respiration.

### Conclusion

In the future, we anticipate that it will be possible to replace CT altogether in the majority of cases. In order to do this, one of the challenges will be the need to substitute CT and provide a surrogate for electron density. As part



of our research agreement with Siemens we are currently investigating the efficacy of ultrashort echo time (UTE) sequences to develop a strategy for MR-only planning<sup>1</sup>. By bringing the TE down to tens of microseconds it becomes possible to obtain signal from materials and tissues that were previously invisible (Fig. 8). These images have the potential to provide more accurate substitute CT datasets as they can map cortical bone and even the RF coil itself which will be useful on the MR-Linac.

In summary, although it is still very much early days for us, the installation of a dedicated scanner in our department has been a great success and crucial in propelling MRI into our practice. We hope that in the not-too-distant future, MR-Sim will become a fairly standard sight in many radiotherapy centres throughout Australia and indeed the rest of the world. This will certainly help to establish a standardised approach for the implementation of MRI into radiotherapy so that the full benefit of this modality can be realised.

### Acknowledgements

We would like to acknowledge the following radiotherapists who make up the MR-Sim team: Lynnette Casapi, Ewa Juresic, Jim Yakobi & Callie Choong. Also thanks to Aitang Xing, Amy Walker (radiotherapy physicists), Mark Sidom and Dion Forstner (oncologists) and Daniel Moses (MR radiologist).

### References

- 1 GP Liney & MA Moerland. Magnetic resonance imaging acquisition techniques for radiotherapy planning, Sem Rad Onc in press, 2014.
- 2 GP Liney, T Al Harthi, E Juresic et al. Quantitative evaluation of diffusion-weighted imaging techniques for radiotherapy planning of prostate cancer. Proc ISMRM 2718: 2014.

<sup>1</sup>Radiotherapy Planning where MR data is the only imaging information is ongoing research. The concepts and information presented in this article are based on research and are not commercially available. Its future availability cannot be ensured.



### Contact

Conjoint Associate Professor Gary Liney (UNSW)  
Hon Principal Fellow, University of Wollongong  
Ingham Institute for Applied Medical  
Research & Radiation Oncology  
Liverpool Hospital, 1 Campbell Street  
Liverpool NSW 2170, Australia  
Phone: +61 2 8738 9221  
gary.liney@sswahs.nsw.gov.au



# Evaluation of the CIVCO Indexed Patient Position System (IPPS) MRI-Overlay for Positioning and Immobilization of Radiotherapy Patients

Th. Koch<sup>1</sup>; K. Freundl<sup>1</sup>; M. Lenhart<sup>2</sup>; G. Klautke<sup>1</sup>; H.-J. Thiel<sup>1</sup>

<sup>1</sup>Klinik und Praxis für Strahlentherapie und Radioonkologie, Sozialstiftung Bamberg, Germany

<sup>2</sup>Klinik für Diagnostische Radiologie, Interventionelle Radiologie und Neuroradiologie, Bamberg, Germany

## Abstract

The emerging development in modern radiotherapy planning (RTP) requires sophisticated imaging modalities. RTP for high precision requires exact delineation of the tumor, but this is currently the weakest link in the whole RTP process [1]. Therefore Magnetic resonance imaging (MRI) is of increasing interest in radiotherapy treatment planning because it has a superior soft tissue contrast, making it possible to define tumors and surrounding healthy organs with greater accuracy. The way to use MRI in radiotherapy can be different. The MRI datasets can be used as secondary images to support the tumor delineation. This is routinely in use in many radiotherapy departments. Two other methods of MRI guidance in the RTP process are until now only research

projects, but interest in them is increasing. The first method is to use MRI data as the primary and only image dataset and the second is the application of the MRI data as reference dataset for a so-called 'MRI-guided radiotherapy in hybrid systems' (Linear Accelerator (Linac) or Cobalt RT units combined with MRI). For all cases it is essential to create the MRI datasets in the radiotherapy treatment position. For this reason the CIVCO Indexed Patient Positioning System (IPPS) MRI-Overlay was introduced and tested with our Siemens MAGNETOM Aera MRI Scanner.

## Introduction

Although computed tomography (CT) images are the current gold standard in radiotherapy planning, MRI

becomes more and more interesting. Whilst CT has limitations in accuracy concerning the visualization of boundaries between tumor and surrounding healthy organs, MRI can overcome these problems by yielding superior soft tissue contrast. Currently there are three different possible strategies by which MRI can help to improve radiotherapy treatment planning:

The MRI datasets can be used as secondary images for treatment planning. These MR images can be used to delineate the tumor and the surrounding organs, whilst the CT images – the primary planning data – are necessary to calculate the 3D dose distribution. The two image datasets have to be co-registered thoroughly to ensure that the anatomy correlates (see for example [2]). The registration

accuracy strongly depends on the MRI scan position. Hanvey et al. [3] and Brunt et al. [4] have shown that it is indispensable for the MRI dataset to be created in the treatment position which is primarily defined by the CT scan.

The MRI dataset can also feasibly be used as the only dataset. Because of the lack of electron density information, which is required for dosimetric calculations, bulk densities have to be applied to the MRI images. For this purpose the different anatomic regions like bone, lung, air cavities and soft tissue have to be overwritten with the physical densities. With this method it is possible to achieve dose calculation results quite similar to the calculation in the CT dataset in the head and neck region [5, 6] as well as in the pelvic region [7]. The advantage of this method is that by avoiding the CT scan you save some time and money. In this case it is necessary for the treatment position to be determined during the MRI scan, hence the MRI scanner has to be equipped with the same positioning and immobilization tools as the Linac. Further problems to overcome are the evaluation and correction of possible image distortions and the determination of accurate bulk densities.

After the RTP process there are a lot of remaining uncertainties such as set-up errors, motion of the target structures and during the treatment changes of the tumor volume and shrinking. This problem can be overcome with the so-called image-guided radiotherapy (IGRT). IGRT involves

a periodical verification (weekly or more frequent) of tumor position and size with appropriate imaging systems. It is evident that IGRT is only as good as the accuracy with which the target structures can be defined. For this reason some groups try to develop hybrid systems, where a Linac or a cobalt treatment unit is combined with an MRI scanner for a so-called MR-guided radiotherapy [8-10]. Again: MR-guided radiotherapy can only be successful when the reference MRI dataset has been created in the treatment position.

In any of the above three cases, where MRI can be helpful to improve the accuracy of radiotherapy, it is strongly advised that one has a robust and reproducible patient positioning and immobilization system, mainly at the MRI scanner, which is used for MR-guided RTP. Siemens provides with the CIVCO IPPS MRI-Overlay a suitable solution. In our clinic we have introduced and tested this MRI-overlay, especially for patients with tumors in the pelvis and for brain tumors and metastasis.

## Method

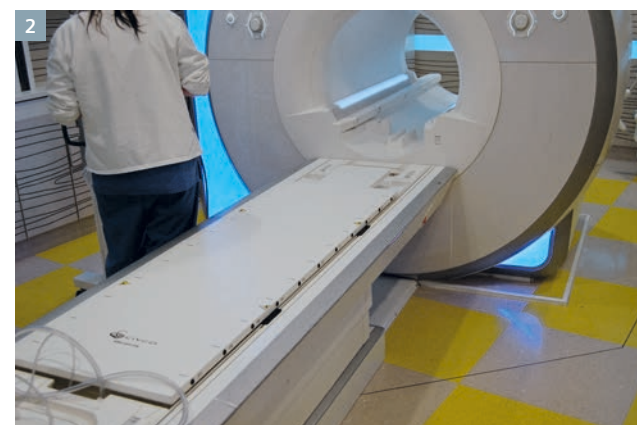
Our 1.5T MAGNETOM Aera system (Siemens Healthcare, Erlangen, Germany) is located in the radiology department and can temporarily be used by the staff of the radiotherapy department. For the purpose of MR-guided RTP we have equipped the MAGNETOM Aera with the CIVCO IPPS MRI-Overlay. This overlay enables the fixation of positioning and immobilization tools necessary for radio-

therapy treatments. For our purpose we have used an MR compatible mask system for head and neck cases and vacuum cushions for patients with diseases in the pelvic region both from Medical Intelligence (Elekta, Schwabmünchen, Germany). These tools can all be fixed with so-called index bars (Figs. 4, 12) at the MRI-Overlay. These index bars are custom designed for our purpose by Innovative Technologies Völp (IT-V, Innsbruck, Austria) for the MRI-Overlay and for use in the high field magnetic environment. For the correct positioning of the patients, the laser system Dorado 3 (LAP, Lüneburg, Germany) was additionally installed in the MRI room. The preliminary modifications and the patient positioning is described in the following for two cases.

The first case describes the procedure for a patient with a head tumor. The first step is the removal of the standard cushion of the MRI couch and the mounting of the MRI-Overlay (Figs. 1–3). One index bar is necessary to fix the mask system on the overlay (Figs. 4, 5) to avoid movements and rotations during the scan. Because the standard head coil set cannot be used with the mask system, two flex coils (Flex4 Large) have to be prepared (Figs. 6–8). In figure 8 one can see, that the correct head angle could be adjusted. Now the patient is placed on the overlay and in the mask system. The patient's head can be immobilized with the real and proper mask made from thermoplastic material called iCAST (Medical Intelligence, Elekta, Schwabmünchen, Germany)



1 1.5T MAGNETOM Aera with the standard cushion on the MRI couch.



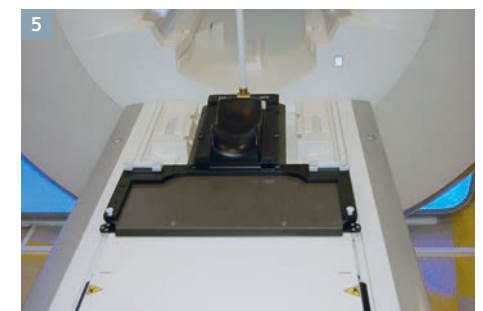
2 After the removal of the standard cushion the CIVCO IPPS MRI-Overlay can be mounted.



3 The lines indicate the position for the index bars.



4 One index bar is latched to the MRI-Overlay.



5 The mask system for head and neck fits to the index bar to avoid movement.

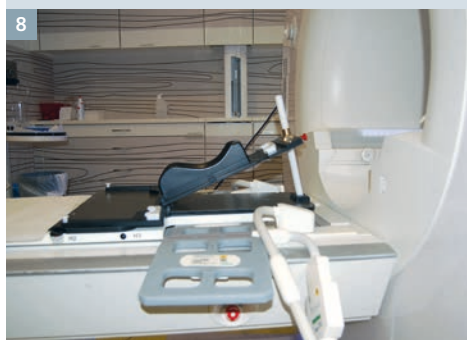




**6**  
Two flex coils (Flex4 Large) are prepared.



**7**  
The flex coils have to be positioned partly under the mask system, because the whole head of the patient should be covered.



**8**  
It is possible to adjust the head angle in an appropriate and reproducible position that is comfortable for the patient.



**9**  
Now the patient is immobilized using a custom-made mask made from thermo-plastic material.



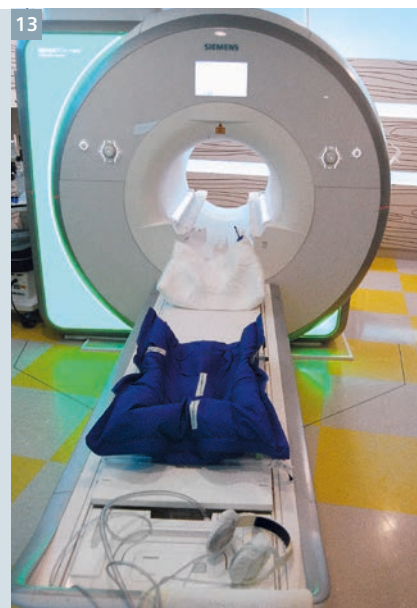
**10**  
The flex coils are closed with hook-and-loop tapes.



**11**  
The patient is ready for the scan.



**12**  
A custom-made vacuum cushion for the lower extremities is latched to the MRI-Overlay with two index bars.



**13**  
A second vacuum cushion is positioned on the table to fix the arms and shoulders and keep the patient in a comfortable position.

as can be seen in figure 9. Now the flex coils can be fixed with hook-and-loop tapes and placed very tight to the patient (Figs. 10, 11). Now the MRI scan can be started.

The second case describes the preparation before the MRI scan for a patient with a tumor in the pelvic region. The first two steps are identical, the remove of the standard cushion followed by the mount of the overlay (Figs. 1, 2). Then a custom-made vacuum cushion for the lower extremities is attached to the overlay with two index bars (Figs. 12, 13). For a robust position of the patients with diseases in the pelvis it is very important to keep the legs in well-defined position – not only during imaging but also throughout the



**14**  
Now the patient can be positioned.



**15**  
The accurate position of the patient can be adjusted with the LAP laser system.



**16**  
A mounting-frame for the flex coil has to be attached to the MRI-Overlay.



**17**  
The mounting-frame from a side view.



**18**  
The flex coil is fixed to the mounting-frame with hook-and-loop tapes.



**19**  
The patient is ready to start the scan.

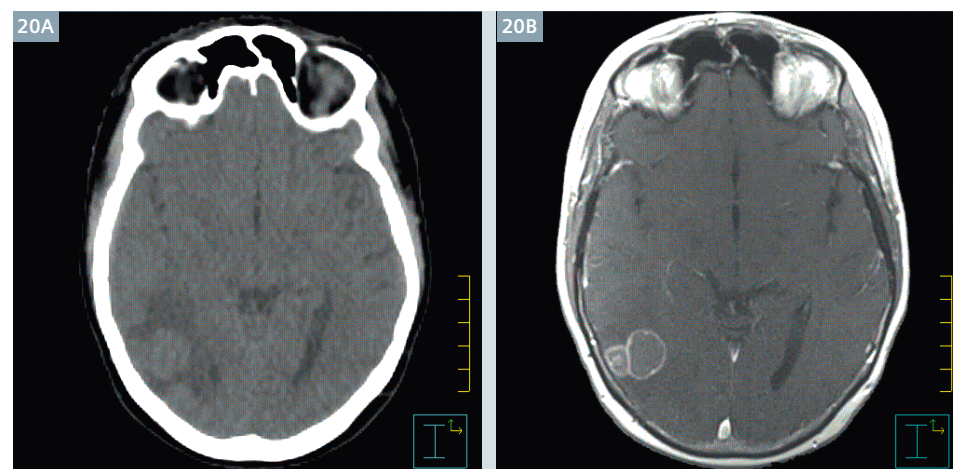
whole treatment course, which spans over seven weeks. Any changes there can result in undesired rotations of the pelvis and in the end the tumor position and shape can also change. In figure 13 a second custom-made vacuum cushion can be seen. The only purpose of this vacuum cushion is to enable a comfortable position of the patient during scan and later during the treatment (Fig. 14). The more comfortably the patient lies on the table the more robust and reproducible is the positioning. Fortunately MAGNETOM Aera has a bore diameter of 70 cm, hence there are almost no limitations concerning patient positioning. Now the accurate position of the patient should be checked with the moveable laser-system (Fig. 15). This is neces-

sary to avoid rotations of the pelvis around the patients longitudinal and lateral axis. For the fixation of the flex-coil for the pelvic region a mounting-frame has to be attached to the overlay (Figs. 16, 17). This can be done with hook-and-loop tapes (Fig. 18). Now the patient set-up is completed and the MRI scan can be started (Fig. 19).

## Results

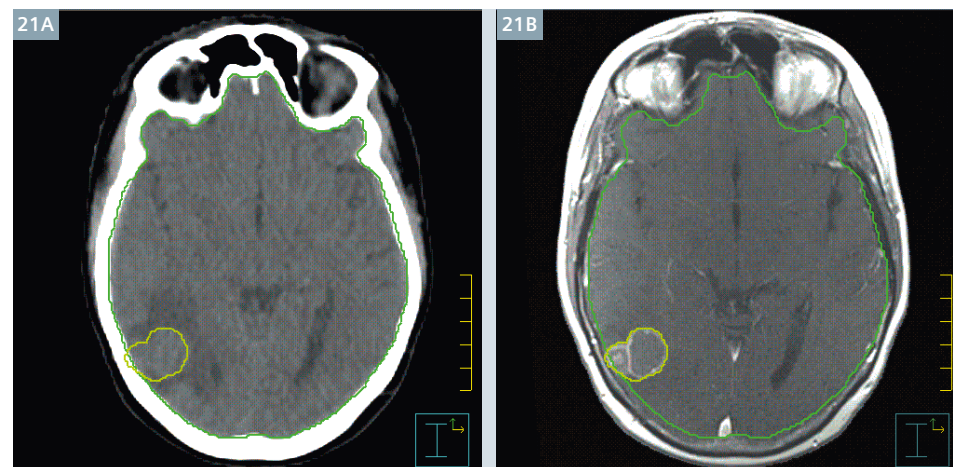
Two examples are shown in the following pictures. In Fig. 20 you can see a brain tumor in two corresponding slices. The left picture shows the CT-slice and the right picture shows the corresponding MRI slice obtained with a T1-weighted sequence with contrast agent. It is clear to see that tumor boundary is much more pronounced in the MRI image. Figure 21 shows the same slices with structures created by the radiotherapists. It is also helpful to create some control structures, such as brain and ventricles, to check the accuracy of the registration. Figures 22 and 23 give an example of a patient with prostate cancer. In this case the MRI images on the right





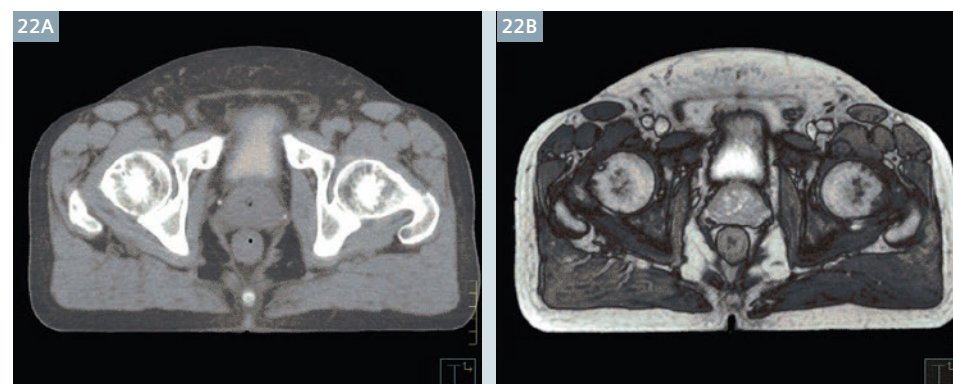
20

Two corresponding slices of a brain scan: (20A) CT slice and (20B) MRI slice obtained using a T1-weighted sequence with contrast agent.



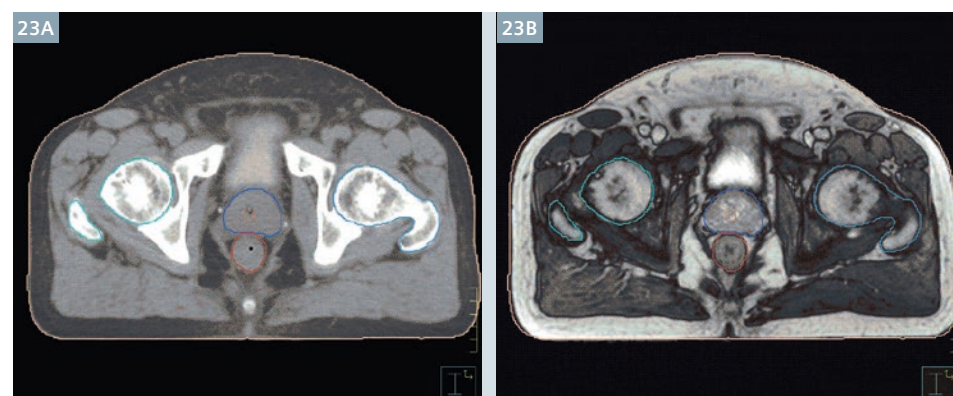
21

The same slices as in figure 20, but now with delineated tumor and help structures.



22

Two corresponding slices in the pelvic region of a patient with a prostate cancer: (22A) CT slice and (22B) MRI slice obtained with a T2-weighted TrueFISP sequence.



23

The important structures rectum and prostate as defined in the MRI slice are shown. The accuracy of the registration can be tested with the coincidence of help structures – like the femoral heads in this case – in both datasets.

are acquired using a T2-weighted TrueFISP sequence. The boundary of the prostate and the differentiation between prostate and rectum is much more easier to define in the MRI images. The control structures in this case are the femoral heads. For the head scans we normally use 3 sequences, a T1w SE with contrast agent, a T2w TSE and a FLAIR sequence. For the pelvis scans we normally use a T2w SPACE, a T2w TrueFISP and a T2w TSE sequence. The coordinate system should be the same for all sequences, that means same slices and same field-of-view. Hence one can use the same registration parameters for all sequences.

#### References

- 1 Njeh C. F. Tumor delineation: the weakest link in the search for accuracy in radiotherapy. *J. Med. Phys.* 2008 Oct-Dec; 33(4): 136-140.
- 2 Dean C.J. et al. An evaluation of four CT-MRI co-registration techniques for radiotherapy treatment planning of prone rectal cancer patients. *Br. J. Radiol.* 2012 Jan; 85: 61-68.
- 3 Hanvey S. et al. The influence of MRI scan position on image registration accuracy, target delineation and calculated dose in prostatic radiotherapy. *Br. J. Radiol.* 2012 Dec; 85: 1256-1262.
- 4 Brunt J.N.H. Computed Tomography – Magnetic Resonance Imaging Registration in Radiotherapy Treatment Planning. *Clin. Oncol.* 2010 Oct; 22: 688-697.
- 5 Beavis A.W. et al. Radiotherapy treatment planning of brain tumours using MRI alone. *Br. J. Radiol.* 1998 May; 71: 544-548.
- 6 Prabhakar R. et al. Feasibility of using MRI alone for Radiation Treatment Planning in Brain Tumors. *Jpn. J. Clin. Oncol.* 2007 Jul; 37(6): 405-411.
- 7 Lambert J. et al. MRI-guided prostate radiation therapy planning: Investigation of dosimetric accuracy of MRI-based dose planning. *Radiother. Oncol.* 2011 Mar 98: 330-334.
- 8 Raymakers B.W. et al. Integrating a 1.5 T MRI scanner with a 6 MV accelerator: proof of concept. *Phys. Med. Biol.* 2009 May; 54: 229-237.
- 9 Hu Y. et al. Initial Experience with the ViewRay System – Quality Assurance Testing of the Imaging Component. *Med. Phys.* 2012 Jun; 39:4013.
- 10 ViewRay. Available at: <http://www.viewray.com>

#### Conclusion and outlook

We can now look back over a period of two years working with the CIVKO IPPS MRI-Overlay. Our experience is very promising. The modifications on the table of the MRI scanner are very easy and can be executed and finished in only a couple of minutes. The procedure is well accepted by the radiologic technologists. To date, we have scanned more than 100 radiotherapy patients, mainly with diseases in the pelvis (rectum and prostate cancer) and in the head (brain tumors and metastasis). So far we have only used MRI dataset as a secondary image dataset. The co-registration with the CT datasets is now much

easier because we have nearly identical transversal slices in both image datasets.

As a conclusion we can say that we are very happy with the options we have to create MRI scans in the treatment positions. It has been demonstrated that the MRI dataset is now much more helpful in the radiotherapy planning process. We should mention the need for a quality assurance program to take possible image distortions into consideration. Our next step is to install such a program, which involves the testing of suitable phantoms. A further step will be to assess whether we can use MRI datasets alone for RTP.



#### Contact

Thomas Koch, Ph.D.  
 Sozialstiftung Bamberg – Medizinisches Versorgungszentrum am Bruderwald  
 Praxis für Radioonkologie und Strahlentherapie  
 Head Medical Physics  
 Buger Straße 80  
 96049 Bamberg  
 Germany  
 Phone: +49 951 503 12931  
[thomas.koch@sozialstiftung-bamberg.de](mailto:thomas.koch@sozialstiftung-bamberg.de)



# RT Dot Engine

Gregor Thörmer, Ph.D.; Martin Requardt, Ph.D.

Siemens Healthcare, Magnetic Resonance Imaging, Erlangen, Germany

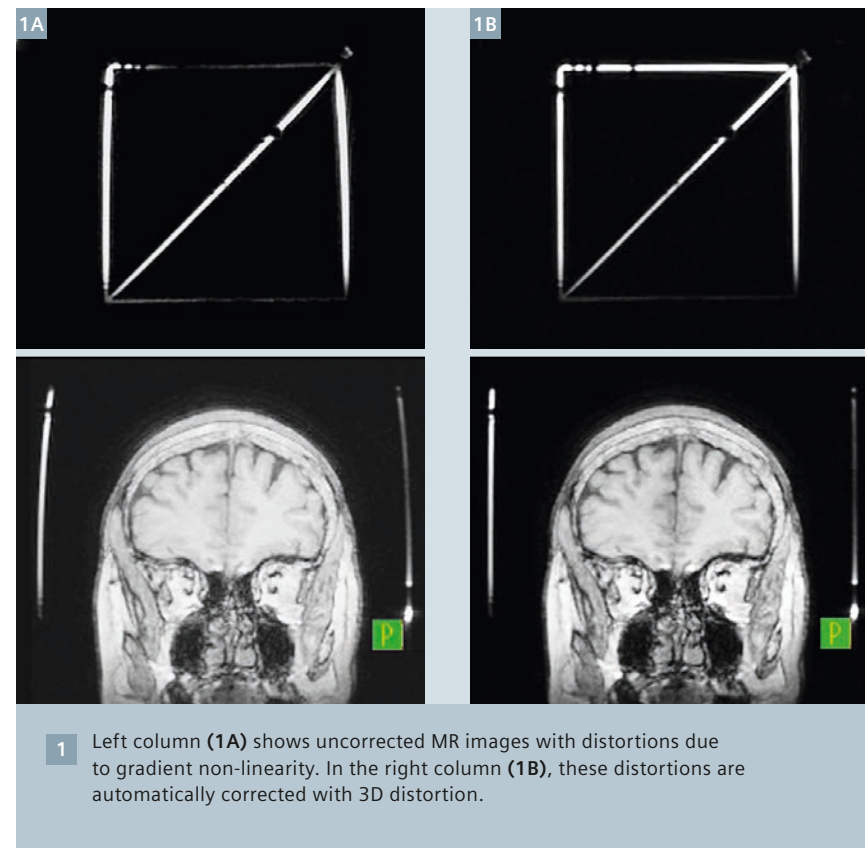
## Background

Magnetic resonance imaging (MRI) is based on different *pulse sequences*, a combination of radio-frequency pulses and gradients that are switched on and off according to a specific scheme. The strength, duration, and spacing of these 'building blocks' are defined by imaging *parameters*. This allows the depiction of tissue in various ways, e.g. for the visualization of vessels, fat or edema, and with different spatial and temporal resolution, depending on the concrete clinical question. An imaging *protocol* allows predefined or customized parameter sets to be saved and retrieved [1].

Standard MR imaging protocols for diagnostic purposes are typically not optimized to meet the requirements of radiation therapy (RT), but can be adjusted for high spatial integrity, isotropic voxels and reduced susceptibility to motion artifacts via the underlying imaging parameters. To do so, however, the user had to be familiar with the complex system of parameters and their mutual interference up to now [2].

## RT Dot Engine

With the RT Dot<sup>1</sup> Engine, a comprehensive package became available addressing specifically the requirements of MR imaging for radiation therapy. The imaging protocols it provides have been developed in collaboration with RT departments experienced in using MR, in particular the group of Prof. James Balter (Michigan University, Ann Arbor, USA). Features like automatic axial image recon-



1 Left column (1A) shows uncorrected MR images with distortions due to gradient non-linearity. In the right column (1B), these distortions are automatically corrected with 3D distortion correction.

struction and 'one click' integration of external laser bridges are easily accessible. All protocols in the RT Dot Engine were carefully optimized to improve spatial integrity, e.g. via high bandwidths [2] and automatic 3D distortion correction (Fig. 1). In the "Dot mode", only a limited set of routine geometry parameters is shown to the user (Fig. 2), while the "Detail mode" provides full access to imaging parameters. The product features different predefined strategies for brain and head & neck imaging and

a protocol to perform external Laser QA (Fig. 3). Using this technology, Radiation Oncology staff can perform MR exams in a reliable and reproducible way. Furthermore, pictograms and hints that exemplary show how to plan an exam can be used to guide less MR-experienced users throughout the workflow. More advanced customers can use the dedicated RT Dot AddIns to build their own RT Dot Engines for other body regions. To support this, Siemens has a team of MR application specialists specifically trained for RT.

## One click integration of external lasers

After patient preparation and positioning with MR compatible immobilization accessories, an external laser bridge (DORADOnova, LAP, Germany) can be used to exactly define the target position on the patient's body. In the past, the technologist had to perform this step with the built-in laser crosshair

of the MRI system again; a handicap of the workflow and a source of inaccuracy. Now, a Dot AddIn takes care with 'one click' ("Laseroffset-Scan", see Fig. 3) that the position defined with the external laser beam directly goes to the center of the magnet where imaging conditions are optimal. One enabler of this technology is the  $\pm 0.5$  mm positioning accuracy of the Tim Table<sup>2</sup>.

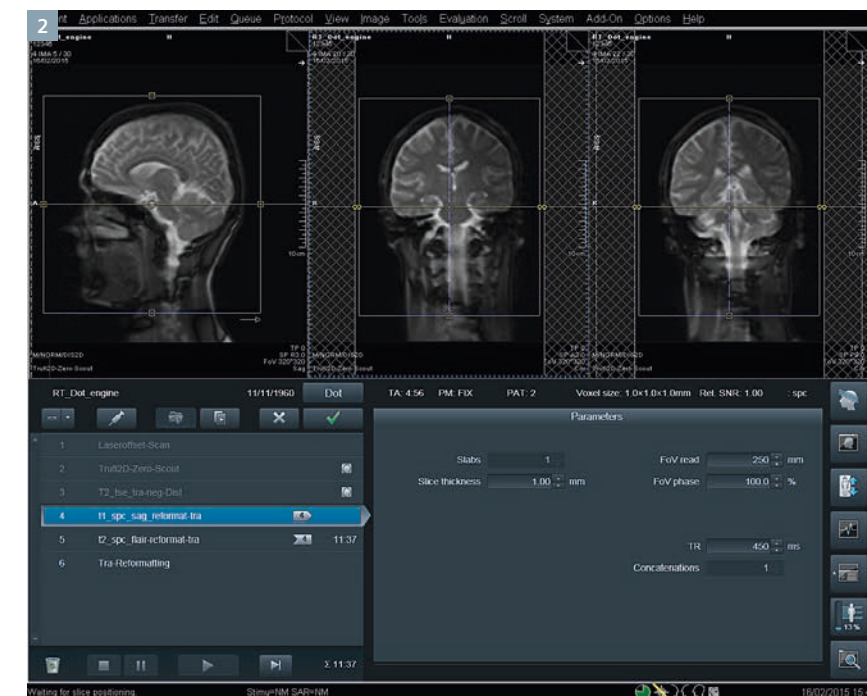
## Fine structured scanning and spatial integrity

Imaging in the treatment position with thermoplastic masks and other equipment requires the use of flexible surface coils. Two such coils wrapped around the patient's head form an '8-channel head coil' providing 17% increase in signal-to-noise-ratio (SNR) compared to a setup with two loop coils positioned left and right of the skull. Nonetheless, the received SNR is still approximately 25% higher with a dedicated 20-channel head & neck coil.

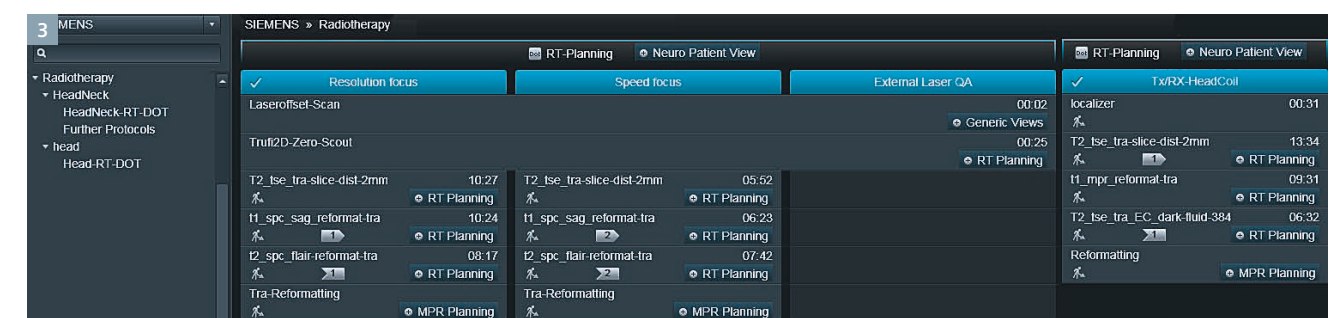
To address this challenge, the RT Dot Engine allows acquisition of two interleaving datasets with an overlap ('negative distance factors') of the neighboring slices. To give an example: 3 mm slice thickness and a negative distance factor of 50% corresponds to an effective interslice distance of only 1.5 mm. This technique of fine structured 2D scanning not only improves the SNR of reconstructed images, it also supports 3D reformatting capabilities (Fig. 4)

## 3D imaging and automatic axial image reconstruction

A majority of imaging protocols in the RT Dot Engine is based on 3D sequences. 3D images inherently provide superior SNR compared to 2D imaging, allow for isotropic voxel size and can be reformatted in any desired orientation. From the point of MR physics it is sometimes beneficial to acquire these datasets with non-axial slice orientation. For some therapy planning systems, however, axial image orientation is mandatory.

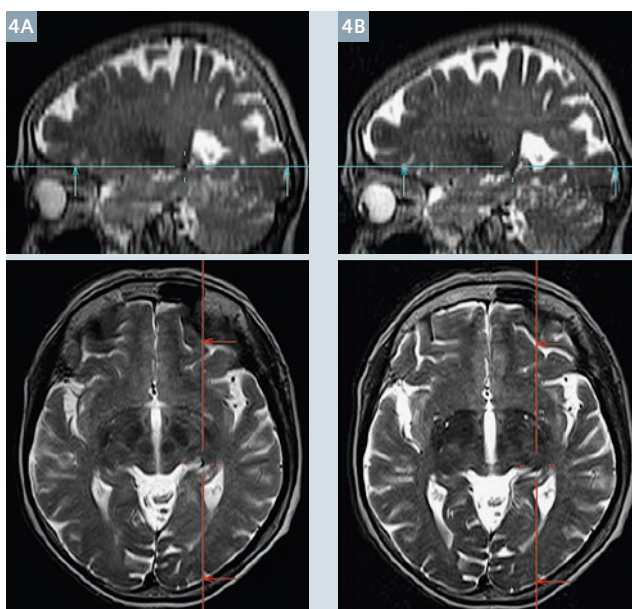


2 User interface shows the predefined scan strategy for a brain exam with the RT Dot Engine. The queue with RT protocols is displayed in the lower half to the left. In "Dot mode" a limited set of geometry parameters is displayed on the right side to adapt scanning to patient's anatomy. By clicking the magnifying glass symbol in the lower right corner you can access and define all imaging parameters on expert level.

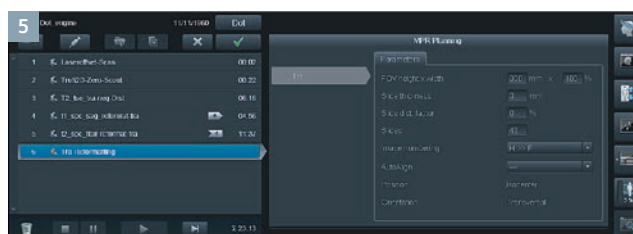


3 Scan strategies within the RT Dot Engine for MAGNETOM Skyra [204x48].





4 Comparison of a standard axial 2D TSE scan with no gap between the slices (4A) and a fine structured 2D TSE volume scan (4B). These images provide both better SNR and good delineation of anatomical structures along the slice axis. The technique is applicable to every 2D sequence protocol.



5 Screenshot of multiplanar reconstruction (MPR) planning AddIn. Assigned image data sets (here: 4 t1\_spc\_sag\_reformat\_tra and 5 t2\_spc\_flair\_reformat\_tra) are automatically reconstructed according to the defined parameters.



6 Left: Coordinate Frame G inside a Tx/Rx (transmit/receive) head coil. By clicking “measure” the B1 rms value for a protocol is calculated. In the example shown here, the flip angle, which correlates with the power of the applied refocusing RF pulses was reduced from 180° to 150° resulting in a respective decrease of the applied average RF power.

In the RT Dot Engine an AddIn ensures that axial images are automatically reconstructed in a predefined way which then can be sent to the planning system (Fig. 5). If a user always wants to have 1.5, 3 and 6 mm axial slices, for example, this can be defined via a respective preset.

#### B1 rms calculation

Some radiation therapy scenarios involve the use of special equipment, like dedicated stereotactic head-

frames to fixate the patient’s skull. For some devices special regulations exist, i.e. to operate these devices with protocols under restricted RF-deposition in order to reduce the risk of heating during imaging<sup>3</sup>. The functionality “B1 rms” (Root mean square of the B1 field) enables easy access to SAR (specific absorption rate) deposition with a specific imaging protocol (Fig. 6). Before starting the actual measurement, the user can verify if certain safety conditions are fulfilled and change imaging parameters if necessary.

#### References

- 1 Rumpel H, et al. How Modules of Imaging Sequences Fit Together: An Overview of Recent Advances in MR Imaging. MAGNETOM Flash #60 (5/2014) p86-92.
- 2 Graessner J. Bandwidth in MRI? MAGNETOM Flash #52 (2/2013) p122-127. <http://www.healthcare.siemens.com/magnetic-resonance-imaging/magnetom-world/clinical-corner/application-tips/bandwidth-mri>

<sup>1</sup> Dot (Day optimizing throughput) includes different features like Dot AddIns to assist the user, standardize procedures and automate recurrent workflow steps.

<sup>2</sup> Specifications MAGNETOM Aera and MAGNETOM Skyra. Datasheet.

<sup>3</sup> Specifications and terms of use are defined and provided by the manufacturer of the equipment.



#### Contact

Gregor Thörmer, Ph.D.  
Global Segment Manager Men’s and Women’s Health  
Siemens Healthcare  
Karl-Schall-Str. 6  
91052 Erlangen  
Germany  
[gregor.thoermer@siemens.com](mailto:gregor.thoermer@siemens.com)

SIEMENS

[siemens.com/imaging-for-RT](http://siemens.com/imaging-for-RT)

## Imaging Solutions that empower Radiation Therapy

Look closer. See further.

As therapeutic and technological capabilities in RT evolve, so does the need for a partner who combines therapy experience with leading imaging expertise. Siemens Healthcare is that partner: For access to high-quality anatomical and functional imaging information that helps RT professionals to make confident treatment decisions.

Siemens’ advanced imaging tools can help you reach your most important clinical goals: achieve a complete response, reduce the risk of normal tissue toxicity,

and improve the chances of disease-free survival for an increasing number of patients.

Siemens solutions can be easily implemented in RT environments and are customized to fit the way RT professionals work – ensuring a smooth and efficient workflow supported by some of the finest imaging tools available.

With tailor-made imaging solutions for RT, Siemens enables you to look closer and see further than ever before, to place you at the forefront of truly individualized therapy.



# Anatomical and Functional MRI for Radiotherapy Planning of Head and Neck Cancers

Maria A. Schmidt, Ph.D.; Rafal Panek, Ph.D.; Erica Scurr, DCR(R), MSc; Angela Riddell, MD FRCS FRCR; Kate Newbold, MD MRCP FRCR; Dow-Mu Koh, MD MRCP FRCR; Martin O. Leach, Ph.D. FMedSci

Cancer Imaging Centre, Royal Marsden NHS Foundation Trust and Institute of Cancer Research, Sutton, UK

## Introduction

Head and Neck cancers are relatively common: squamous cell carcinoma of the head and neck (SCCHN) has a worldwide incidence of approximately 500,000 cases per annum [1]. Treatment is a combination of surgery, chemotherapy and radiotherapy (RT), devised to maximize the probability of eradicating the disease while retaining organ function [2-5]. Recent technical advances in RT include high-precision conformal techniques such as intensity-modulated RT (IMRT) and volumetric intensity modulated arc therapy (VMAT), which enable dose escalation to lesions without exceeding recommended exposure levels for organs at risk (OAR). However, these

techniques require accurate anatomical information to contribute towards improving disease control.

High-resolution Magnetic Resonance Imaging (MRI) has increasingly been used to plan Head and Neck RT [6-10]. MRI and CT images are registered, combining the advantageous soft tissue contrast of MRI examinations and the required CT-based electron density. However, MR images are often distorted due to magnetic field inhomogeneity and non-uniform gradients [11-13], and the use of CT-MR fusion requires geometrically accurate MRI datasets. This article describes the equipment, protocols and techniques used in Head and Neck MRI at the Royal Marsden NHS Foundation Trust to

ensure that the MRI examinations undertaken for RT planning purposes achieve the required geometric accuracy.

## High resolution anatomical imaging in the radiotherapy planning position

At the Royal Marsden NHS Foundation Trust clinical Head and Neck MRI examinations for RT planning are undertaken at 1.5T in the 70 cm bore MAGNETOM Aera (Siemens Healthcare, Erlangen, Germany). Patients are scanned in the RT position using an appropriate head rest and thermoplastic shell immobilisation attached to an MR-compatible headboard, modified to remain accurately positioned on the Aera patient couch. In addition to the elements of the posterior spine coil selected at the level of the lesion, a large flex-coil is also placed anteriorly, in line with the tumor, employing a custom-built plastic device to keep the coil curved, following the neck anatomy. This arrangement achieves a high signal-to-noise ratio, allows effective use of parallel imaging and keeps patient comfort in the RT planning position (Fig. 1).

The MRI protocol covers the primary tumor and neck lymph nodes with approximately isotropic T1-weighted sagittal 3D acquisition (TE 1.8 ms, TR 880 ms, 160 x 1 mm slices, 250 mm x 250 mm FOV, 256 x 256 image matrix). Images are acquired post contrast-agent injection (single dose). This dataset is subsequently registered with the RT planning CT examination, and for this reason its geometric integrity is checked periodically with a large linear test object, previously described [14], consisting of sets of straight tubes in three

orthogonal directions. Figure 2 shows images of the test object without and with post processing to correct image distortion. The 3D distortion correction built into the scanner software is essential for RT planning, and always used. The maximum displacement found within the volume encompassed by head and neck examinations is less than 1 mm. In addition, the imaging protocol employs a 500 Hz/pixel bandwidth, ensuring chemical shift related displacements in the readout direction remain under 0.5 mm.

Having characterized the geometric integrity of the protocol employed, it is also essential to characterize any further distortion associated with the distribution of magnetic susceptibility values within the subjects. In Head and Neck a large number of air-tissue interfaces in the vicinity of the tumors gives rise to localized magnetic field inhomogeneity, detrimental to the geometric integrity of the images. For this purpose, the field inhomogeneity in this region was estimated in five Head and Neck subjects. Transaxial gradient-echo images were acquired with fat and water in phase (TE values 4.76 and 9.53 ms), and the phase

images were subtracted. The local field inhomogeneity was measured after phase unwrapping. Displacements associated with the airways were mostly under 0.5 mm with this sequence. Displacements only reach 1 mm in the vicinity of dental implants, and only very few pixels are affected.

## Functional imaging

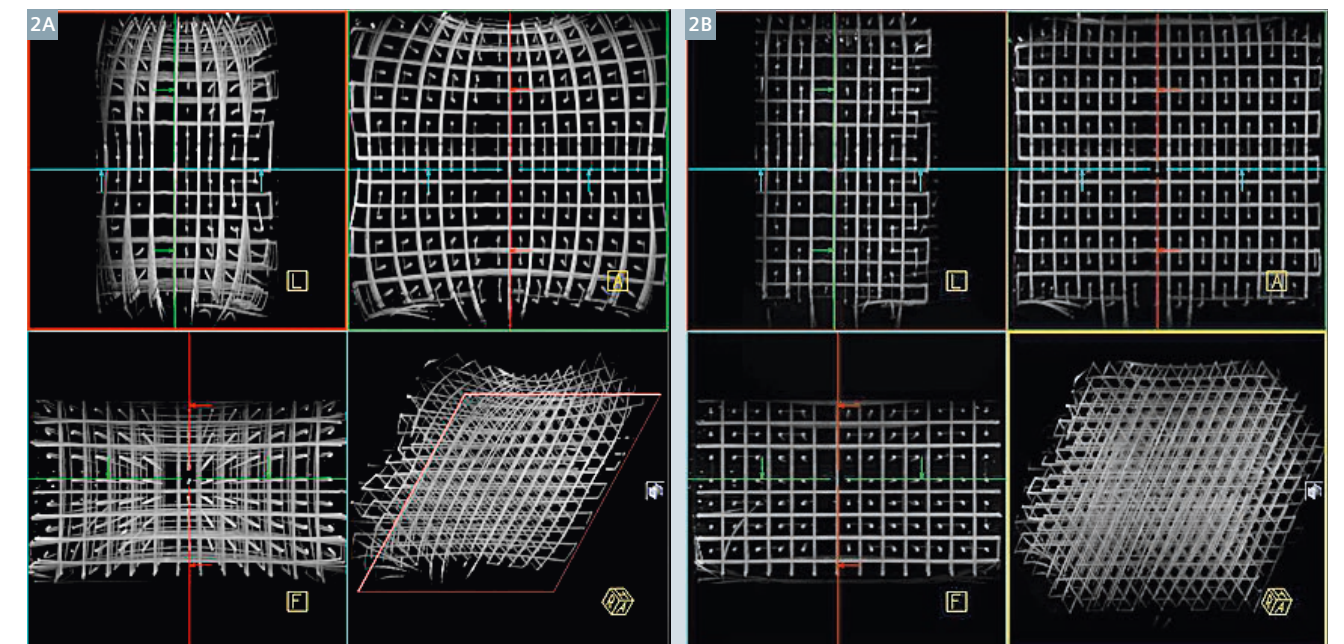
In addition to the clinical service providing anatomical images for RT planning, functional MRI is also employed to characterize lesions pre and post treatment and to investigate prediction of treatment response both at 1.5T (MAGNETOM Aera) and 3T (MAGNETOM Skyra). In RT planning, the ultimate aim of functional imaging techniques is to identify radio-resistant disease and thus provide a biological target volume for dose boosting. Geometric accuracy is therefore essential to allow correct registration of functional MR images with anatomical MRI and CT datasets. In Head and Neck cancers, both diffusion-weighted imaging (DWI) and Dynamic Contrast-Enhanced (DCE) MRI have been explored [15-21].

**Diffusion-weighted imaging with readout segmentation of long variable echo-trains (RESOLVE):** EPI-based DWI is sensitive to the mobility of water molecules and to their environment. In cancer, cell proliferation is often associated with an increase in cell density and in extracellular space tortuosity. This leads to lower values of the Apparent Diffusion Coefficient (ADC), compared to healthy tissues [22-23]. ADC values have thus been used for tumor detection, prediction and assessment of treatment response.

EPI in regions adjacent to air-tissue interfaces is known to suffer from poor geometric integrity [24]. Because this affects Head and Neck studies, strategies to reduce the echo-train length were sought. In addition to parallel imaging, the RESOLVE technique was also employed to acquire multi-shot DWI using a navigator signal to enable accurate multi-echo combinations. In Head and Neck studies, DWI with RESOLVE was employed, covering the volume of interest to identify restricted diffusion within primary lesions and affected lymph nodes.



1 Receiver coil arrangement used at the Royal Marsden NHS Foundation Trust to perform Head and Neck MRI for RT planning. A standard MR-compatible baseboard is employed, enabling the use of a thermoplastic mask. The large flex-coil is positioned above the neck and used in conjunction with elements of the spine array.



2 Images of the Linear Test Object (described by Doran et al. [14]) acquired using a 3D T1-weighted sequence with bandwidth 500 Hz/pixel, without distortion correction (2A) and with 3D distortion correction (2B). Each picture shows three maximum intensity projections (sagittal, coronal and transaxial) and a 3D view of the test object.





3 A comparison of conventional single shot DWI (3A) and RESOLVE DWI (3B) in a head examination. The ADC calculated with the RESOLVE DWI (3C) retains the geometric integrity. Standard DWI parameters: TE 98 ms, TR 7000 ms, receiver bandwidth 1040 Hz/pixel, matrix 192 x 192, FOV 230 mm x 230 mm, 3 averages, slice thickness 4 mm. RESOLVE DWI parameters: TE 58 ms, TR 5700 ms, receiver bandwidth 950 Hz/pixel, matrix 128 x 128, FOV 240 mm x 240 mm, slice thickness 4 mm.



4 Head and Neck T2-weighted image (4A) with co-registered RESOLVE diffusion-weighted image (4B). Restricted diffusion (high intensity) can be observed in nodes, spinal cord, tonsils and submandibular glands with no apparent geometrical distortion.

Figure 3 compares DWI acquired without and with the RESOLVE technique for a Head subject, in a slice comprising air spaces. The clear improvement in geometric integrity achieved with RESOLVE DWI allows the registration of anatomical and functional images, thus allowing the use of DWI in RT planning for Head and Neck cancers (Fig. 4).

#### Dynamic contrast-enhanced MRI with CAIPIRINHA-VIBE and TWIST view-sharing\*:

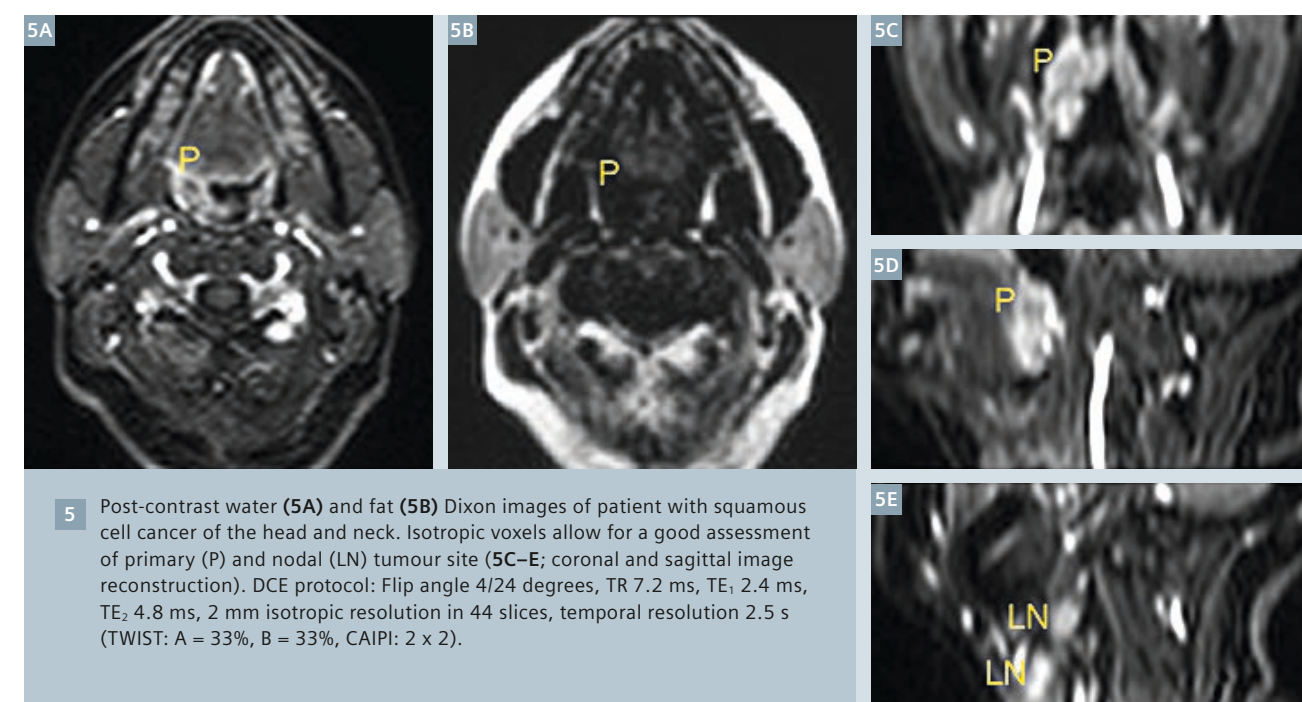
In dynamic contrast-enhanced (DCE)-MRI a series of 3D T1-weighted images is acquired to monitor contrast-agent uptake following an intravenous injection of contrast-agent. Using reference images, this technique can be quantitative and provide a dynamic calculation of T1

for each voxel. This enables pharmacokinetic modelling, providing information on tumor microcirculation, vascularity, blood volume and vessel permeability [25, 26]. This quantitative approach to DCE requires high temporal resolution to maintain accuracy. However, this conflicts with the need for high spatial resolution in RT planning applications.

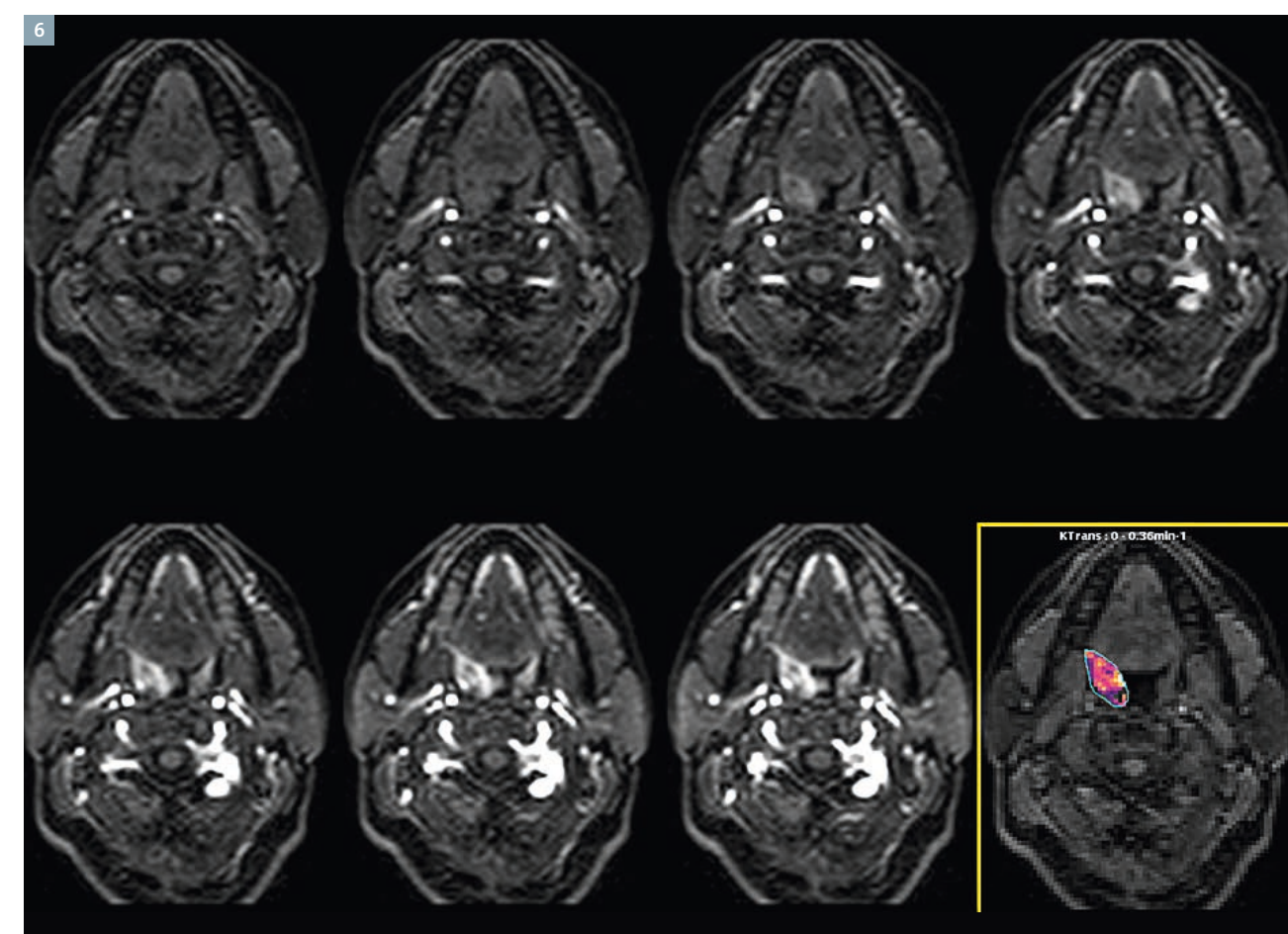
The combination of flex-coil and spine coil elements has been used for DCE employing TWIST view-sharing and CAIPIRINHA reconstruction to produce high resolution images (voxel size 2 mm isotropic x 44 slices, CAIPIRINHA parameters: 2x2) with 2.5 s temporal resolution (TWIST parameters: A = 33% B = 33%). An example of TWIST/CAIPIRINHA DCE with a generous superior/inferior

coverage to include both primary site and local involved lymph nodes is shown in figure 5. Isotropic voxels allow for a good 3D delineation of a biological target volume. In addition, Dixon reconstruction of fat and water images also provides information on fat content within the imaged volume, which might be important in the context of tumor response to treatment. Figure 6 shows T1-weighted water-Dixon signal change after Gd injection for a given representative slice containing a primary tumour. Last frame shows K<sub>trans</sub> map within the region of interest.

\* Work in progress. The product is still under development and not commercially available yet. Its future availability cannot be ensured.



5 Post-contrast water (5A) and fat (5B) Dixon images of patient with squamous cell cancer of the head and neck. Isotropic voxels allow for a good assessment of primary (P) and nodal (LN) tumour site (5C-E; coronal and sagittal image reconstruction). DCE protocol: Flip angle 4/24 degrees, TR 7.2 ms, TE<sub>1</sub> 2.4 ms, TE<sub>2</sub> 4.8 ms, 2 mm isotropic resolution in 44 slices, temporal resolution 2.5 s (TWIST: A = 33%, B = 33%, CAIPI: 2 x 2).



6 T1-weighted Dixon/water signal change after contrast agent injection, showing progressive enhancement and washout of Head and Neck cancer lesion. Last frame shows K<sub>trans</sub> for a region of interest over a primary tumor site.



## Conclusion

Geometrically accurate anatomical and functional imaging for RT planning of Head and Neck cancers were acquired in the RT planning position in standard clinical scanners; this service was developed to meet the clinical and research needs of the users, using custom built coil positioning devices and test objects.

## Acknowledgments

The authors wish to thank D. Nickel, R. Kroeker and P. Ravell (Siemens Healthcare) for the provision of the works-in-progress package WIP771 (VIBE with View Sharing TWIST). The authors acknowledge the support of CRUK and EPSRC to the Cancer Imaging Centre at ICR and RMH in association with MRC & Department of Health C1060/A10334, C1060/A16464 and NHS funding to the NIHR Biomedicine Research Centre and the Clinical Research Facility in Imaging. This work was also supported in part by Cancer Research UK Programme Grants C46/A10588 and C7224/A13407. MOL is an NIHR Senior Investigator.

Radiotherapy Planning where MR data is the only imaging information is ongoing research. The concepts and information presented in this article are based on research and are not commercially available. Its future availability cannot be ensured.

## Contact

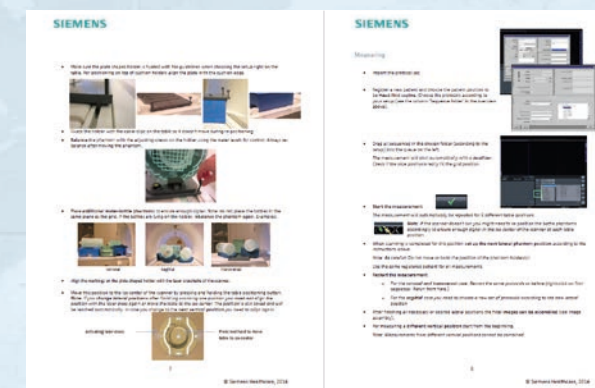
Dr. Maria A. Schmidt  
MRI Unit  
Royal Marsden NHS  
Foundation Trust  
Downs Rd  
Sutton SM2 5PT  
UK  
Phone: +44 (0)20 8661 3353  
maria.schmidt@icr.ac.uk

## References

- Parkin DM, Bray F, Ferlay J, Pisani P. Estimating the world cancer burden: Globocan 2000. *International Journal of Cancer*. 2001;94(2):153–6.
- Bentzen SM, Trotti A. Evaluation of early and late toxicities in chemoradiation trials. *J Clin Oncol* 2007; 25:4096–4103.
- Harrington KJ, et al. Interactions between ionising radiation and drugs in head and neck cancer: how can we maximise the therapeutic index? *Curr Opin. Investig Drugs* 2002; 3: 807–11.
- Lefebvre JL, et al. Larynx preservation clinical trial design: key issues and recommendations - a consensus panel summary. *Int J Radiat Oncol Bio Phys*. 2009; 73: 1293–303.
- Kazi R, et al. Electroglottographic comparison of voice outcomes in patients with advanced laryngopharyngeal cancer treated by chemoradiotherapy or total laryngectomy. *Int J Radiat Oncol Bio Phys*. 2008; 70: 344–52.
- Ahmed M, Schmidt M, Sohaib A, Kong C, Burke K, Richardson C, Usher M, Brennan S, Riddell A, Davies M, Newbold K, Harrington KJ & Nutting CM. The value of magnetic resonance imaging in target volume delineation of base of tongue tumours – a study using flexible surface coils. *Radiother Oncol* 2010; 94, 161–7.
- Bhide SA, Ahmed M, Barbachano Y, Newbold K, Harrington KJ & Nutting CM. Sequential induction chemotherapy followed by radical chemo-radiation in the treatment of locoregionally advanced head-and-neck cancer. *Br J Cancer* 2008; 99, 57–62.
- Gregoire V et al. Radiotherapy for head and neck tumours in 2012 and beyond: conformal, tailored, and adaptive? *Lancet Oncol*. 2012; 13(7), pp.e292–300.
- Nuyts S. Defining the target for radiotherapy of head and neck cancer. *Cancer Imaging*. 2007;7(Special Issue A):S50–S55.
- Newbold K, Partridge M, Cook G, Sohaib SA, Charles-Edwards E, Rhys-Evans P, et al. Advanced imaging applied to radiotherapy planning in head and neck cancer: a clinical review. *Br J Radiol*. 2006 Jul 1;79(943):554–61.
- Wang D & Doddrell DM. Geometric distortion in structural magnetic resonance imaging. *Current Medical Imaging Reviews* 2005; 1: 49–60.
- Wang H, Balter J & Cao Y. Patient-induced susceptibility effect on geometric distortion of clinical brain MRI for radiation treatment planning on a 3T scanner. *Phys Med Biol*. 2013; 58: 465–77.
- Reinsberg SA, Doran SJ, Charles-Edwards EM & Leach MO. A complete distortion correction for MR images: II. Rectification of static-field inhomogeneities by similarity-based profile mapping. *Phys Med Biol* 2005; 50: 2651–61.
- Doran SJ, Charles-Edwards L, Reinsberg SA & Leach MO. A complete distortion correction for MR images: I. Gradient warp correction. *Phys Med Biol*. 2005; 50: 1343–61.
- Thoeny HC, de Keyser F & King AD. Diffusion-weighted MR imaging in the head and neck. *Radiology*. 2012; 263(1): pp.19–32.
- Vandecaveye, V. et al. Evaluation of the larynx for tumour recurrence by diffusion weighted MRI after radiotherapy: initial experience in four cases. *The British Journal of Radiology* 2006; 79: 681–687.
- Sumi M, Sakihama N, Sumi T, Morikawa M, Uetani M, Kabasawa H, et al. Discrimination of metastatic cervical lymph nodes with diffusion-weighted MR imaging in patients with head and neck cancer. *AJNR Am J Neuroradiol* 2003; 24(8):1627–34.
- Powell C, Schmidt M, Borri M, Koh DM, Partridge M, Riddell A, Cook G, Bhide S A, Nutting CM, Harrington KJ & Newbold KL. Changes in functional imaging parameters following induction chemotherapy have important implications for individualised patient-based treatment regimens for advanced head and neck cancer. *Radiother Oncol*. 2013; 106, 112–
- Quon H, Brizel DM. Predictive and prognostic role of functional imaging of head and neck squamous cell carcinomas. *Semin Radiat Oncol*. 2012 Jul; 22(3):220–32.
- Wang P, Popovtzer A, Eisbruch A, Cao Y. An approach to identify, from DCE MRI, significant subvolumes of tumours related to outcomes in advanced head-and-neck cancer. *Medical Physics*. 2012; 39(8):5277–85.
- Srinivasan A, Mohan S & Mukherji SK. Biological imaging of head and neck cancer: the present and the future. *AJNR Am J Neuroradiol*. 2012; 33(4), pp. 1–9.
- Padhani et al. Diffusion-Weighted Magnetic Resonance Imaging as a Cancer Biomarker: Consensus and Recommendations, *Neoplasia* 2009; 11(2):102–125.
- Galbán CJ et al. The parametric response map is an imaging biomarker for early cancer treatment outcome. *Nature medicine*. 2009;15(5): pp.572–6.
- Jezzard P. Correction of geometric distortion in fMRI data. *Neuroimage* 2012; 62: 648–51.
- Walker-Samuel S, Leach MO, Collins DJ. Evaluation of response to treatment using DCE-MRI: the relationship between initial area under the gadolinium curve (IAUGC) and quantitative pharmacokinetic analysis. *Phys Med Biol*. 2006 Jul 21; 51(14):3593–602.
- O'Connor J P B, Jackson A, Parker G J M and Jayson G C. DCE-MRI biomarkers in the clinical evaluation of antiangiogenic and vascular disrupting agents. *British Journal of Cancer* 2007; 96: 189–195. doi:10.1038/sj.bjc.6603515.

# Relevant clinical information at your fingertips

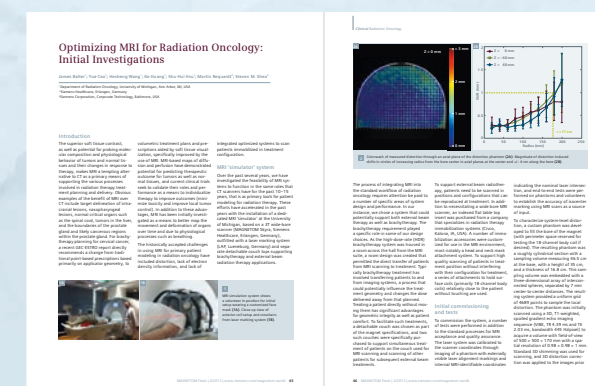
From technology to tips and tricks, you will find the news on all aspects of MRI in Radiation Therapy at [www.siemens.com/magnetom-world](http://www.siemens.com/magnetom-world)



Just a mouse click away you will find application tips allowing you to optimize your daily work.

**MRI Geometric Distortion QA**  
Using the ACR MRI Accreditation Phantom

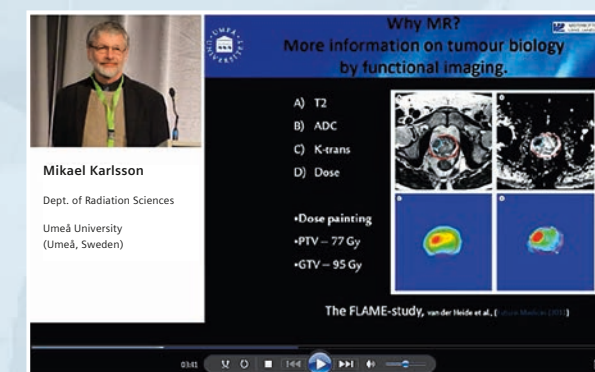
**Nina Niebuhr**  
*Siemens Healthcare*



The centerpiece of the MAGNETOM World Internet platform consists of our users' clinical results. Here you will find case reports, review articles and clinical methods.

**Optimizing MRI for Radiation Oncology**

**James Balter**  
*Dept. of Radiation Oncology, University of Michigan*



Don't miss the talks of international and renowned experts on MRI in RT.

**MRI in the Radiotherapy Process. Now and in the Future**

**Mikael Karlsson**  
*Umeå University Hospital (Umeå, Sweden)*

Visit us at

[www.siemens.com/magnetom-world-rt](http://www.siemens.com/magnetom-world-rt)



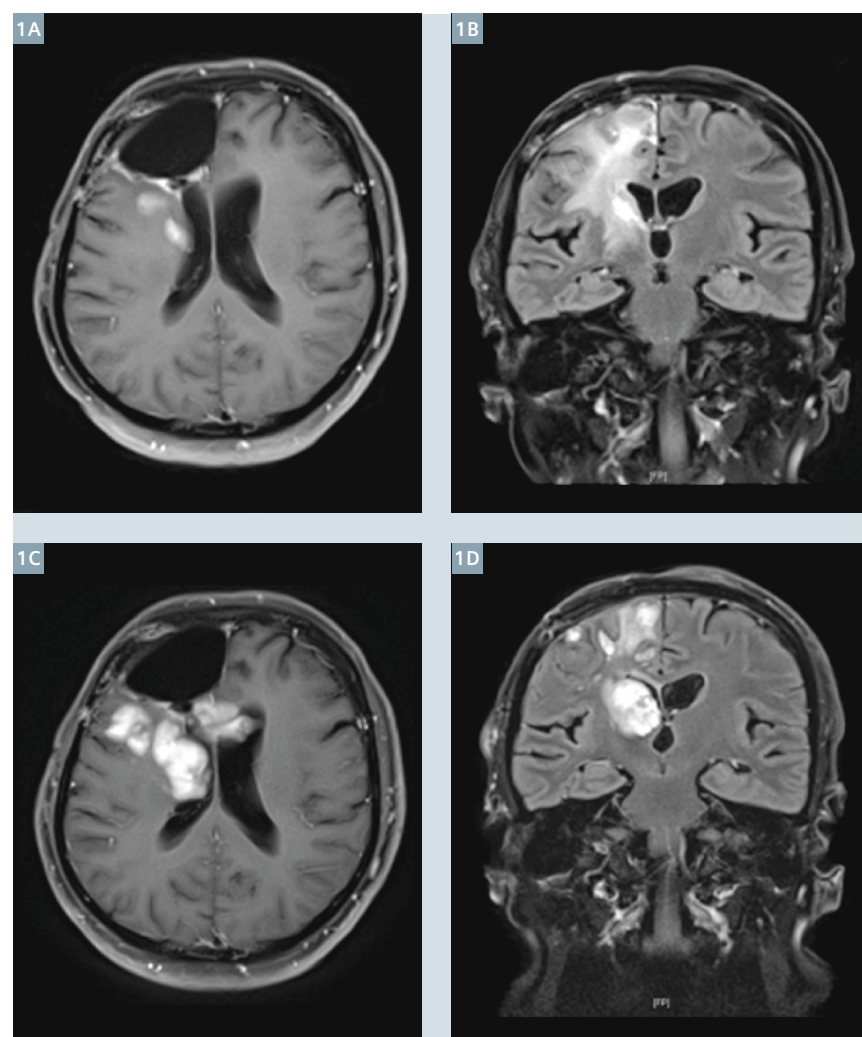
# Clinical Application of Diffusion Tensor Imaging in Radiation Planning for Brain Tumors

S. Rogers<sup>1</sup>; S. Bodis<sup>1</sup>; G. Lutters<sup>1</sup>; L. Remonda<sup>2</sup>; J Berberat<sup>1,2</sup>

<sup>1</sup>Radiation Oncology, Canton Hospital, Aarau, Switzerland

<sup>2</sup>Neuro-radiology, Canton Hospital, Aarau, Switzerland

Malignant brain tumors (glioma WHO grade III-IV) are notoriously difficult to treat despite an intensive combination of surgery, radiation and chemotherapy. Although there is an increasing number of 5-year survivors with this combined modality therapy, the median survival remains in the order of 14 months [1]. Pathological studies have demonstrated preferential tumor cell dissemination spread along white matter tracts and brain vessels [2], which limits the efficacy of both microsurgical resection and radiation therapy. The target for post-operative therapeutic radiation after maximal safe resection includes the resection cavity and any residual tumor visible on the postoperative T1-weighted Gadolinium-enhanced MRI. When surgery is not possible due to a high risk of neurological damage, a diagnostic biopsy is undertaken, followed by radiotherapy. To maximise the probability of including relevant microscopic spread from a glioblastoma (glioma WHO grade IV), uniform wide planning margins of up to 30 mm are typically added (Fig. 2B, green line). Some centres further extend this to include all visible edema on the T2-weighted imaging. Recent studies on the pattern of relapse in patients with high-grade glioma (HGG), predominantly glioblastoma, have suggested that tumor recurrence after maximal combined modality therapy occur within 2 cm of the original tumor location [3, 4]. This has led to a suggestion that a

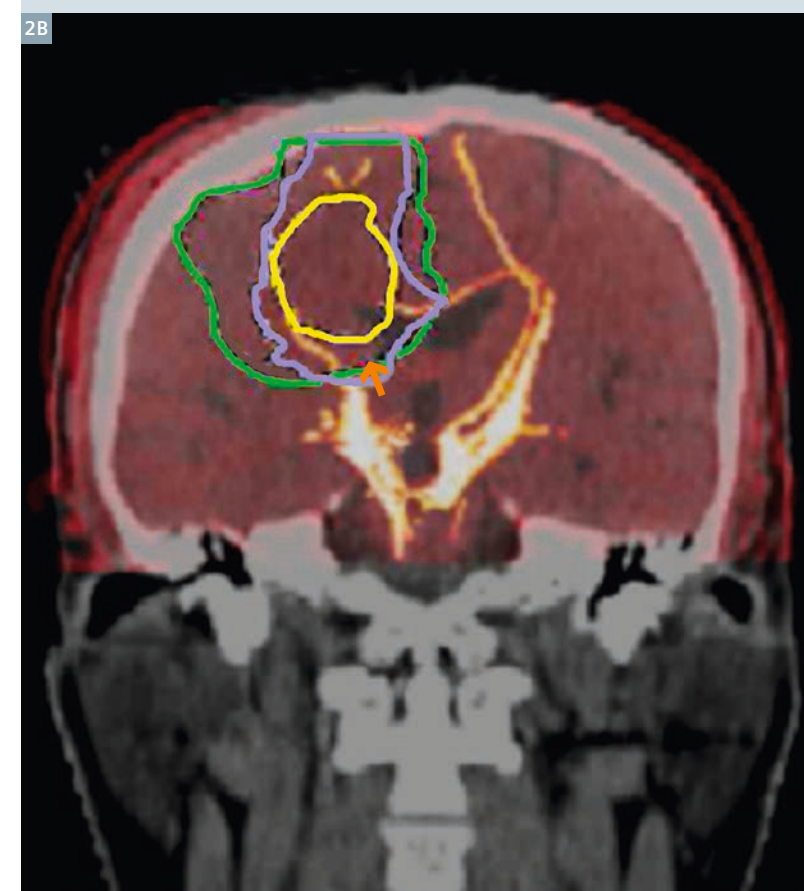
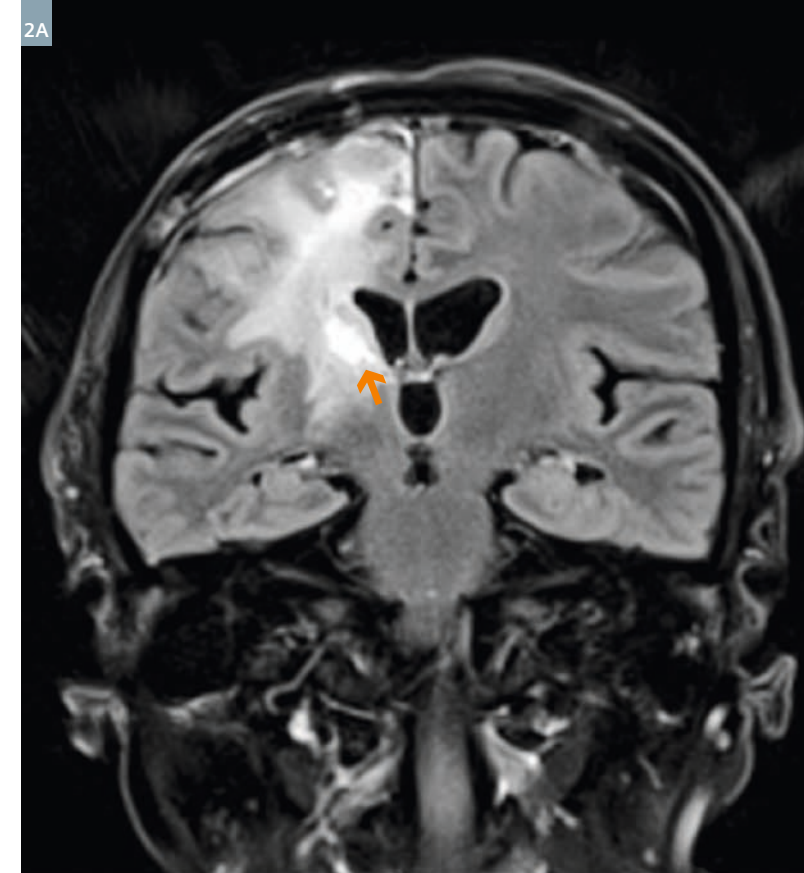


**1** Transverse (T1w BLADE fs) and coronal (T2w TIRM dark fluid fs) MR images (1A, B) 12 months and (1C, D) 16 months after the operation. The patient developed a progressive tumor recurrence contiguous with residual tumor with subsequent extension along neighboring white matter tracts.

reduced margin, for example 1 cm, may be sufficient for the high-dose volume [3].

The addition of temozolomide chemotherapy as a radiation sensitizer and as adjuvant therapy is reported to be associated with an increased risk of normal brain toxicity (radionecrosis) of up to 20% [5]. Radiation-related side effects are dependent on both the prescription dose and the irradiated volume. A dose of at least 60 Gy has been shown to be necessary to control HGG, therefore it is compelling to instead reduce the planning target volume (PTV) where possible without compromising efficacy. Our aim is to derive a biologically targeted volume to ensure coverage of the regions at greatest risk of microscopic infiltration whilst excluding uninvolved brain. To this end, we have explored diffusion tensor imaging (DTI) and fractional anisotropy (FA) to identify areas of tumor infiltration, beyond that visible on T1w contrast-enhanced MRI. The method is derived from the isotropic (p) and anisotropic (q) maps of water diffusivity [6] and based on clinically validated data from patients with HGG [7].

Our technique is best illustrated using a clinical case as an example. This patient with histologically confirmed glioblastoma (GBM), showed tumor progression after surgery and radiation and developed a new lesion in the right thalamus (Fig. 1). The initial pre-operative work-up included DTI to assist the neurosurgeons in the identification and avoidance of apparently uninvolved white matter tracts to minimize the neurological sequelae of the surgery. All the MR imaging was done using a MAGNETOM Avanto 1.5T whole body scanner (Siemens Healthcare, Erlangen, Germany). These same scans were further analysed to extract data



**2** Fusion of the MRI at recurrence 12 months post op with the DTI at recurrence 12 months post op suggests a route of spread via the radiologically abnormal right corticospinal tract.



regarding water diffusivity. The initial steps of the radiation planning technique were to co-register the T1w contrast-enhanced MRI with the planning CT scan. The residual enhancing tumor was contoured accordingly and the volume expanded by 1 cm (Fig. 2B, yellow line) to include brain at highest risk of infiltration. In addition, the DTI scan was co-registered and the volume was extended further along the tracts (Fig. 2B, purple line) in contact with the tumor to encompass likely microscopic spread. Any additional regions of tumor and infiltration, as detected by the p and q

maps, were delineated and then combined into the target volume by the planning software. This final volume was used to generate intensity modulated radiotherapy (IMRT) plans that were not used for clinical treatment (Fig. 2).

Using an in-house software program, we have developed a technique to incorporate regions of altered water diffusivity, reported to correspond with macroscopic tumor or microscopic infiltration, into the radiotherapy planning process. Conventional large volume irradiation for high-grade glioma carries an inevitable

risk of neuro-toxicity, which may be enhanced by combination with radiosensitizers. DTI and FA have previously been reported as diagnostic tools to assist with differential diagnosis, tumor grading, identifying tumor margins and predicting tumor relapse [7-9]. As white matter tracts and alterations in water diffusivity can also be targeted, we believe that future developments in radiation planning for HGG should endeavour to reduce the irradiated volume whilst maintaining adequate coverage of such regions likely to mediate relapse and spread.

# References

- 1 Stupp R, Hegi ME, Mason WP, van den Bent MJ, Taphoorn MJ, Janzer RC, Ludwin SK, Allgeier A, Fisher B, Belanger K, Hau P, Brandes AA, Gijtenbeek J, Marosi C, Vecht CJ, Mokhtari K, Wesseling P, Villa S, Eisenhauer E, Gorlia T, Weller M, Lacombe D, Cairncross JG, Mirimanoff RO; European Organisation for Research and Treatment of Cancer Brain Tumour and Radiation Oncology Groups; National Cancer Institute of Canada Clinical Trials Group. Effects of radiotherapy with concomitant and adjuvant temozolomide versus radiotherapy alone on survival in glioblastoma in a randomized phase III study: 5-year analysis of the EORTC-NCIC trial. *Lancet Oncol.* 2009 10(5):459-66.
- 2 Giese A, Westphal M. Glioma invasion in the central nervous system. *Neurosurgery* 1996 39(2):235-50.
- 3 McDonald MW, Shu HK, Curran WJ Jr, Crocker IR. Pattern of failure after limited margin radiotherapy and temozolomide for glioblastoma. *Int J Radiat Oncol-Biol Phys* 2011 1;79(1):130-6.

- 4 Milano MT, Okunieff P, Donatello RS, Mohile NA, Sul J, Walter KA, Korones DN. Patterns and timing of recurrence after temozolomide-based chemoradiation for glioblastoma. *Int J Radiat Oncol Biol Phys.* 2010 15;78(4):1147-55.
- 5 Rusthoven KE, Olsen C, Franklin W, Kleinschmidt-DeMasters BK, Kavanagh BD, Gaspar LE, Lillehei K, Waziri A, Damek DM, Chen C. Favorable prognosis in patients with high grade glioma with radiation necrosis: the University of Colorado experience. *Int J Radiat Oncol Biol Phys.* 2011 1;81(1):211-7.
- 6 Basser PJ, Mattiello J, LeBihan D. Estimation of the effective self-diffusion tensor from the NMR spin echo. *J Magn Reson B* 1994 103(3):247-54.
- 7 Price SJ, Jena R, Burnet NG, Hutchinson PJ, Dean AF, Peña A, Pickard JD, Carpenter TA, Gillard JH. Improved delineation of glioma margins and regions of infiltration with the use of diffusion tensor imaging: an image-guided biopsy study. *AJNR Am J Neuroradiol* 2006 27(9):1969-74.

- 8 Byrnes TJ, Barrick TR, Bell BA, Clark CA. Diffusion tensor imaging discriminates between glioblastoma and cerebral metastases in vivo. *NMR Biomed* 2011 24(1):54-60.
- 9 Mohsen LA, Shi V, Jena R, Gillard JH, Price SJ. Diffusion tensor invasive phenotypes can predict progression-free survival in glioblastomas. *Br J Neurosurg* 2013 27 [Epub ahead of print].

## Contact

Jatta Berberat, Ph.D.  
Canton Hospital  
Tellstrasse  
5001 Aarau  
Switzerland  
jatta.berberat@ksa.ch



# Advance your clinical capabilities with the MAGNETOM RT Pro edition

For more information please visit us at: [siemens.com/mri](https://www.siemens.com/mri)

Go to: [MRI in Therapy](#) > [MAGNETOM RT Pro edition](#)



# MR-guided Gynecological High Dose Rate (HDR) Brachytherapy

Joann I. Prisciandaro<sup>1</sup>; James M. Balter<sup>1</sup>; Yue Cao<sup>1</sup>; Katherine Maturen<sup>2</sup>; Amir Owraangi<sup>1</sup>; Shruti Jolly<sup>1</sup>

<sup>1</sup> Department of Radiation Oncology, University of Michigan, Ann Arbor, MI, USA

<sup>2</sup> Department of Radiology, University of Michigan, Ann Arbor, MI, USA

## Introduction

Brachytherapy is a form of radiation therapy that is delivered using sealed radioactive sources positioned in close proximity to tissues with cancer. The term derives from the Greek meaning short distance therapy. It is one of the original forms of radiation therapy, and emerged shortly after the discovery of radium in the early 1900's. Up until the 1990's, little had changed in the way brachytherapy treatments were planned and delivered. The nominal workflow consisted of the selection and *in vitro* placement of the appropriate applicator (a device that contains the radioactive source(s)), acquisition of 2D radiographic images to determine the position of the applicator and sources relative to the patient's anatomy, determination of the desired dose to the cancerous tissues and dose limits to neighboring normal tissues, and development of a treatment strategy to deliver the dose. The last two steps are iterative, as one tries to optimize the position and length of time the radioactive source(s) may reside in

the applicator to deliver the highest possible dose to the defined region of interest, while minimizing dose to neighboring normal tissues. However, 2D imaging presents limitations to the development of an optimal treatment plan. Although radiographs provide sharp subject contrast and detail between objects with highly varying attenuation, such as bone and air, the limited differences in attenuation between different types of soft tissue make them difficult to discern (Fig. 1A). As a result, brachytherapy treatment plans have traditionally been designed to deliver the desired dose to a geometrically defined reference point relative to the applicator to which anatomic significance is attached. This approach limits the ability to individualize the patient's radiation to their specific tumor and normal tissues.

In the 1990's, as computed tomography (CT) and magnetic resonance imaging (MRI) became more widely available at clinics and hospitals,

brachytherapy imaging began to transition from the use of planar to volumetric imaging. Unlike radiographs, volumetric images support some visualization of tumors and adjacent normal soft tissues (Figs. 1B, C). Compared to CT, MR images have the advantage of superior soft tissue resolution, and clear distinction of pelvic structures such as the uterus and cervix. Since local tumor control is strongly dependent on appropriately defined tumor volumes and the accurate delivery of radiation, the ability to visualize and delineate soft tissue is expected to improve target coverage and normal tissue sparing [1].

Beginning in 2000, GEC-ESTRO (the Groupe Européen de Curiethérapie – European Society for Radiotherapy & Oncology) recognized the significance of volumetric imaging in the movement toward 3D treatment planning for gynecological diseases, namely cervical cancer, with the formation of the gynecological (GYN) GEC-ESTRO work group [1]. In the fourteen years

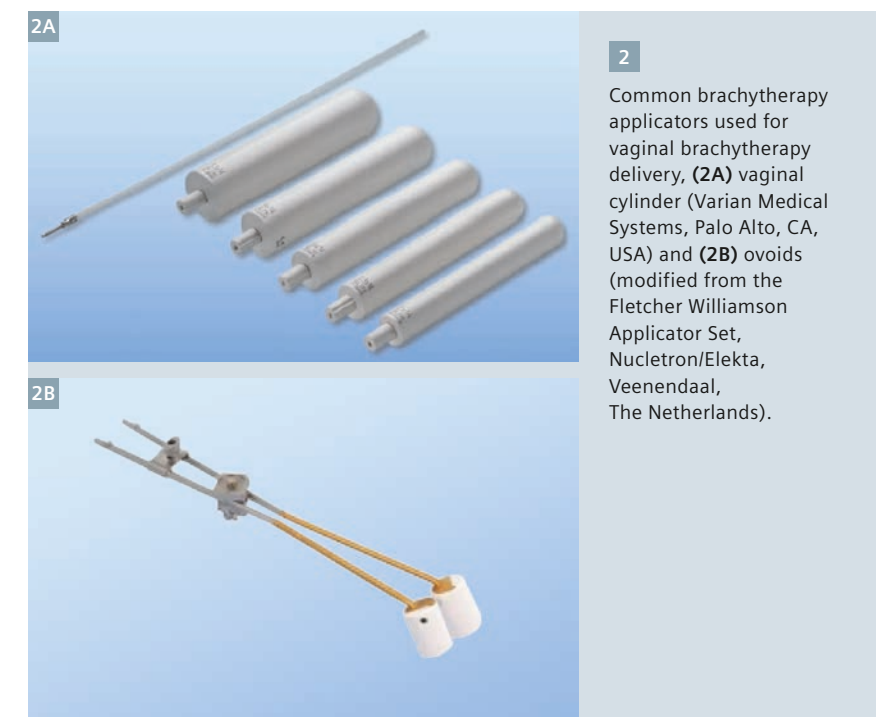
since its creation, the work group has released a series of recommendations to help standardize the approach to image-based brachytherapy treatment planning [1-4]. This has included the definition of a common language and means of delineating the target volumes (i.e., Low Risk-Clinical Target Volume (CTV), Intermediate Risk-CTV and High Risk-CTV for definitive treatment of cervix cancer), discussion on issues related to applicator reconstruction, and suggestions on the appropriate MR imaging sequences to utilize for treatment planning. Although these recommendations are helpful, there is a significant learning curve for each clinic during the clinical commissioning of MR-guided brachytherapy that is dependent on their specific MRI unit and brachytherapy applicators.

## MR-simulator

In 2012, a 3T wide-bore MRI-simulator was installed in the department of Radiation Oncology at the University of Michigan (MAGNETOM Skyra, Siemens Healthcare, Erlangen, Germany). This unit was purchased for the express purpose of complementing, and at times, replacing CT treatment simulations, and has been outfitted with a laser marking system (LAP, Lueneburg, Germany) and detachable couch [5]. The couch supports imaging and treatment of brachytherapy patients, eliminating the need to transfer patients to other tables and the risk of inadvertently modifying the local geometry of the applicator and surrounding tissues. The brachytherapy suite is directly across the hall from the MRI-simulator, and an access door and path was built into the room design to permit wheeling the couch directly to the treatment suite following scanning.

## Clinical commissioning

Prior to the clinical implementation of MR-guided brachytherapy, it is imperative to commission the process and workflow. Commissioning varies based on the desired treatment site, and involves the determination of the optimal imaging sequences for anatomical and applicator visualization. Care must be taken to ensure an MR conditional or compatible applicator is selected prior to the simulation. For treatment



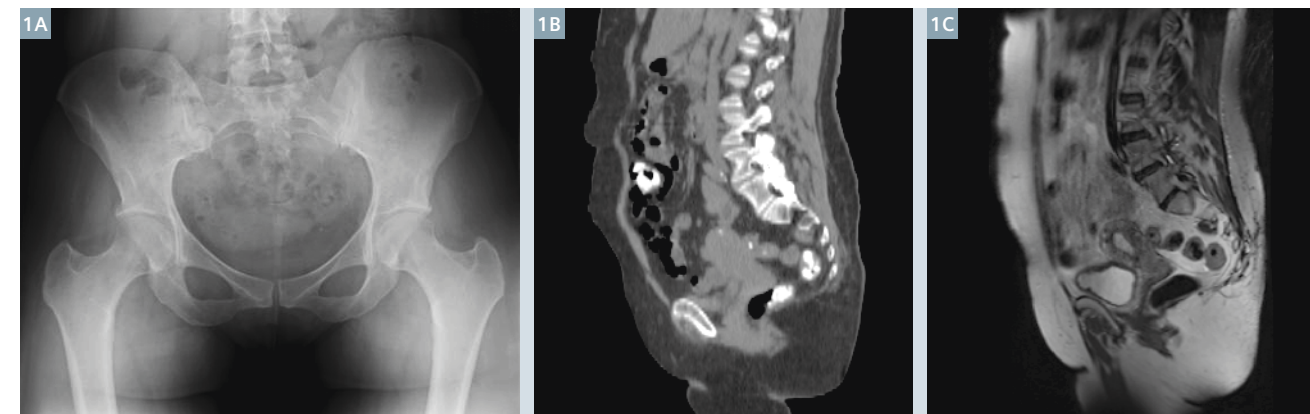
2 Common brachytherapy applicators used for vaginal brachytherapy delivery, (2A) vaginal cylinder (Varian Medical Systems, Palo Alto, CA, USA) and (2B) ovoids (modified from the Fletcher Williamson Applicator Set, Nucletron/Elekta, Veenendaal, The Netherlands).

planning purposes, the images are imported into a software package (treatment planning system) that allows the user to identify the position of the applicator/potential source positions (a process known as applicator reconstruction) and the relevant patient anatomy. This software can then be used to optimize the length of time the radioactive source(s) should reside in various positions along the length of the applicator in order to deliver the desired dose and dose distribution to the patient. While the applicator, in particular the source channel (i.e., the hollow channel within the applicator where the source(s) may reside), is well-visualized in planar and CT imaging with the use of x-ray markers, this task is challenging with MRI. At present there are few MR markers that are commercially available to assist with applicator reconstruction. Additionally, the presence of the applicator, especially titanium applicators, produces image artifacts and distortions. Since dose calculations are dependent on the accurate definition of the applicator, namely the source position(s), relative to the patient's anatomy, geometrical uncertainties may result in dosimetric uncertainties to the target volume(s) and neighboring normal structures

[3]. Thus, it is critical to evaluate these uncertainties prior to the clinical implementation of MR-guided brachytherapy.

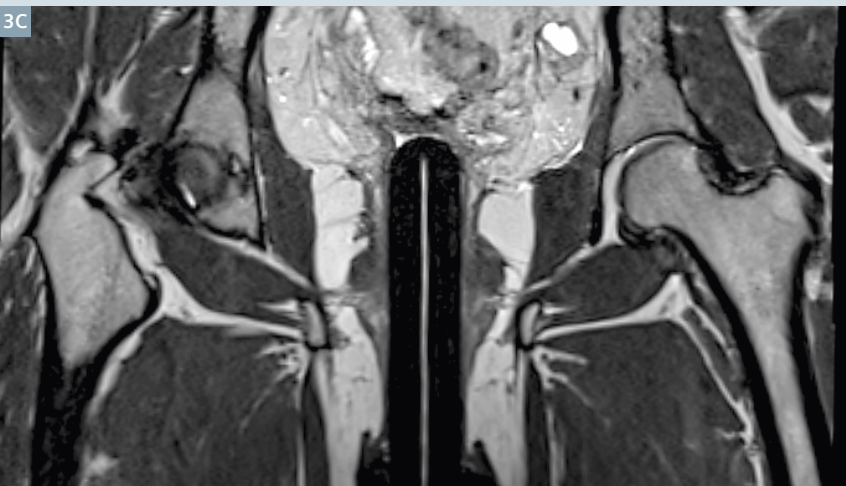
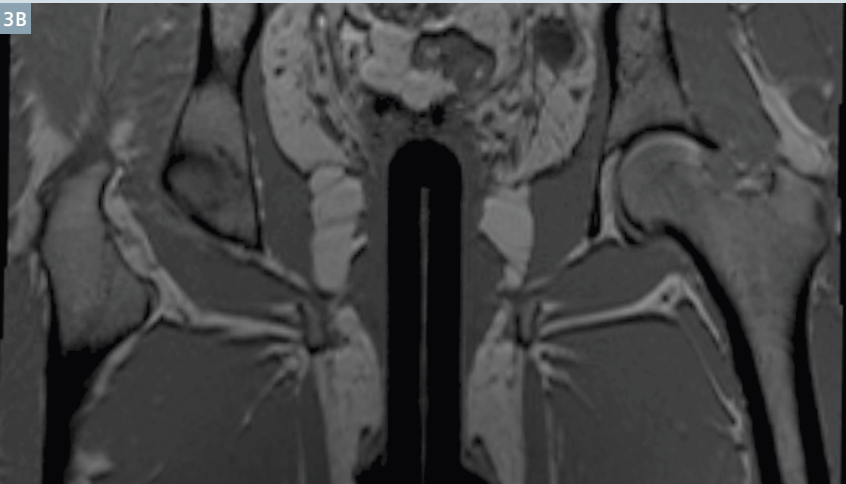
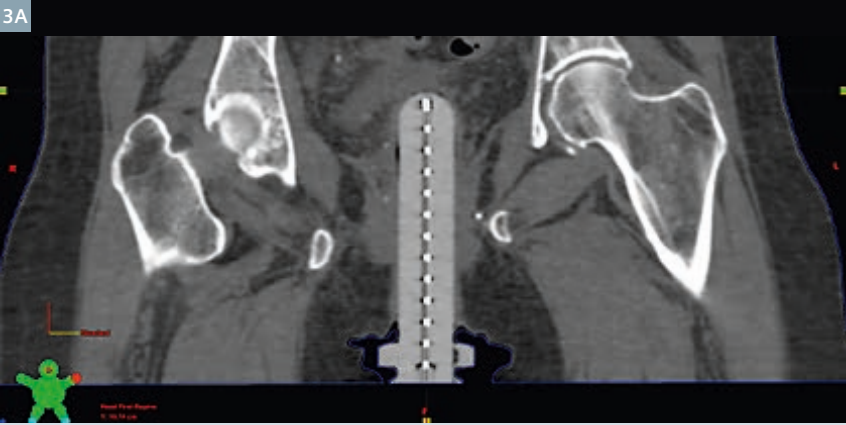
### a. Vaginal high dose rate (HDR) brachytherapy

Clinically, vaginal brachytherapy is most often used in the adjuvant treatment of uterine cancer post hysterectomy to reduce the risk of cancer recurrence in the vagina. Vaginal brachytherapy can also be used for treatment of other gynecologic cancers, including cervix, primary vaginal and vulvar cancer as clinically indicated. The typical applicators used for the delivery of vaginal brachytherapy are the vaginal cylinder and ovoids [6] (see Fig. 2). A vaginal cylinder is typically a smooth, plastic cylinder with a dome shaped apex that is available in diameters ranging from approximately 2.0–4.0 cm, depending on the patient's anatomy. The applicator typically has a single, hollow channel that runs along the center of the device; however, multi-channel variants are also available. Ovoids are hollow egg or cylinder-shaped capsules that are inserted into a patient's vagina and pressed up against the cervix if present or apex of the vaginal vault. Whereas the ovoids may be used to treat the upper



1 Example (1A) anterior pelvic radiograph [10], (1B) sagittal view of a pelvic CT simulation, and (1C) a sagittal reconstruction of a T2w 3D (SPACE) coronal image.





3 Coronal view of a patient with a vaginal cylinder on (3A) CT, (3B) 3D T1w (MPRAGE) MR, and (3C) 3D T2w (SPACE) MR. To assist with the visualization of the central source channel, the appropriate marker (x-ray for CT and contrast filled for MR) was inserted in the applicator prior to simulations.

portion of the vagina (known as the vaginal cuff), the vaginal cylinder offers the flexibility of treating the entire length of the vaginal vault [6].

During the clinical commissioning of MR-guided vaginal brachytherapy at the University of Michigan between August and September of 2013, three patients received a CT simulation preceding each HDR treatment

with a Philips Brilliance CT scanner (Philips Medical, Chesterfield, MO, USA), followed by an MRI simulation using a Siemens MAGNETOM Skyra 3T scanner. The patients were positioned supine with their legs straight. The CT scan was acquired with a 1 mm slice thickness with an x-ray marker in place (see Figure 3A). The MRI was acquired with T1 and T2-weighted 3D imaging sequences.

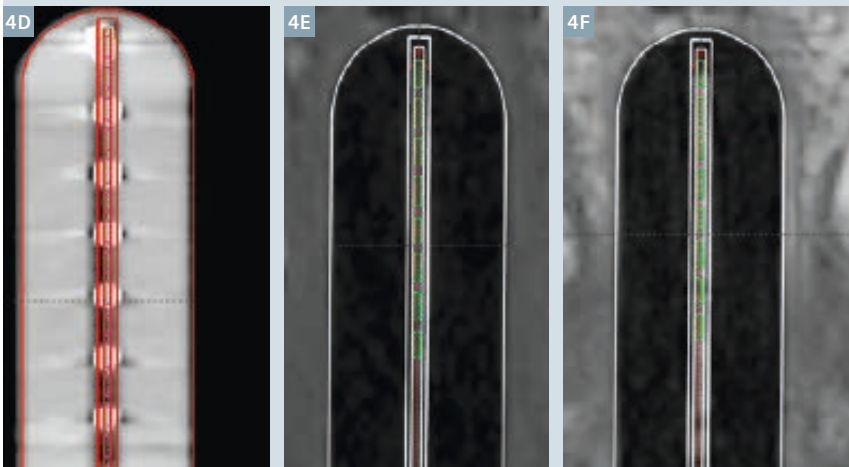
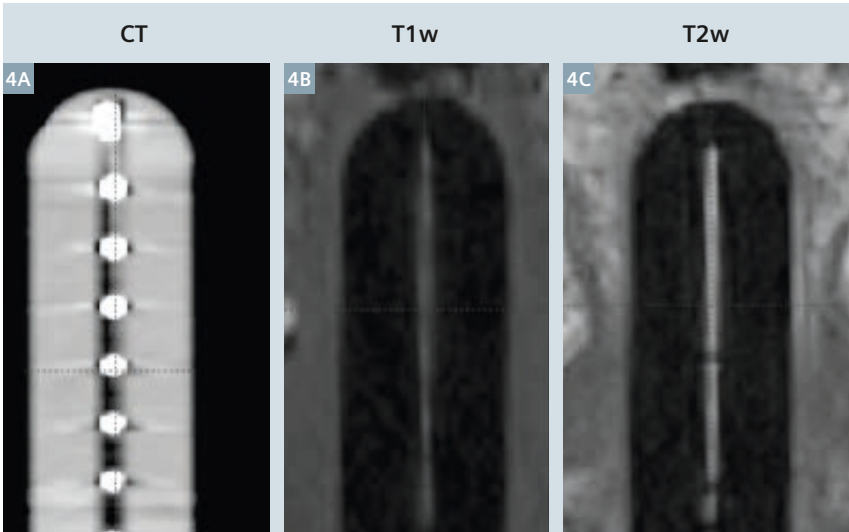
The following MRI sequences were used: 3D T2 (SPACE) coronal (FOV 320 × 320 × 176 mm, voxel size 0.94 × 0.94 × 1 mm, TR 1700 ms, TE 88 ms) and 3D T1 (MPRAGE) coronal (FOV 300 × 300 × 166.4 mm, voxel size 1.17 × 1.17 × 1.3 mm, TR 1900 ms, TE 2.35 ms, TI 900 ms, flip angle 9°). In order to identify the applicator channel, an MR marker was made in-house using a thin (0.046" outer diameter), hollow nylon tube (Best Medical International, Springfield, VA, USA) filled with gadolinium-doped water (T1 contrast) or either water or 0.2% Agarose Gel (T2 contrast), then sealed. Several different techniques were tested to seal the catheter ends including a heat seal with and without hot glue, bone wax with cyanoacrylate, and Water Weld™ with and without cyanoacrylate.

Although the applicator channel was easily visualized with the presence of the appropriate MR marker in both the T1w and T2w images as illustrated in Figures 3B and 3C, the applicator tip proved difficult to identify due to challenges in achieving a watertight seal. This resulted in observed displacements of the catheter tip, at times exceeding 1 cm. As such, an alternative method was investigated for applicator reconstruction using a solid model of the applicator available in the treatment planning software (BrachyVision 8.11, Varian Medical Systems, Palo Alto, CA, USA). Using T1w and/or T2w images, the solid model was aligned to the perimeter of the applicator (see Fig. 4). Deviations between the central source positions identified via aligning the applicator surface model to MR versus using the x-ray marker on CT to reconstruct the applicator (the conventional method) ranged from 0.07–0.19 cm and 0.07–0.20 cm for T1w and T2w images, respectively. Based on this study, vaginal brachytherapy patients at the University of Michigan now routinely undergo a single, T2w SPACE scan with approximately 1 mm isotropic voxel size. The applicator and related source positions for treatment planning are determined by alignment of the applicator model to the vaginal cylinder outline as observed on MRI.

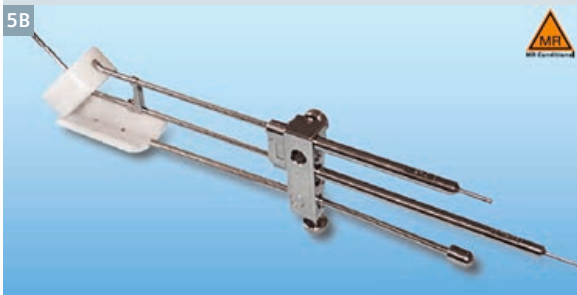
**b. Cervical HDR brachytherapy**

While cervical cancer remains the most common gynecologic cancer worldwide, in the United States, the incidence of cervical cancer has decreased significantly since the widespread use of Papanicolaou (pap) smears in preventative care. Currently, approximately 12,000 new cases of cervical cancer are diagnosed per year. Treatment options are dependent on the stage of the disease upon clinical exam. Early stage cervical cancers are treated primarily by surgery. Occasionally, post-operative radiation or chemotherapy may be needed. When cervical tumors are not considered to be small enough to be removed by definitive hysterectomy, then curative or neoadjuvant radiation therapy with chemotherapy is the standard of care. In such situations, the patient undergoes combined external beam radiation with brachytherapy to provide high doses of radiation close to the tumor. Such treatments employ a variety of brachytherapy applicators. For most cases, the cervix can be treated using a combination of a tandem and ovoids, ring, or cylinder applicators [7]. However, when significant vaginal and/or parametrial involvement are present, then an interstitial brachytherapy implant may be needed to safely bring the required high doses of radiation to those areas.

At the University of Michigan, a plastic MR compatible ring and tandem applicator (GM11001220 and GM1100760, Varian Medical Systems, Palo Alto, CA, USA) has typically been used for HDR brachytherapy treatment of cervical cancer. This applicator system consists of an intrauterine catheter (tandem) and a circular, ring shaped device that allows the sealed source to be placed adjacent to the cervix (see Fig. 5A). During applicator commissioning which commenced in November 2013, 3D T2 (SPACE) sagittal images (FOV 300 × 300 × 79.2 mm, voxel size 0.94 × 0.94 × 0.9 mm, TR 1700 ms, TE 88 ms), 3D T1 (MPRAGE) sagittal images (FOV 300 × 300 × 79.2 mm, voxel size 1.17 × 1.17 × 0.9 mm, TR 1900 ms, TE 2.49 ms, TI 932 ms, flip angle 9°), and multi-planar 2D T2w images at 2–3 mm slice thickness, were acquired with in-house MR markers in each applicator. Although the



4 Para-coronal view of the vaginal cylinder on (4A) CT, (4B) 3D T1w (MPRAGE) MR, and (4C) 3D T2w (SPACE) MR. Following alignment, the overlay of the solid applicator model is depicted for each imaging set in (4D–F).



5 The (5A) plastic and (5B) titanium ring and tandem applicator system used at the University of Michigan (Varian Medical Systems, Palo Alto, CA, USA).

The MRI restrictions (if any) of the metal implant must be considered prior to patient undergoing MRI exam. MR imaging of patients with metallic implants brings specific risks. However, certain implants are approved by the governing regulatory bodies to be MR conditionally safe. For such implants, the previously mentioned warning may not be applicable. Please contact the implant manufacturer for the specific conditional information. The conditions for MR safety are the responsibility of the implant manufacturer, not of Siemens.

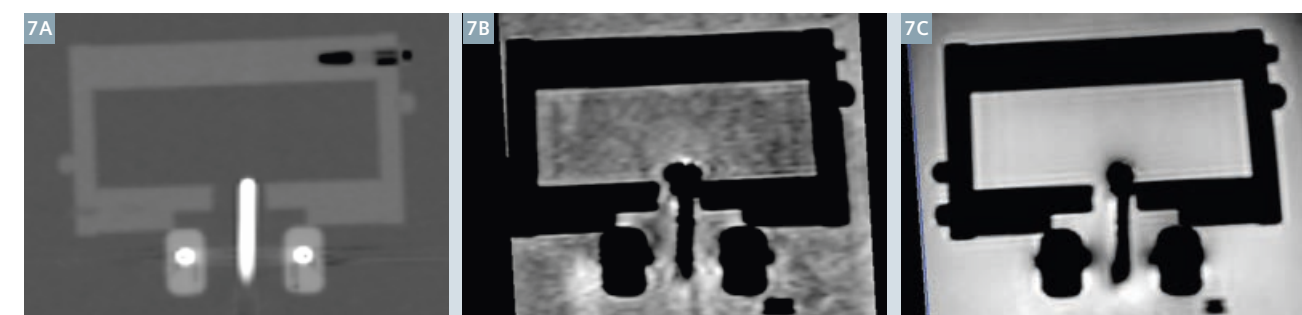


tip of the tandem and ring was not visualized reproducibly due to the compromised seal of the MR markers, the source path and MR marker was discernable on the T1w images (see Fig. 6). As a result of the significantly higher acquisition time for the T2w versus T1w images (nearly twice the scan time), the source channel and MR markers were blurred due to patient and organ motion on the T2w images (see Fig. 6). To minimize scan time, multi-planar 2D T2w images as well as a 3D T1 (VIBE) sagittal scan

with approximately 1 mm voxel size are acquired. Although the 2D T2w planar scans improve the quality of the resulting images, due to the large slice thickness of the 2D versus 3D MRI images, the MR marker was not visible on the 2D images. Therefore, 2D multi-planar T2w images as well as a small FOV 3D T2 (SPACE) sequence are acquired for soft tissue details, and 3D T1 (VIBE) sagittal images are acquired for applicator reconstruction. Prior to treatment planning, the registration of the T1w and T2w images

is verified. If significant patient motion is observed, the images are manually registered in the treatment planning software.

Unlike the vaginal cylinder, a solid applicator model was not available in the treatment planning system for the utilized plastic ring and tandem system. As such, a user defined library plan and applicator model was developed based on the CT reconstruction of the applicator. When a new treatment planning simulation is acquired, the library plan is imported, and the



7 Comparison of (7A) CT, (7B) 3D T1w (MPRAGE), and (7C) 3D T2w (SPACE) sagittal images of the titanium ring and tandem system. The applicator set was scanned in a custom phantom designed to hold the applicator in a fixed position (based on [8, 9]). Prior to imaging, the phantom was filled with gadolinium-doped water. As compared to the CT image, magnetic susceptibility effects produce a mushroom effect off the tip of the tandem in the T1w and T2w images, resulting in uncertainties in the identification of the applicator tip on MRI.

applicator model is aligned based on the visible portions of the source channel, specifically focusing on the curvature of the tandem and/or ring.

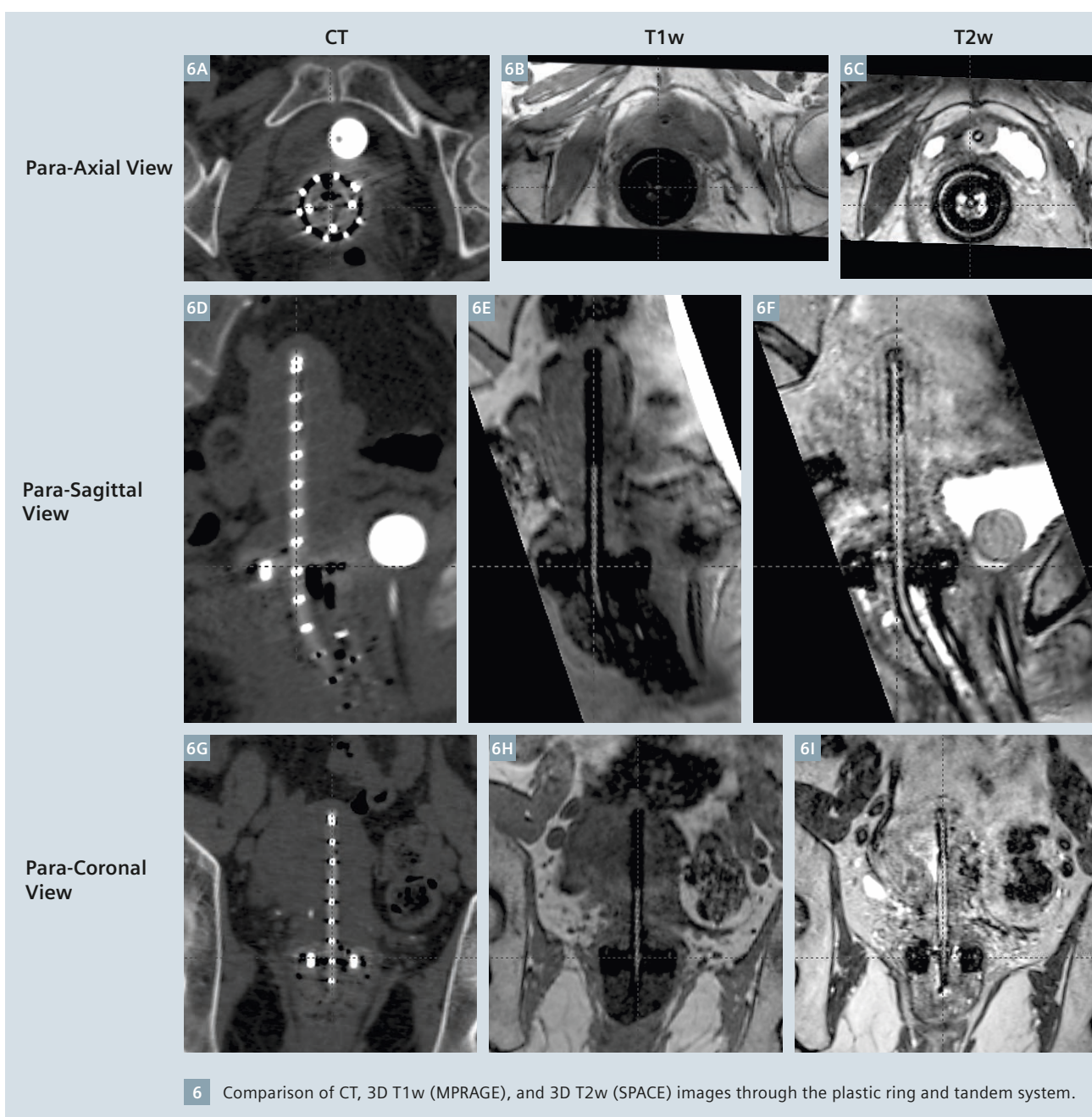
Following a recent recall of the plastic ring and tandem system (PN BT-01366 Rev A, Varian Medical Systems, Palo Alto, CA, USA), a new titanium ring and tandem system (AL13017000, Varian Medical Systems, Palo Alto, CA, USA) has been purchased by the University of Michigan (see Fig. 5B). Due to susceptibility artifacts, the MR marker is not visible in the titanium applicator [8]. Additionally, these artifacts result in a mushroom effect

off the tip of the applicator, making it challenging to accurately identify the applicator tip on MR (see Fig. 7). Kim *et al.* [9] have reported this effect to be considerably smaller when using a small slice thickness (i.e., 1 mm) T1w versus T2w MRI. With the recent arrival of the titanium ring and tandem system at our institution, the clinical commissioning of this applicator set is currently in progress.

## Conclusions

MRI based image guided brachytherapy has the potential to significantly change the treatment planning pro-

cess. Soft tissue contrast allows the user to customize treatment plans to accurately deliver therapeutic doses to the region-of-interest, while minimizing dose to the normal structures in the vicinity of the tumor, potentially resulting in fewer treatment-related complications. However, the transition from point to volume-based planning requires the user to perform a thorough set of commissioning tests to determine the geometric uncertainties related to their imaging and the associated dosimetric uncertainties.



6 Comparison of CT, 3D T1w (MPRAGE), and 3D T2w (SPACE) images through the plastic ring and tandem system.

## References

- Haie-Meder C, R. Potter, E. Van Limbergen *et al.*, Recommendations from Gynaecological (GYN) GEC-ESTRO Working Group (I): concepts and terms in 3D image based 3D treatment planning in cervix cancer brachytherapy with emphasis on MRI assessment of GTV and CTV, *Radiotherapy & Oncology*, 2005;74:235-245.
- R. Potter CH-M, E. Van Limbergen *et al.*, Recommendations from gynaecological (GYN) GEC ESTRO working group (II): Concepts and terms in 3D image-based treatment planning in cervix cancer brachytherapy – 3D dose volume parameters and aspects of 3D image-based anatomy, radiation physics, radiobiology, *Radiotherapy & Oncology*, 2006;78:67-77.
- Hellebust TP, C. Kirisits, D. Berger *et al.*, Recommendations from Gynaecological (GYN) GEC-ESTRO Working Group: Considerations and pitfalls in commissioning and applicator reconstruction in 3D image-based treatment planning of cervix cancer brachytherapy, *Radiotherapy & Oncology*, 2010;96:153-160.
- Dimopoulos JCA, P. Petrow, K. Tanderup *et al.*, Recommendations from Gynaecological (GYN) GEC-ESTRO Working Group (IV): Basic principles and parameters for MR imaging within the frame of image based adaptive cervix cancer brachytherapy, *Radiotherapy & Oncology*, 2012;103: 113-122.
- Balter J, Y. Cao, H. Wang *et al.*, Optimizing MRI for Radiation Oncology: Initial Investigations, *MAGNETOM Flash*, 2013(April): 45-49.
- Small W, S. Beriwal, D.J. Demanes *et al.*, American Brachytherapy Society consensus guidelines for adjuvant vaginal cuff brachytherapy after hysterectomy, *Brachytherapy*, 2012;11:58-67.
- Viswanathan AN, and B. Thomadsen, American Brachytherapy Society consensus guidelines for locally advanced carcinoma of the cervix. Part I: General principles, *Brachytherapy*, 2012;11:33 - 46.
- Haack S, S.K. Nielsen, J.C. Lindegaard *et al.*, Applicator reconstruction in MRI 3D image-based dose planning of brachytherapy for cervical cancer, *Radiotherapy & Oncology*, 2009;91:187-193.
- Kim Y, M. Muruganandham, J. M Modrick *et al.*, Evaluation of artifacts and distortions of titanium applicators on 3.0-Tesla MRI: Feasibility of titanium applicators in MRI-guided brachytherapy for gynecological cancer, *Int. J. Radiation Oncology Biol. Phys.*, 2011;80(3):947-955.
- Jones, Jeremy. <http://images.radiopaedia.org/images/16912/7bb87421cbd7be3955346f5c27ef93.jpg>. Accessed June 29, 2014.

## Contact

Joann I. Prisciandaro, Ph.D.,  
FAAPM, Associate Professor  
Dept. of Radiation Oncology  
University of Michigan  
Ann Arbor, MI  
USA  
Phone: +1 (734) 936-4309  
[joann@med.umich.edu](mailto:joann@med.umich.edu)



Joann Prisciandaro Shrutti Jolly



# syngo.via RT Image Suite: Empower Radiation Therapy with MRI Information

Elena Nioutsikou

Siemens Healthcare, Imaging & Therapy Division, Forchheim, Germany

## What if you could bring your clinical capabilities to a higher level?

With cancer incidents expected to rise by as much as 45% by 2030, oncologists are under pressure to perform more efficiently [1]. This global healthcare trend affects, amongst others, Radiation Therapy (RT) providers who treat approximately one in every two patients presenting with cancer.

The last decade has seen a rapid growth in the utilization of MR

images in treatment planning of radiation therapy. This is partially owing to the fact that MR information brings additional clarity to the clinical image, enabling more confident treatment decisions. But even when clinics have access to the latest imaging devices, making the most of imaging data remains cumbersome and time-consuming with current software solutions. Consequently, healthcare institutions could expand their clinical capabilities by introducing solutions that maximize RT imaging intelligence.

syngo.via RT Image Suite has been developed by Siemens to fulfill this need. It helps oncologists to devise and assess routine and complex treatment strategies. And by providing a comprehensive view of the patient, its flexible, intuitive design supports even the very complex cases. Efficient 3D and 4D image assessment, precise contouring and streamlined collaboration among physicians will help to advance the quality and efficiency of radiation therapy treatments.

## What if you could drive improved outcomes with a comprehensive view of your patient?

### See clearly

Your institution is striving to provide high-quality, tailor-made treatments. You have at your disposal a wide spectrum of images from 3D or 4D CT, to PET and MRI, which can form a basis for treatment decisions. And their optimal use will help meet the ultimate goal of optimizing outcomes for each patient.

With syngo.via RT Image Suite you can visualize a wide range of clinical images including anatomical and physiological images, for example through multiparametric MRI. A concurrent display of up to eight image series<sup>1</sup> (four single or four fused series) is possible on up to two monitors<sup>2</sup>. Rigid and state-of-the-art Deformable<sup>3</sup> Registration supports a confident inclusion of images, even if those were not acquired in treatment position. These powerful capabilities enable a comprehensive clinical view of the patient, for example when preparing initial consultations for a tumor board, during the course of consulting Radiotherapy on how to optimally plan their treatment strategy, or even when evaluating the progress of a particular patient.

By providing the complete picture at great clarity, you have a solution that enables easier and more intuitive clinical decision making.

## What if you could streamline your contouring tasks with an elegant and easy-to-use solution?

### Contour efficiently

Your institution is required to meet increasing quality demands and increasing patient numbers, despite budgetary and staffing constraints. Achieving these objectives requires you to adopt processes that are more efficient, a difficult challenge given the essential task of contouring.

Although contouring on CT images has been a task of Radiation Oncologists for over a decade, contouring on MRI is still an evolving field where cross-department collaboration is highly desirable.

syngo.via RT Image Suite is an intuitive and easy-to-use software solution that enables this collaboration, by facilitating the contouring of both routine as well as advanced cases efficiently. It can be deployed in a variety of ways, for instance as a server-based solution with one or more clients installed in Radiology. Simple import from CDs and DVDs, pre-fetching from PACS, and easy patient data reconciliation allow you to get started quickly. A set of modern tools including Deformable Registration<sup>3</sup> or 3D Smart Freehand Segmentation in any orientation, support fast 3D and 4D CT, MR and PET delineation. In particular, contour changes performed on any image are immediately reflected on all other images: this parallel contouring capability significantly accelerates the segmentation in multi-modality cases while letting you use all available information to their full extent. In cases where a multitude of images is available, the ability to simultaneously display on the screen up to eight<sup>1</sup> image series eases the otherwise cumbersome and time-consuming process of switching panes and exchanging data between applications.

Contouring for treatments that rely heavily on MRI information, such as radiosurgery and brachytherapy, is also supported. Figure 2 illustrates this with a clinical case of vaginal high-dose brachytherapy (explained in detail in MAGNETOM Flash #59, 4/2014, p14-19). Finally, the ability to configure for automatic send to TPS (Treatment Planning System) saves valuable time in completing cases.

From start to finish, syngo.via RT Image Suite supports you in achieving high-quality results, efficiently.

## What if you could strengthen your clinical practice by enabling image-based cancer care pathways?

### Advance your clinical practice

Your team constantly strives to advance its clinical capabilities. Imaging is frequently the critical factor, whether investigating the optimal treatment for a recurrence, adapting a strategy during the course of treatment, monitoring the progress of therapies, or simply exploring the added value of functional imaging in treatment planning. However, providing image-based care pathways seems impractical partially owing to the lack of adequate tools.

syngo.via RT Image Suite enables you to make imaging part of the daily clinical and research practice. To assess the need for re-contouring, you can visualize previously drawn structures on your current image series, supporting clear decision making. And when adaptation is needed, contour warping using Deformable Registration<sup>3</sup> supports new segmentation and further re-planning.

The application also aids in preparing the treatment of patients presenting with tumor recurrences. In this case, the ability to display images and visualize structure sets used during prior treatment on the current dataset guide new contouring smoothly.

All these cases profit greatly from the Advanced Visualization<sup>1</sup> functionality allowing you to compare and contour a variety of images such as diffusion-weighted and contrast-enhanced MRI, Dual Energy CT, 'Cone Beam CT-of-the-day' or PET images acquired with different tracers. Additional syngo.via applications<sup>2</sup> support you in tasks such as quantification, aiding therapy prognosis and monitoring treatment

<sup>1</sup> Requires Advanced Visualization option

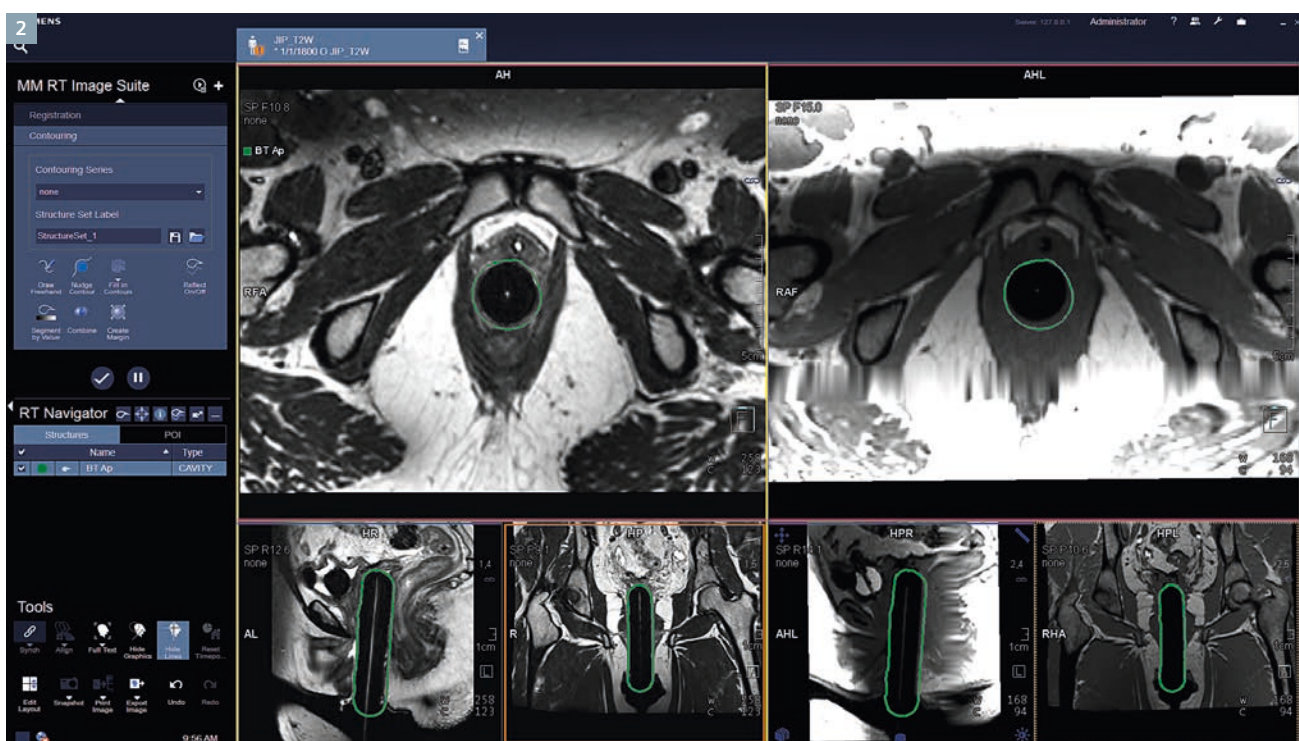
<sup>2</sup> Optional

<sup>3</sup> Requires Deformable Registration option



1 Exploiting all imaging information at hand to its full potential: A CT image of a brain tumor that will later be used for dose calculation, shown side-by-side with two MR contrasts. The contours were drawn on MR and are shown on all images.





2 Contouring a vaginal cylinder in preparation for brachytherapy treatment planning. Left: 3D T2w SPACE, Right: 3D T1w MPRAGE. Images courtesy of Dr. Prisciandaro, University of Michigan, Ann Arbor, MI, USA.

response. Whether you are a Radiologist contouring for the Radiation Therapy department or a Radiation Oncologist with a dedicated MRI, the client-server architecture greatly facilitates efficient communication and teamwork.

From adaptive therapy, to treating recurrences and performing imaging in Radiation Therapy research, syngo.via RT Image Suite supports you and your team in advancing your clinical practice.

### Clinical Example: Adding MRI soft tissue clarity to CT images of the prostate for reducing normal tissue toxicity in whole gland radiotherapy

Radiotherapy treatment to prostate tumors has traditionally targeted the whole prostatic gland, even when the extent of the disease was suspected to be confined to a smaller region. Today, state-of-the-art treatment planning is based on CT images, which are considered

essential due to their capability to provide both the electron density information needed for dose calculation and the geometric accuracy that is expected for planning a precise treatment.

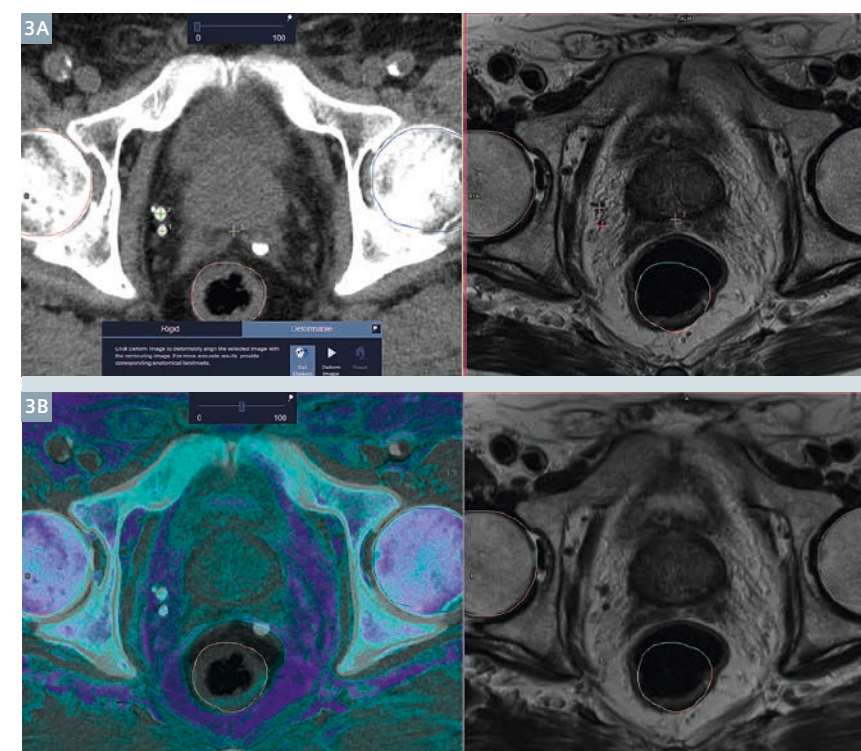
A number of clinical studies [2, 3, 4] have shown that adding the soft tissue information that MRI brings to the picture can help reduce the target volume which is often overestimated by CT alone. Furthermore, Villeirs et al. [5] have shown that the use of MRI in combination with CT improves the accuracy of prostate gland as well as organ-at-risk (OAR) delineation, with decreased inter-observer variability. It is anticipated that this will make an impact on the regions of the surrounding anatomy that would otherwise be exposed to the high-dose region. Reducing, for example, dose to healthy/functional tissue will have a direct effect on any treatment complications experienced by the patient, whether they are manifested as acute or late effects. Alternatively, a dose escalation of 2-7 Gy can be achieved for the same rectal wall dose when MRI is used in organ definition [6].

In the example illustrated below, (Fig. 3) the MR image was acquired in a radiology setting; the patient was not lying on a flat table-top<sup>4</sup> in the 'treatment position'. As a consequence, in order for MRI information to enhance that provided by CT, a Deformable Registration of the MR images was necessary. In figure 3A, the images prior to registration can be seen, while figure 3B shows the results of the registration.

Contouring of all ROI can then proceed on the image that carries the relevant information (e.g. femoral heads on CT, prostate, rectum and bladder on MRI) and those contours can be associated to the CT and sent to a treatment planning system (TPS) for further dosimetric planning.

Deformable registration is also often needed when the CT and MRI were acquired with a significant time difference between the two scans, without following the same protocols; this could give rise to diverse organ filling, making rigid registration lead to odd results.

<sup>4</sup> See [7] for further information.



3 CT and MRI of the same patient acquired in different positions and therefore requiring Deformable Registration before proceeding to contouring. (3A) Landmarks selected to guide the registration and (3B) result of the registration with the MR overlaid on the planning CT.

### Conclusion

syngo.via RT Image Suite helps to leverage MRI and other multi-modality information in Radiation Therapy. syngo.via RT Image Suite improves decision-making with a clear and comprehensive view of your patients, efficient and precise contouring, as well as treatment monitoring and adaptation capabilities that enable personalized therapy.



### Contact

Elena Nioutsikou  
Siemens Healthcare  
Imaging & Therapy Division  
Forchheim  
Germany  
elena.nioutsikou@siemens.com

The product syngo.via RT Image Suite is based on syngo.via VB10. It is still under development and not yet commercially available. Its future availability cannot be ensured.

### Further Reading

For further articles, application tips and clinical talks from experts focusing on the role of MRI in Radiation Therapy, please visit us at:

[www.siemens.com/magnetom-world-rt](http://www.siemens.com/magnetom-world-rt)

### References

- 1 Benjamin D. Smith, Grace L. Smith, Arti Hurria, Gabriel N. Hortobagyi, Thomas A. Buchholz. "Future of Cancer Incidence in the United States: Burdens Upon an Aging, Changing Nation", J Clin Oncol 27. 2009.
- 2 Debois et al, M. (1999). The contribution of magnetic resonance imaging to the three-dimensional treatment planning of localized prostate cancer. Int J Radiat Oncol Biol Phys. 45 (4), pp. 857-865.
- 3 Rasch et al, C. (1999). Definition of the prostate in CT and MRI: a multi-observer study. Int J Radiat.Oncol.Biol.Phys. 43(1), pp. 57-66.
- 4 Roach et al, M. (1996). Prostate volumes defined by magnetic resonance imaging and computerized tomographic scans for three-dimensional conformal radiotherapy. Int. J. Radiat. Oncol. Biol. Phys. 35(5), pp. 1011-1018.
- 5 Villeirs et al. (2005). Interobserver Delineation Variation Using CT versus Combined CT + MRI in Intensity-Modulated Radiotherapy for Prostate Cancer. Strahlenther Onkol 181 (7), pp. 424-430.
- 6 Steenbakkers et al. (2003). Reduction of dose delivered to the rectum and bulb of the penis using MRI delineation for radiotherapy of the prostate. Int J Radiat Oncol Biol Phys 57 (5), pp. 1269-1279.
- 7 MAGNETOM RT Pro edition. (s.d.). Available at <http://www.healthcare.siemens.com/medical-imaging/magnetic-resonance-imaging/mri-guided-therapy/magnetom-rt-pro-edition>



# Whole Body Diffusion-Weighted MRI for Bone Marrow Tumor Detection

Heminder Sokhi, MBCHB, MRCS, FRCR; Anwar R. Padhani, MB BS, FRCP, FRCR

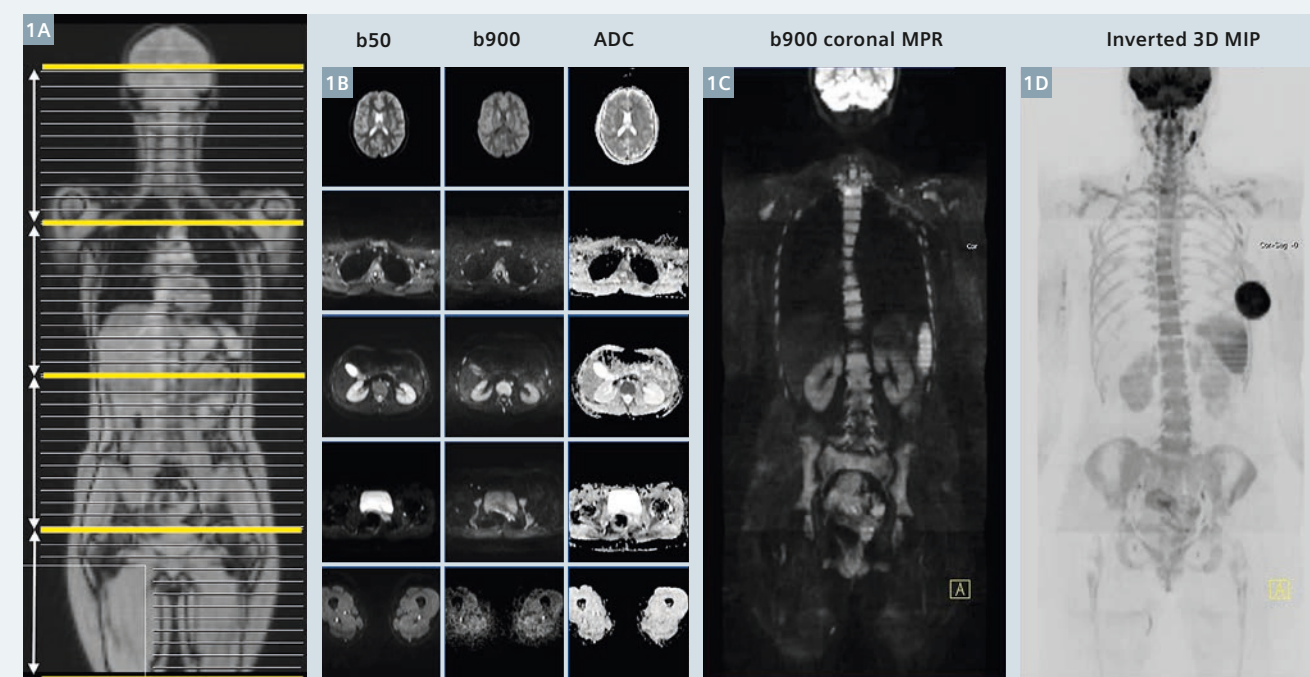
Paul Strickland Scanner Centre, Mount Vernon Cancer Centre, Northwood, Middlesex, UK

## Background

Recent years have seen the evolution of body diffusion-weighted MRI (DWI) into an exciting, whole body (WB-DWI) imaging technique with a distinct clinical utility, particularly in the context of cancer imaging [1-3]. It is clear that, with its excellent sensitivity for detecting marrow infiltration and good spatial resolution, WB-DWI has the capability of providing functional information which complements conventional anatomic

MRI methods. At our institution, we use WB-DWI principally for evaluation of bone marrow metastases, both for detection and for evaluating disease response to therapy, where we have found particular utility for multiple myeloma, breast and prostate cancer. The technique is particularly useful when there is a need to minimize radiation exposure for serial evaluation of younger patients, pregnant women with cancer and in those in

whom intravenous contrast medium is contraindicated (allergy or impaired renal function). This article focuses on the technique for Siemens systems, common artifacts encountered in clinical practice, and alludes to its clinical utility regarding skeletal metastases detection. We do not discuss response assessment of malignant bone marrow disease in any detail but there are clear strengths in this regard also [2].



**1 WB-DWI workflow.** 27-year-old woman with sarcomatoid left breast cancer. The bone marrow pattern is normal for age. Axial DWI from the skull base to the mid-thigh is performed using 2 b-values (50 and 900 s/mm<sup>2</sup>) with a slice thickness of 5 mm in 4 stations. The b900 images are reconstructed into the coronal plane (5 mm) and displayed as thick 3D MIPs (inverted grey scale). ADC images are computed inline with mono-exponential fitting of b50 and b900 signal intensities.

## Technique of whole body DWI

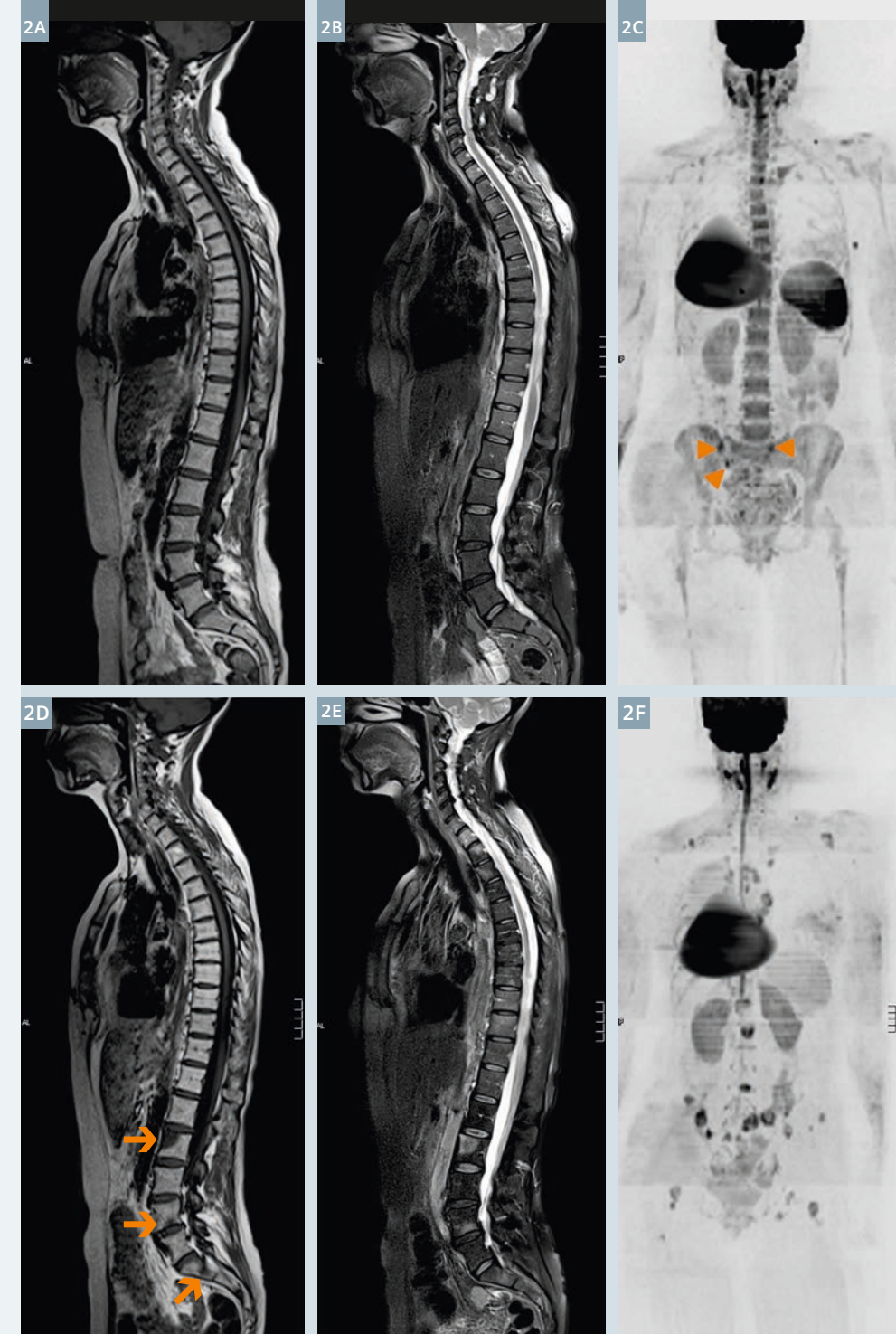
Although imaging at 3T increases the signal-to-noise ratio, WB-DWI at this field strength remains challenging because of increased susceptibility artifacts and poorer fat suppression; currently, we find that WB-DWI is best performed on a longer bore 1.5T scanner. All our WB-MRI scans are done on a Siemens MAGNETOM Avanto scanner equipped with a continuous moving table option (TimCT) and total imaging matrix (Tim) body surface coils. We always acquire morphologic images to accompany the WB-DWI images.

Our morphologic images consist of

- 1 whole spine: T1-weighted, turbo spin-echo sagittal images (acquisition time 2:21 minutes),
- 2 whole spine: T2-weighted, turbo spin-echo sagittal images with spectral fat suppression (acquisition time 2:36 minutes),
- 3 whole body: T1-weighted, gradient-echo axial 2-point Dixon sequence (acquisition time 3:00 minutes) that automatically generates four image-sets (in-phase, opposed phase, water-only (WO), and fat-only (FO)) from which T1w fat% and non-fat% images can be calculated if needed.
- 4 Finally whole body (vertex to upper mid thighs): T2-weighted, short-tau inversion recovery (STIR) axial images with half-Fourier single shot turbo spin-echo (HASTE) readouts (acquisition time 4:00 minutes) is also undertaken.

The axial images from the skull vault to the mid-thighs are acquired using the continuous table movement technology, employing multiple breath-holds for image acquisitions of the chest, abdomen, pelvis and upper thighs.

Axial DWI from the skull vault to the mid-thighs is then performed using b-values of 50 s/mm<sup>2</sup> and a b-value of 900 s/mm<sup>2</sup> with a slice thickness of 5 mm. The axial DWI acquisition is usually achieved in 4 contiguous stations using a free-breathing technique, with each station taking approximately 6 minutes to acquire. Our preferred



**2 Bone marrow hypoplasia due to chemotherapy with disease progression.** 49-year-old woman with metastatic breast cancer before and after 3 cycles of carboplatin chemotherapy. Both rows left-to-right: spine T1w spin-echo, spine T2w spin-echo with spectral fat saturation and b900 3D MIP (inverted scale) images. Top row before chemotherapy shows normal background bone marrow pattern with superimposed small volume bone metastases (arrow heads). Bottom row after chemotherapy shows disease progression with enlarging and new bony metastases (arrows). Note that bone marrow hypoplasia has developed in the ribs, spine and pelvis. Note reductions of signal intensity of the spleen secondary to iron deposition due to blood transfusions. There is a right sided silicone containing breast enhancement bra pad in place on both examinations.





**3 Poor visibility of treated metastases and osteoblastic metastases.** 69-year-old with metastatic prostate cancer on long term, third line hormonal therapy with abiraterone being evaluated for rising serum prostate specific antigen (PSA) levels. He has had an excellent response to 2 years of treatment with residual abnormalities in his bone marrow visible on T1w (3A) and T2w (with fat suppression) spinal images. No hyperintensity is seen on the b900 3D MIP (inverted scale) image (3C) indicating the absence of highly cellular infiltrative disease. Bone scan (3D) shows a focal area of osteoblastic uptake in the intertrochanteric region of the left femur (arrow) which is not visible as a discrete region on the b900 3D inverted MIP image.

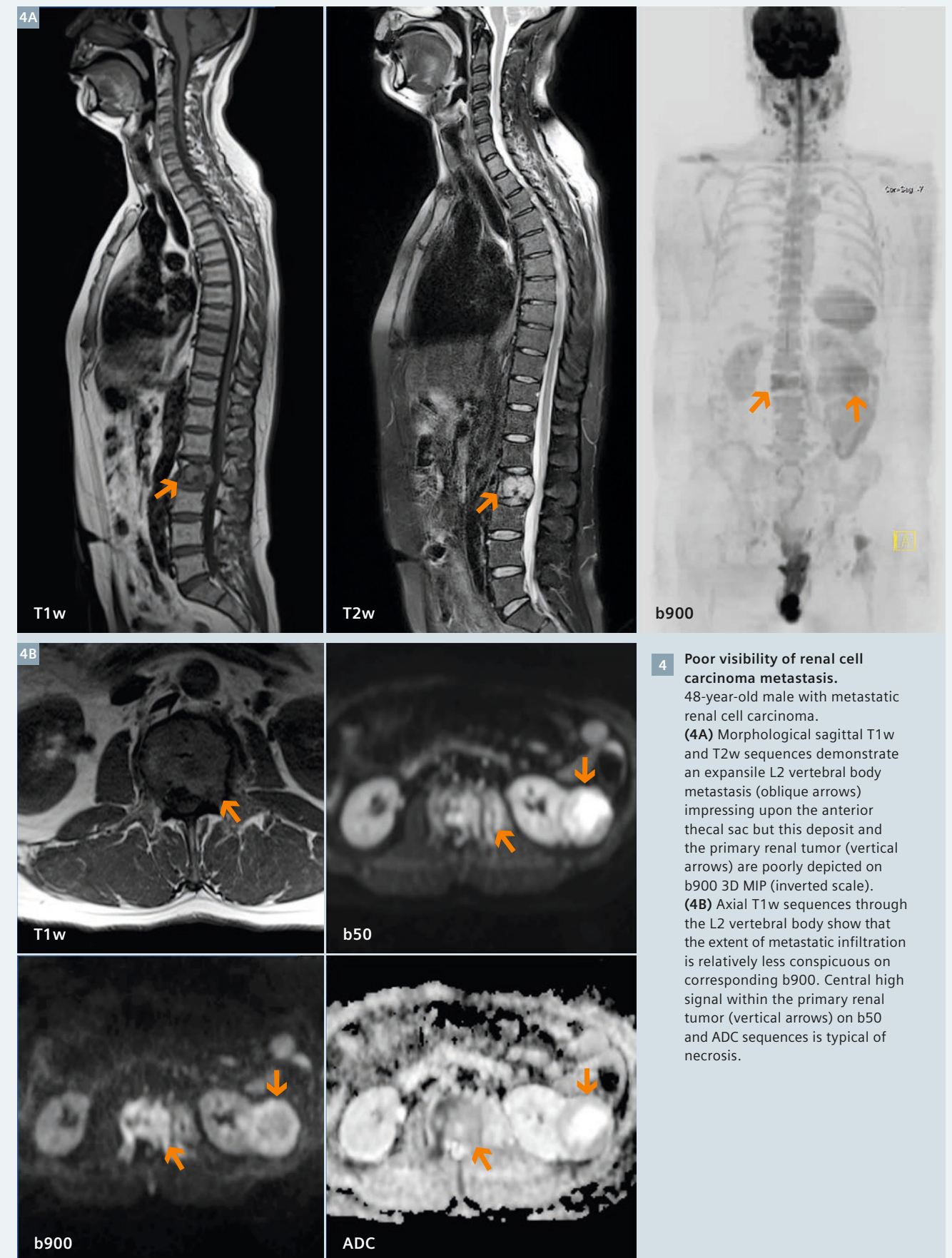
method for fat suppression uses inversion recovery because it allows uniform fat suppression over large fields-of-view [4]. An artificially 'fractured spine' observed on the post processed stitched images as a consequence of alignment mismatch can be minimized by manually adjusting and maintaining the transmitter frequency for each station. The b900 value images are reconstructed in the coronal plane (5 mm) and as thick 3D maximum intensity projections (MIPs) which are displayed using an inverted grey scale. ADC maps are computed inline with system software using mono-exponential fitting in which each voxel reflects the tissue diffusivity (units:  $\mu\text{m}^2/\text{s}$ ) (Fig. 1).

Detailed scanning parameters for each sequence have been published [4, 5]; the entire examination takes 52 minutes to complete. The illustrations of this article were obtained from more than 2,000 WB-DWI scans done at our institution in the last 4 years using this protocol.

#### Normal bone marrow signal on WB-DWI

A thorough understanding of normal bone marrow signal distribution on b900 value images is vital for the accurate detection, characterization and treatment assessment of skeletal metastases [5]. This is because the bone marrow distribution can be visu-

alized by WB-DWI. The normal adult bone marrow pattern which is established by the age of 25 years can be seen as uniformly distributed, intermediate high signal intensity distributed in the axial skeleton (mixed red bone marrow); yellow marrow in the appendicular skeleton shows no/lower signal intensity (Fig. 1). The changing distribution of the normal marrow is also exquisitely demonstrated on WB-DWI. Red marrow conversion to yellow marrow is dependent on patient age, gender and underlying medical conditions [6]. Both bone marrow hypo- and hypercellularity are well depicted on WB-DWI.



**4 Poor visibility of renal cell carcinoma metastasis.** 48-year-old male with metastatic renal cell carcinoma. (4A) Morphological sagittal T1w and T2w sequences demonstrate an expansile L2 vertebral body metastasis (oblique arrows) impressing upon the anterior thecal sac but this deposit and the primary renal tumor (vertical arrows) are poorly depicted on b900 3D MIP (inverted scale). (4B) Axial T1w sequences through the L2 vertebral body show that the extent of metastatic infiltration is relatively less conspicuous on corresponding b900. Central high signal within the primary renal tumor (vertical arrows) on b50 and ADC sequences is typical of necrosis.



The relationship between bone marrow cellularity and ADC values is non linear and highly dependent on the water, cellular and fat content of the marrow. The reduced water content [6], the larger-sized fat cells, the hydrophobic nature of fat and poorer perfusion all contribute to lower diffusion-weighted signal intensities and ADC values of the yellow bone marrow. On the other hand, with increasing cellularity and water content and greater perfusion, mixed yellow-red bone marrow returns higher signal intensities and paradoxically higher ADC values [5, 7-9].

### Skeletal metastases detection

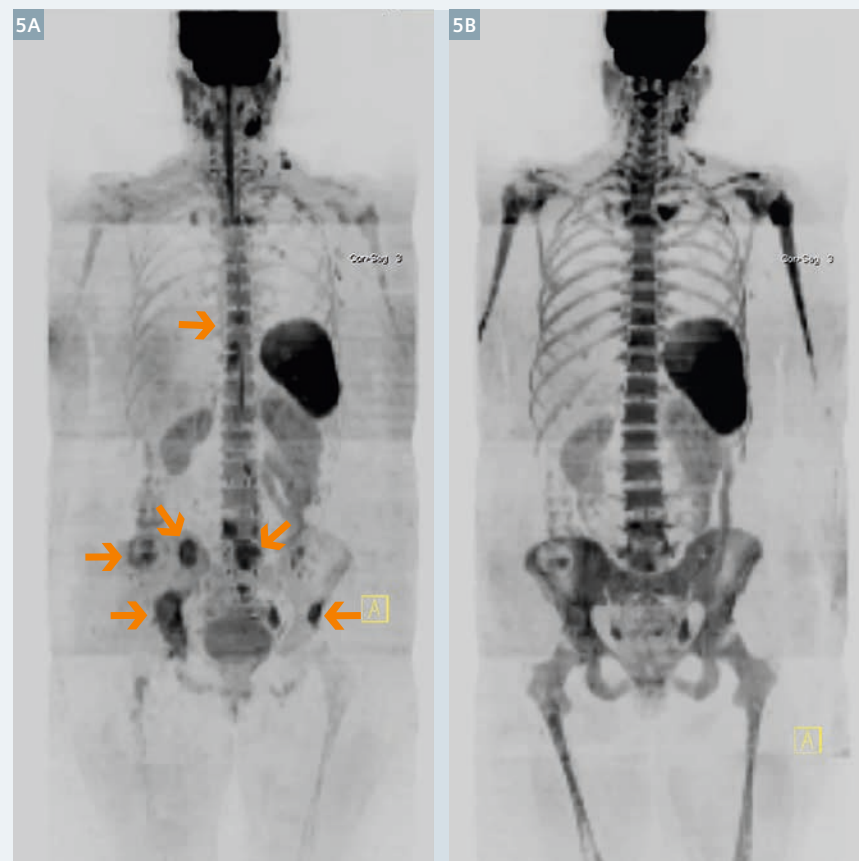
Skeletal metastases appear as focal or diffuse areas of high-signal intensity on high b-value WB-DWI (Fig. 2). The ability to detect bone marrow lesions is dependent on the intrinsic signal intensity of the deposits and the background bone marrow. Other factors determining the visibility of bone lesions include their anatomic location and treatment status. It is imperative that WB-DWI is performed and interpreted in conjunction with conventional morphological WB-MRI sequences rather than in isolation.

This is because false positive and negative lesions do occur. This assertion was highlighted by a recent meta-analysis, which demonstrated that the high sensitivity of WB-DWI to detect metastases was at the expense of specificity [1].

Generally, infiltrative cellular lesions are better detected than *de-novo* sclerotic or treated lytic/sclerotic lesions (Fig. 3). This is due to the lower water and cellular content of sclerotic and treated metastases [7, 10]. This is the likely reason for the improved visibility of bone metastases of untreated breast cancer compared to prostate cancer; *de-novo* sclerotic metastases are commoner in prostate cancer. WB-DWI is better at detecting skeletal lesions from smaller cancer cell infiltrations such as those due to breast cancer, myeloma, lymphoma and small cell cancers as well as neuroendocrine tumors. On the other hand, bony metastases from clear cell renal cancers are sometimes poorly depicted (the presence of necrosis, large sized tumor cells and inherent lipogenesis contribute to the poorer visualization) (Fig. 4). On occasion, the high magnetic field susceptibility of melanin can also impair depiction of melanoma metastases.

The detection of skeletal metastases on WB-DWI may be impaired in areas of movement such as the anterior ribs and sternum. Visibility of skull vault infiltrations can be impaired because of the adjacent high signal of the normal brain. The visibility of skull base disease is impaired because of susceptibility effects.

Other causes for false-negative findings are low levels of bone marrow infiltration such as in smoldering multiple myeloma (when plasma cell infiltration fraction is less than background cell bone marrow cellularity) or when bone marrow hyperplasia results in diffuse increase in signal on high b-value images obscures the presence of metastases [2, 5] (Fig. 5). Relative bone marrow hypercellularity is observed in children and adolescents, chronic anemia, in smokers, chronic cardiac failure, in pregnancy

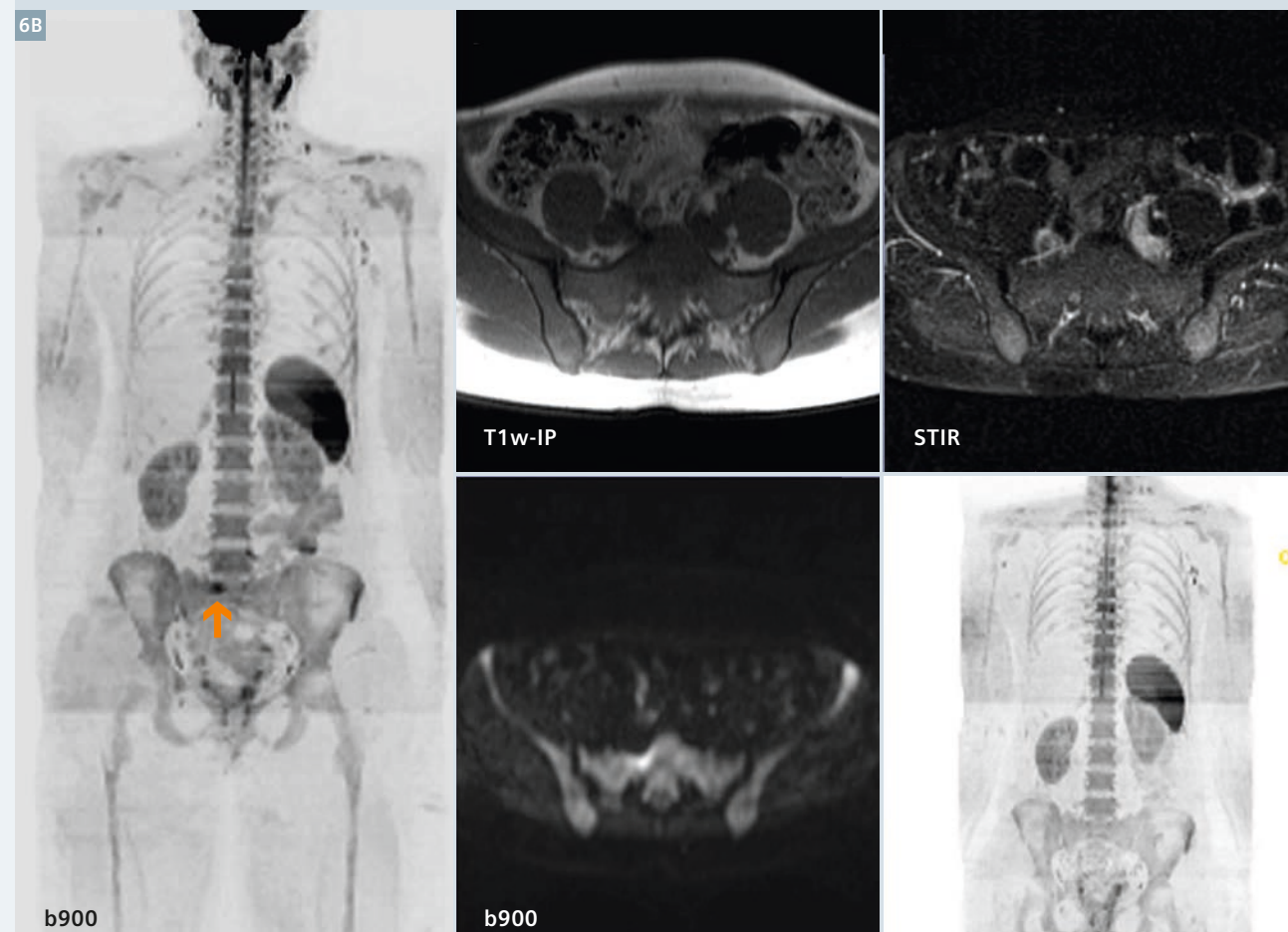


**5 Bone marrow hyperplasia induced by G-CSF therapy obscuring metastases.** 50-year-old woman with metastatic breast cancer before and after 3 cycles of erubulin chemotherapy with growth-colony stimulating factor (G-CSF) given to prevent neutropenia. b900 3D MIP (inverted scale) images. Image 5A shows multiple bone metastases (arrows). Image 5B after 3 cycles of chemotherapy shows increases in signal intensity of the bone marrow leading to the decreased visibility of the bone metastases. The splenic size has also increased. The increased signal intensity of the background bone marrow should not be misinterpreted as malignant progression.

6A



6B



### 6 False positive whole body diffusion MRI.

64-year-old female with breast cancer treated with right mastectomy, radiotherapy and chemotherapy. (6A) Bone scan shows increased uptake at L4/L5 – query metastases. (6B) Subsequent WB-DWI imaging 1 month later shows normal signal at L4/L5 with normal anatomic MRI images, but reveals a small focus of high signal intensity overlying the sacrum on b900 3D MIP (vertical arrow) and axial images. Corresponding anatomical T1w and STIR sequences show no focal abnormality within the sacrum; the high signal seen on b900 images is artifact from adjacent bowel. Note normal marrow signal on WB-DWI done eight months later (bottom right) with no development of metastases.



and in patients treated with hematopoietic growth factors such as granulocyte-colony stimulating factors (G-CSF).

Causes for false-positive findings include bone marrow edema caused by fractures, osteoarthritis, infection, bone infarcts, vertebral hemangiomas, isolated bone marrow islands and 'T2 shine through' – the latter observed in treated metastases. A variety of internal metallic (orthopedic) and silicone (breast) prostheses are routinely encountered in clinical practice. Magnetic field inhomogeneities secondary to metal and air interfaces will cause artifacts that cause false positive lesions (Fig. 6) and at the same time may obscure metastatic lesions in the adjacent bones. Many of these false-positive findings can be identified as not representing metastases by correlating the appearances of DW images with corresponding ADC maps and anatomical sequences [5].

## Conclusions

WB-DWI is a contemporary imaging technique serving as an adjunct to conventional morphological whole body MRI, with high intrinsic sensitivity for detecting skeletal bone marrow metastases. However, there are several pitfalls that are encountered in routine clinical practice, the majority of which can be overcome by judicious interpretation of images in conjunction with standard anatomical sequences in light of relevant clinical knowledge.

## References

- 1 Wu LM, Gu HY, Zheng J, et al. Diagnostic value of whole-body magnetic resonance imaging for bone metastases: a systematic review and meta-analysis. *J Magn Reson Imaging* 2011;34:128-135.
- 2 Padhani AR, Gogbashian A. Bony metastases: assessing response to therapy with whole-body diffusion MRI. *Cancer Imaging* 2011;11 Spec No A:S129-145.
- 3 Padhani AR. Diffusion magnetic resonance imaging in cancer patient management. *Semin Radiat Oncol* 2011;21:119-140.
- 4 Koh DM, Blackledge M, Padhani AR, et al. Whole-Body Diffusion-Weighted MRI: Tips, Tricks, and Pitfalls. *AJR Am J Roentgenol* 2012;199:252-262.
- 5 Padhani AR, Koh DM, Collins DJ. Whole-body diffusion-weighted MR imaging in cancer: current status and research directions. *Radiology* 2011;261:700-718.
- 6 Hwang S, Panicek DM. Magnetic resonance imaging of bone marrow in oncology, Part 1. *Skeletal Radiol* 2007;36:913-920.
- 7 Messiou C, Collins DJ, Morgan VA, Desouza NM. Optimising diffusion weighted MRI for imaging metastatic and myeloma bone disease and assessing reproducibility. *Eur Radiol* 2011;21:1713-1718.
- 8 Hillengass J, Bauerle T, Bartl R, et al. Diffusion-weighted imaging for non-invasive and quantitative monitoring of bone marrow infiltration in patients with monoclonal plasma cell disease: a comparative study with histology. *Br J Haematol* 2011;153:721-728.
- 9 Nonomura Y, Yasumoto M, Yoshimura R, et al. Relationship between bone marrow cellularity and apparent diffusion coefficient. *J Magn Reson Imaging* 2001;13:757-760.
- 10 Eiber M, Holzapfel K, Ganter C, et al. Whole-body MRI including diffusion-weighted imaging (DWI) for patients with recurring prostate cancer: Technical feasibility and assessment of lesion conspicuity in DWI. *J Magn Reson Imaging* 2011;33:1160-1170.

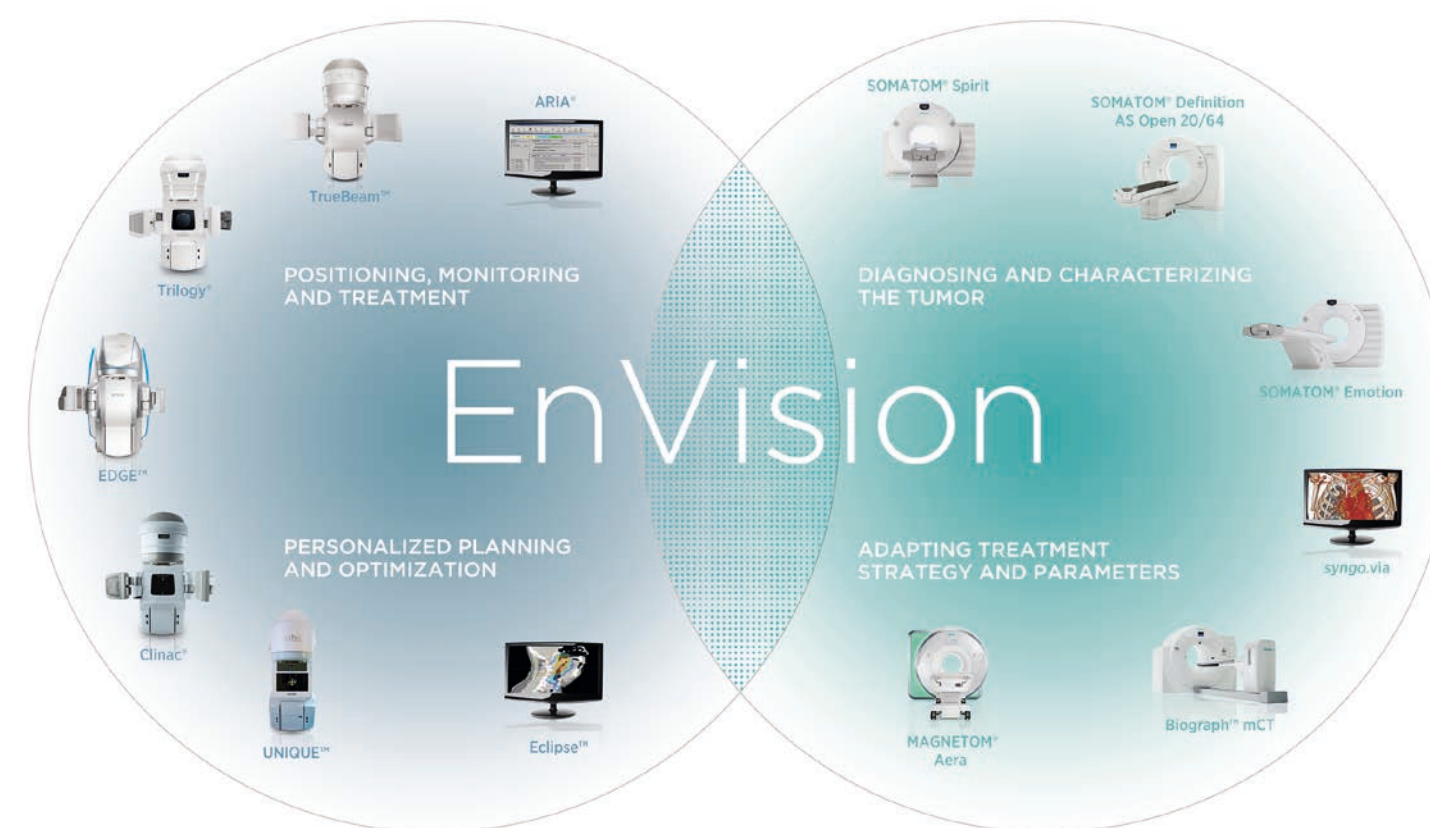


## Contact

Professor Anwar R. Padhani,  
MB BS, FRCP, FRCR  
Paul Strickland Scanner Centre  
Mount Vernon Cancer Centre  
Rickmansworth Road  
Northwood  
Middlesex HA6 2RN  
United Kingdom  
Phone: +44 (0) 1923-844751  
Fax: +44 (0) 1923-844600  
anwar.padhani  
@stricklandscanner.org.uk

## TOGETHER WE MOVE FORWARD IN THE FIGHT AGAINST CANCER

When two leading companies join forces in the fight against cancer, it broadens the realm of what's possible. That's why Varian and Siemens have partnered. Siemens' advanced diagnostic imaging capabilities coupled with Varian's powerful delivery systems and treatment planning tools give even more of an edge in the pursuit of our common goal: to **EnVision better cancer care**. Together we offer more personalized treatment and expanded care options that aid you in making the best possible decisions for your patients—with confidence. By gathering our strengths, we have the energy and vision to better help healthcare professionals detect, diagnose and treat cancer while paving the way for the future of cancer care.



**VARIAN**  
medical systems

**SIEMENS**  
Strategic Partner  
of Varian for  
Radiation Therapy

© 2013 Varian, Varian Medical Systems, Trilogy, and ARIA are registered trademarks, and TrueBeam, Edge Radiosurgery and Eclipse are trademarks of Varian Medical Systems, Inc. All other trademarks are property of Siemens AG.

Varian Medical Systems  
International AG  
Zug, Switzerland  
Tel: +41-41 749 88 44  
Fax: +41-41 740 33 40  
varian.com  
info.europe@varian.com

Global Siemens Healthcare  
Headquarters  
Siemens AG  
Healthcare Sector  
Henkestrasse 127  
91052 Erlangen, Germany  
Tel: +49 9131 84-0  
siemens.com/healthcare



# Case Report: Functional, Volumetric, Treatment Response Assessment Using MR OncoTreat

Susanne Bonekamp; Ihab R. Kamel

The Russell H. Morgan Department of Radiology and Radiological Science, The Johns Hopkins Hospital, Baltimore, MD, USA

## Introduction

Hepatocellular carcinoma (HCC) is one of the most common malignancies worldwide and is associated with a very low survival rate [1]. Because the majority of HCC lesions are diagnosed at an advanced stage, few patients qualify for surgical resection or liver transplantation [2]. Loco-regional treatment methods, most commonly transarterial chemoembolization (TACE), are considered the standard of care in patients with unresectable HCC [3, 4]. Response to treatment is often assessed using cross-sectional imaging. Current guidelines include EASL (European Association for the Study of Liver Disease) and modified RECIST (Response Evaluation Criteria in Solid Tumors). Both metrics rely on the measurement of viable tumor burden in a single axial plane [5, 6]. However, assessment of a single axial slice can be misleading and may have low reproducibility. Furthermore, residual enhancement assessed by contrast-enhanced MRI or CT can be difficult to evaluate owing to the presence of changes in signal intensity (hyperintensity on unenhanced T1-weighted images) related to a combination of iodized oil injection and hemorrhagic necrosis.

Several recent publications have highlighted the advantage of volumetric assessment of tumor anatomy and function as a method of response assessment. Functional volumetric assessment of diffusion-weighted MRI (DWI) using apparent diffusion coefficient (ADC) maps and post-contrast-enhancement MRI have been successfully applied in the brain and liver [7, 8]. Using a prototype software



(MR OncoTreat\*; Fig. 1) developed by Siemens Corporation; Corporate Technology, USA and Siemens Healthcare, Erlangen, Germany we have published several recent manuscripts that outline the feasibility of a volumetric, functional assessment of treatment response in patients with primary

and metastatic liver cancer [8-13]. This case report outlines the functional, volumetric analysis of response to TACE in a patient with HCC.

\* Work in progress: The product is still under development and not commercially available yet. Its future availability cannot be ensured.

## Patient history

The patient is a 61-year-old male with a history of hepatitis B, liver cirrhosis, and hepatocellular carcinoma. After diagnosis of a large lesion in the liver (14 cm in diameter) on CT imaging, he underwent one session of hepatic artery chemoembolization to the right lobe of the liver. MR imaging was performed one day before TACE to more accurately assess the lesion. Follow-up MRI was done one month after TACE.

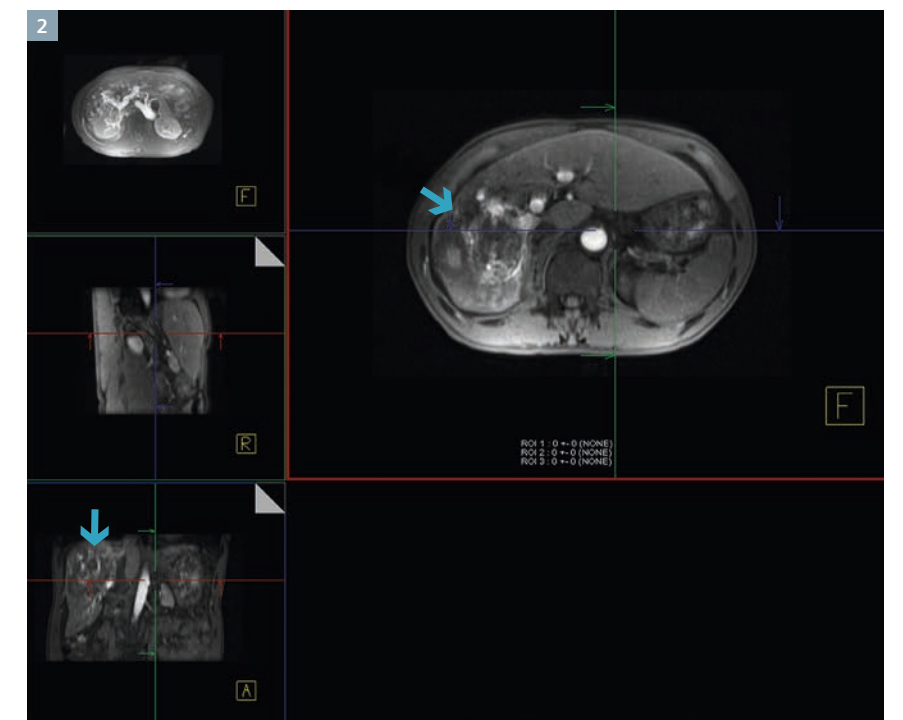
## Sequence details

All images have been acquired on a 1.5T MAGNETOM Avanto (Siemens Healthcare, Erlangen, Germany). The patient underwent our standardized clinical imaging protocol. Which included breath-hold diffusion-weighted echo planar images (matrix, 128 × 128; slice thickness 8 mm; interslice gap, 2 mm; b-value, 0 s/mm<sup>2</sup>, 750 s/mm<sup>2</sup>; repetition time (TR) 3000 ms; echo time (TE) 69 ms; received bandwidth 64 kHz) as well as breath-hold unenhanced and contrast-enhanced (0.1 mmol/kg intravenous gadobenate dimeglumine; Multihance; Bracco Diagnostics, Princeton, NJ, USA) T1-weighted three-dimensional fat suppressed spoiled gradient-echo images (field-of-view 320–400 mm; matrix 192 × 160; slice thickness 2.5 mm; TR 5.77 ms; TE 2.77 ms; received bandwidth 64 kHz; flip angle 10°) in the hepatic arterial phase (AE) (20 s), and portal venous phase (VE) (70 s).

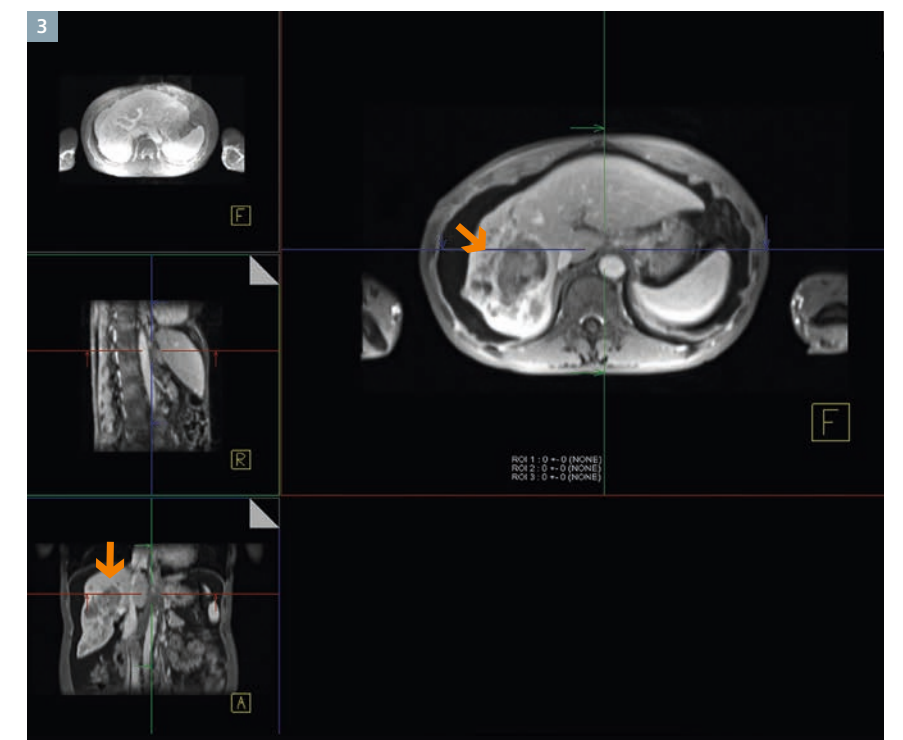
## Volumetric functional MRI response

Image analysis was performed by an MRI researcher (S.B.) with 8 years experience in MR imaging using proprietary, non-FDA approved software, MR OncoTreat (Siemens Healthcare, Erlangen, Germany). A single, treated HCC index lesion was selected as the representative index lesion for the patient. Figure 2 shows the arterial phase images of the lesion (arrow) before treatment. Figure 3 shows the same lesion after treatment.

Lesion segmentation is shown in figure 4 (pre-treatment) and figure 5

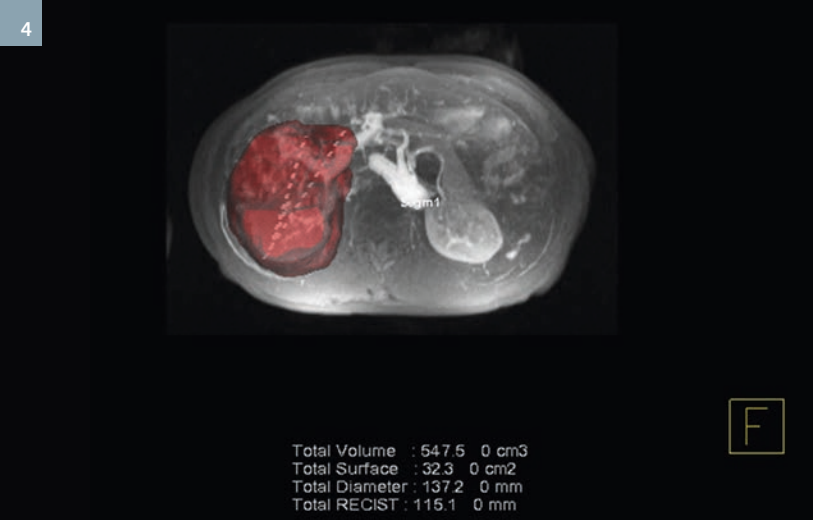


2 Arterial phase images of a liver with a large heterogeneously enhancing HCC lesion (arrows) in a 61-year-old male with a history of hepatitis B before loco-regional therapy.

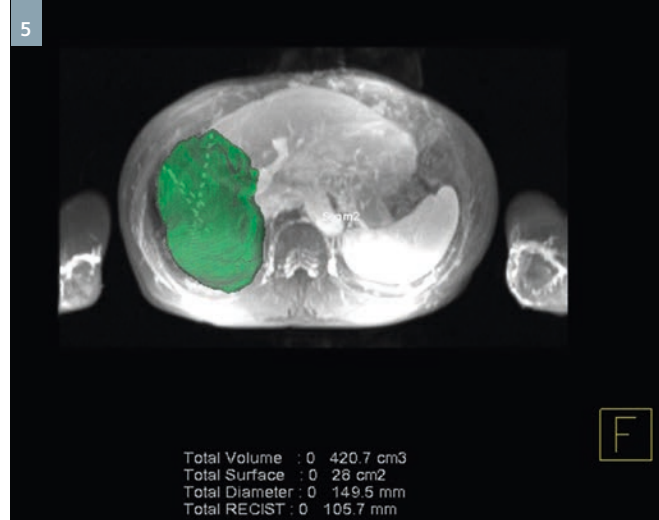


3 Arterial phase images of a liver with a large heterogeneously enhancing HCC lesion (arrows) of the same patient after loco-regional therapy.

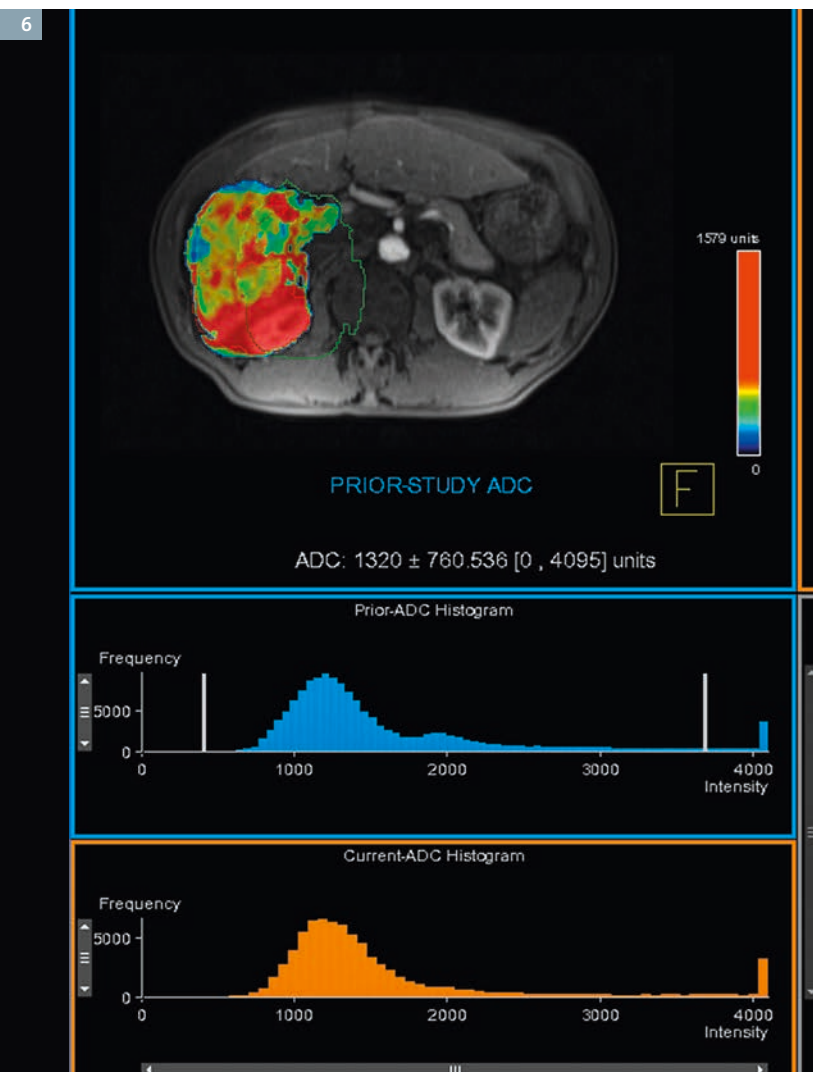




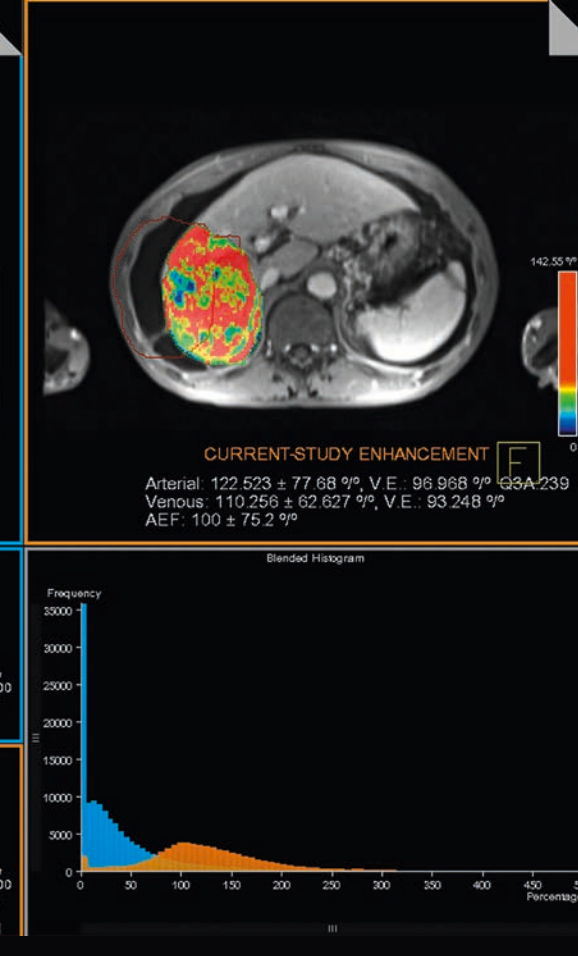
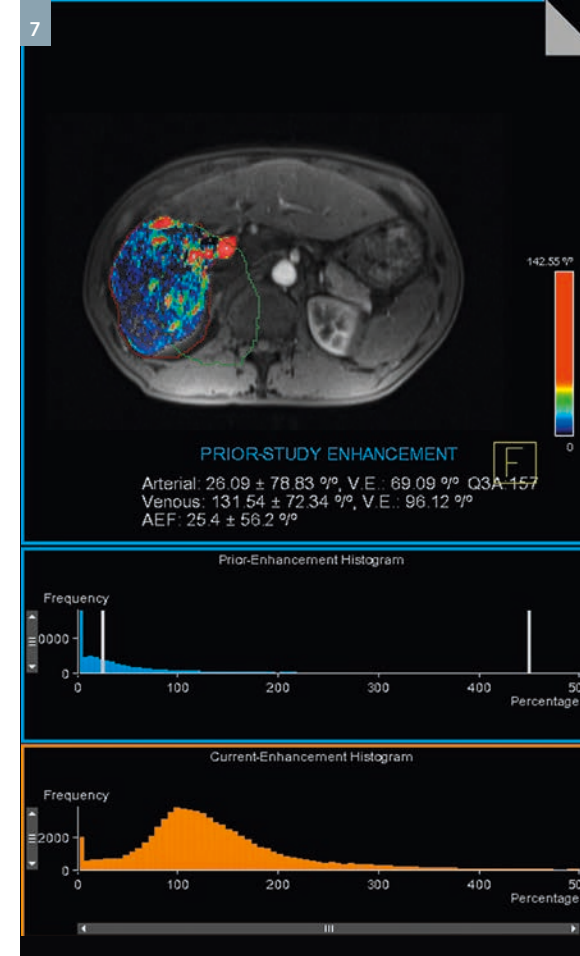
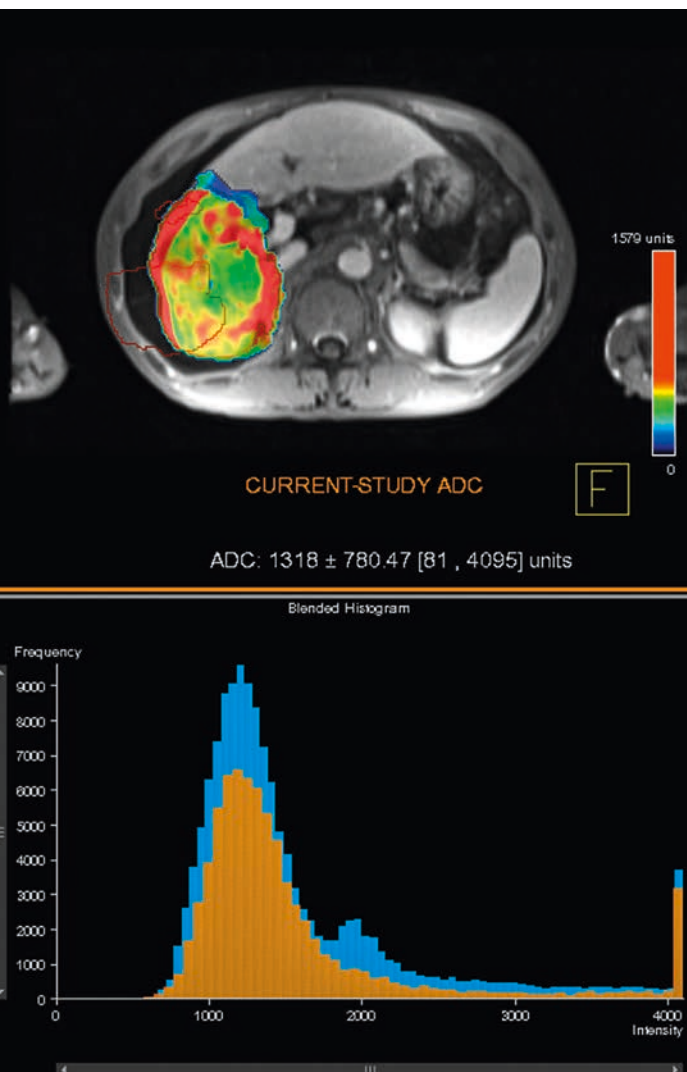
4 Segmentation of the HCC lesion before treatment performed using seed placement and 'Random Walker', a semi-automatic 3D segmentation technique.



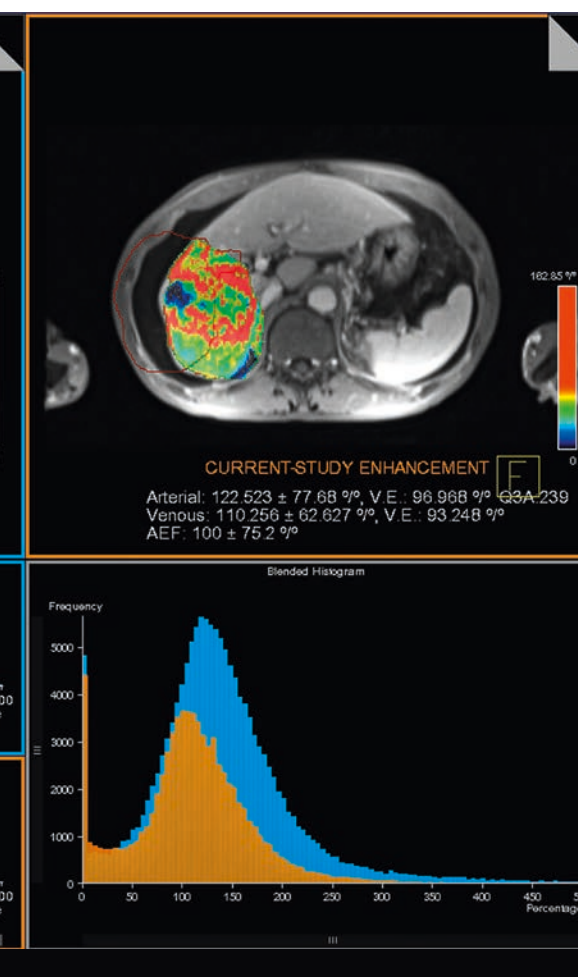
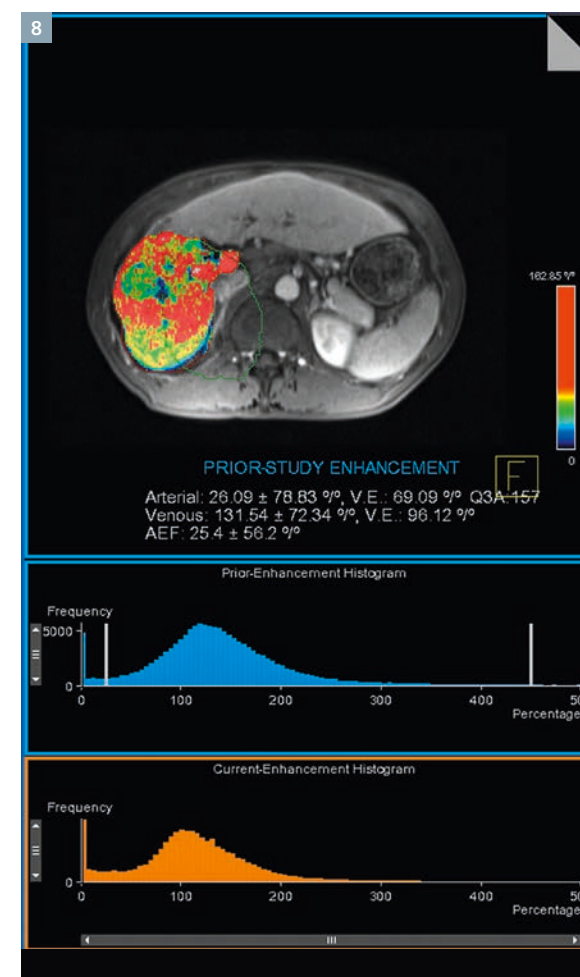
5 Segmentation of the HCC lesion after treatment performed using seed placement and 'Random Walker', a semi-automatic 3D segmentation technique. No co-registration of the HCC lesion was performed due to the change in size and structure.



6 Comparison of the ADC values before and after TACE within the entire segmented tumor volume. The upper left window and the blue histogram show the heterogeneous distribution of ADC values before treatment, the upper right window and the orange histogram show the distribution of ADC values after treatment. The window in the lower left shows an overlay of the pre- and post-treatment ADC values and their distribution, allowing for easy visual assessment of treatment induced changes in ADC.



7 Comparison of the arterial enhancement (AE) values before and after TACE within the entire segmented tumor volume. The upper left window and the blue histogram show the heterogeneous distribution of AE values before treatment, the upper right window and the orange histogram show the distribution of AE values after treatment. The window in the lower left shows an overlay of the pre- and post-treatment AE values and their distribution, allowing for easy visual assessment of treatment induced changes in AE.



8 Comparison of the portal venous enhancement (VE) values before and after TACE within the entire segmented tumor volume. The upper left window and the blue histogram show the heterogeneous distribution of VE values before treatment, the upper right window and the orange histogram show the distribution of VE values after treatment. The window in the lower left shows an overlay of the pre- and post-treatment VE values and their distribution, allowing for easy visual assessment of treatment induced changes in VE.



(post-treatment). The software automatically generated tumor diameter, tumor volume, volumetric ADC and volumetric enhancement in the arterial (AE) and portal venous phase (VE).

ADC maps were reconstructed using a monoexponential fit between two b-values of 0 and 750 s/mm<sup>2</sup>. Figure 6 depicts a comparison of the ADC values of the pre-treatment lesion (segment 1), along with the pre-treatment ADC histogram in blue, and the post-treatment lesion (segment 2), with the post-treatment ADC histogram in orange.

For the assessment of treatment response the percent change in volumetric tumor ADC at follow-up compared with baseline values can be calculated using the formula  $\{(ADC_{post} - ADC_{pre})/ADC_{pre}\} \times 100$ , where  $ADC_{pre}$  is the mean baseline volumetric ADC value and  $ADC_{post}$  is the mean follow up volumetric ADC value.

Enhancement in the portal venous phase was calculated by subtracting the native phase signal intensity from the venous phase signal intensity multiplied by 100 to obtain percentage change. Similar to the ADC results, figures 7 (AE) and 8 (VE) show a comparison of the pre-treatment enhancement values (segment 1, blue histogram) compared to the post-treatment enhancement values (segment 2, orange histogram).

Again, for the assessment of response to treatment the percent change in volumetric tumor AE or VE at follow up compared with baseline values can be calculated using the formula  $\{(E_{post} - E_{pre})/E_{pre}\} \times 100$ , where  $E_{pre}$  represents the mean baseline volumetric enhancement value and  $E_{post}$  represents the mean 3–4 weeks follow up volumetric enhancement value.

## Diagnosis

Figures 4–8 show the large, heterogeneously enhancing HCC lesion before and after treatment. ADC values did not change significantly after TACE (1.320 × 10<sup>-3</sup> mm<sup>2</sup>/s to 1.318 × 10<sup>-3</sup> mm<sup>2</sup>/s, fig. 6). Enhancement values in the hepatic arterial phase were highly variable with

a standard deviation of 79% and increased after treatment (26.09% to 122.52%, fig. 7), while portal venous enhancement was also highly variable (standard deviation of 72%) and showed a slight decrease after TACE (131.54% to 110.26%, fig. 8). Together these functional parameters indicate that the lesion did not respond to treatment. The patient subsequently underwent treatment with doxorubicin eluting microspheres (DEB-TACE) which resulted in a more favorable outcome than the initial TACE.

## Conclusion

The case shows how functional, volumetric analysis of MR imaging data using MR Oncotreat can assist diagnostic and interventional radiologist in the assessment of treatment response and planning of follow-up treatment.

## Acknowledgement

We would like to thank Atilla Kiraly, Mehmet Akif Gulsun, and Li Pan (Siemens Corporation, Corporate Technology, USA), Peter Gall and Berthold Kiefer (Siemens Healthcare, Erlangen, Germany) for the development and the help and support with the MR OncoTreat software used for image processing.

### References

- 1 Altekruse SF, McGlynn KA, Reichman ME. Hepatocellular carcinoma incidence, mortality, and survival trends in the United States from 1975 to 2005. *J Clin Oncol* 2009;27(9):1485-1491.
- 2 Jemal A, Siegel R, Xu J, Ward E. Cancer Statistics, 2010. *CA Cancer J Clin* 2010
- 3 Llovet JM, Bruix J. Systematic review of randomized trials for unresectable hepatocellular carcinoma: Chemoembolization improves survival. *Hepatology* 2003;37(2):429-442.
- 4 Camma C, Schepis F, Orlando A, et al. Transarterial chemoembolization for unresectable hepatocellular carcinoma: meta-analysis of randomized controlled trials. *Radiology* 2002;224(1):47-54.
- 5 Suzuki C, Jacobsson H, Hatschek T, et al. Radiologic measurements of tumor response to treatment: practical approaches and limitations. *Radiographics* 2008;28(2):329-344.

- 6 Suzuki C, Torkzad MR, Jacobsson H, et al. Interobserver and intraobserver variability in the response evaluation of cancer therapy according to RECIST and WHO-criteria. *Acta Oncol* 2010;49(4):509-514.
- 7 Moffat BA, Chenevert TL, Lawrence TS, et al. Functional diffusion map: a non-invasive MRI biomarker for early stratification of clinical brain tumor response. *Proc Natl Acad Sci U S A* 2005;102(15):5524-5529.
- 8 Bonekamp S, Jolepalem P, Lazo M, Gulsun MA, Kiraly AP, Kamel IR. Hepatocellular Carcinoma: Response to TACE Assessed with Semiautomated Volumetric and Functional Analysis of Diffusion-weighted and Contrast-enhanced MR Imaging Data. *Radiology* 2011;260(3):752-761.
- 9 Bonekamp S, Li Z, Geschwind JF, et al. Unresectable Hepatocellular Carcinoma: MR Imaging after Intraarterial Therapy. Part I. Identification and Validation of Volumetric Functional Response Criteria. *Radiology* 2013.
- 10 Bonekamp S, Halappa VG, Geschwind JF, et al. Unresectable Hepatocellular Carcinoma: MR Imaging after Intraarterial Therapy. Part II. Response Stratification Using Volumetric Functional Criteria after Intraarterial Therapy. *Radiology* 2013.
- 11 Gowdra Halappa V, Corona-Villalobos CP, Bonekamp S, et al. Neuroendocrine Liver Metastasis Treated by Using Intraarterial Therapy: Volumetric Functional Imaging Biomarkers of Early Tumor Response and Survival. *Radiology* 2012.
- 12 Halappa VG, Bonekamp S, Corona-Villalobos CP, et al. Intrahepatic cholangiocarcinoma treated with local-regional therapy: quantitative volumetric apparent diffusion coefficient maps for assessment of tumor response. *Radiology* 2012;264(1):285-294.
- 13 Li Z, Bonekamp S, Halappa VG, et al. Islet cell liver metastases: assessment of volumetric early response with functional MR imaging after transarterial chemoembolization. *Radiology* 2012;264(1):97-109.

## Contact

Ihab R. Kamel, M.D., Ph.D.  
The Johns Hopkins Hospital  
Department of Radiology  
600 N. Wolfe St, MRI 143  
Baltimore, MD 21287  
USA  
Phone: +1 410-955-4567  
ikamel@jhmi.edu

# Optimizing MRI for Radiation Oncology: Initial Investigations

James Balter<sup>1</sup>; Yue Cao<sup>1</sup>; Hesheng Wang<sup>1</sup>; Ke Huang<sup>1</sup>; Shu-Hui Hsu<sup>1</sup>; Martin Requardt<sup>2</sup>; Steven M. Shea<sup>3</sup>

<sup>1</sup> Department of Radiation Oncology, University of Michigan, Ann Arbor, MI, USA

<sup>2</sup> Siemens Healthcare, Erlangen, Germany

<sup>3</sup> Siemens Corporation, Corporate Technology, Baltimore, USA

## Introduction

The superior soft tissue contrast, as well as potential for probing molecular composition and physiological behavior of tumors and normal tissues and their changes in response to therapy, makes MRI a tempting alternative to CT as a primary means of supporting the various processes involved in radiation therapy treatment planning and delivery. Obvious examples of the benefit of MRI over CT include target delineation of intracranial lesions, nasopharyngeal lesions, normal critical organs such as the spinal cord, tumors in the liver, and the boundaries of the prostate gland and likely cancerous regions within the prostate gland. For brachytherapy planning for cervical cancer, a recent GEC-ESTRO report directly recommends a change from traditional point-based prescriptions based primarily on applicator geometry, to

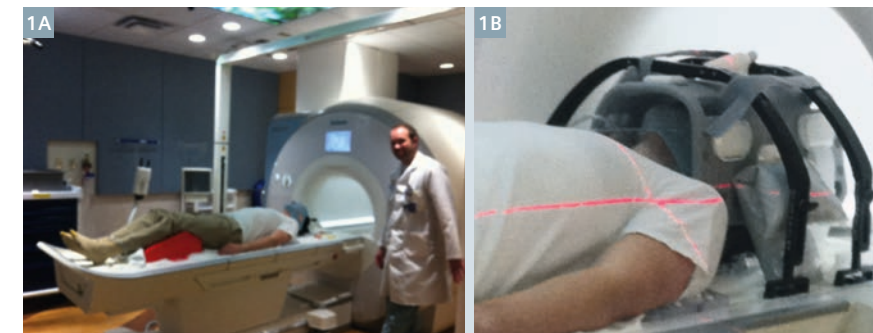
volumetric treatment plans and prescriptions aided by soft tissue visualization, specifically improved by the use of MRI. MRI-based maps of diffusion and perfusion have demonstrated potential for predicting therapeutic outcome for tumors as well as normal tissues, and current clinical trials seek to validate their roles and performance as a means to individualize therapy to improve outcomes (minimize toxicity and improve local tumor control). In addition to these advantages, MRI has been initially investigated as a means to better map the movement and deformation of organs over time and due to physiological processes such as breathing.

The historically accepted challenges in using MRI for primary patient modeling in radiation oncology have included distortion, lack of electron density information, and lack of

integrated optimized systems to scan patients immobilized in treatment configuration.

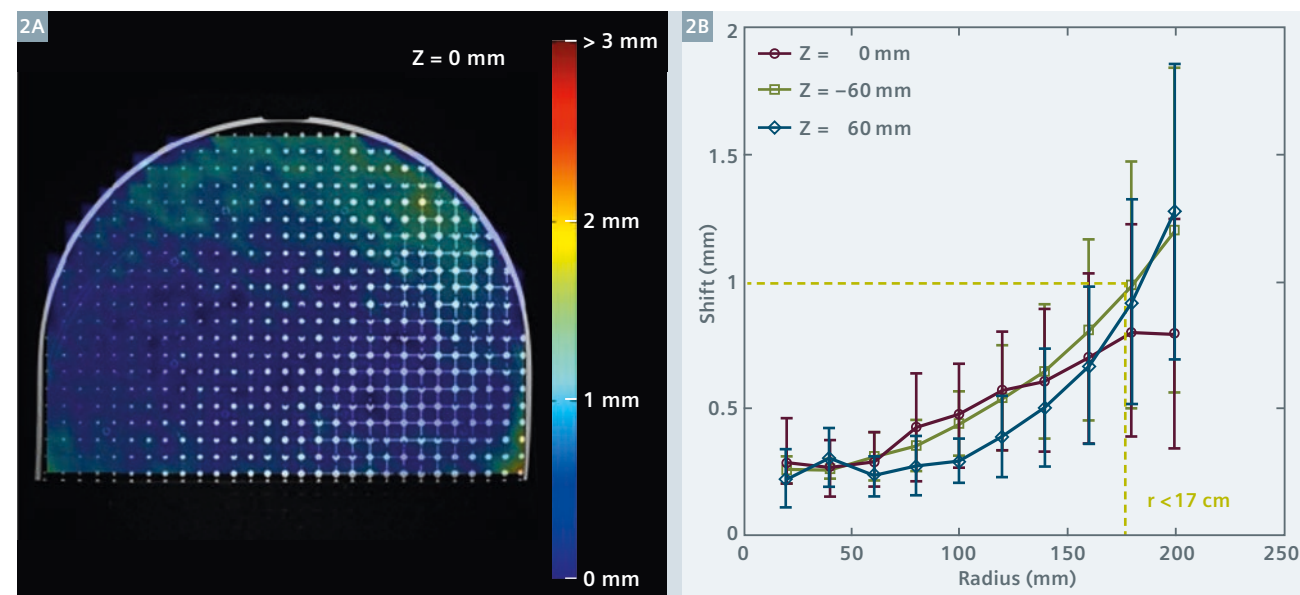
## MRI ‘simulator’ system

Over the past several years, we have investigated the feasibility of MRI systems to function in the same roles that CT scanners have for the past 10–15 years, that is as primary tools for patient modeling for radiation therapy. These efforts have accelerated in the past years with the installation of a dedicated MRI ‘simulator’ at the University of Michigan, based on a 3T wide-bore scanner (MAGNETOM Skyra, Siemens Healthcare, Erlangen, Germany), outfitted with a laser marking system (LAP, Lueneburg, Germany) and separate detachable couch tops supporting brachytherapy and external beam radiation therapy applications.



**1** MRI simulation system shows a volunteer in position for initial setup wearing a customized face mask (1A). Close-up view of anterior coil setup and crosshairs from laser marking system (1B).





2 Colorwash of measured distortion through an axial plane of the distortion phantom (2A). Magnitude of distortion-induced shifts in circles of increasing radius from the bore center in axial planes at the center and  $\pm 6$  cm along the bore (2B).

The process of integrating MRI into the standard workflow of radiation oncology requires attention be paid to a number of specific areas of system design and performance. In our instance, we chose a system that could potentially support both external beam therapy as well as brachytherapy. The brachytherapy requirement played a specific role in some of our design choices. As the high-dose-rate (HDR) brachytherapy system was housed in a room across the hall from the MRI suite, a room design was created that permitted the direct transfer of patients from MRI scanning to treatment. Typically brachytherapy treatment has involved transferring patients to and from imaging systems, a process that could potentially influence the treatment geometry and changes the dose delivered away from that planned. Treating a patient directly without moving them has significant advantages for geometric integrity as well as patient comfort. To facilitate such treatments, a detachable couch was chosen as part of the magnet specifications, and two such couches were specifically purchased to support simultaneous treatment of patients on the couch used for MRI scanning and scanning of other patients for subsequent external beam treatments.

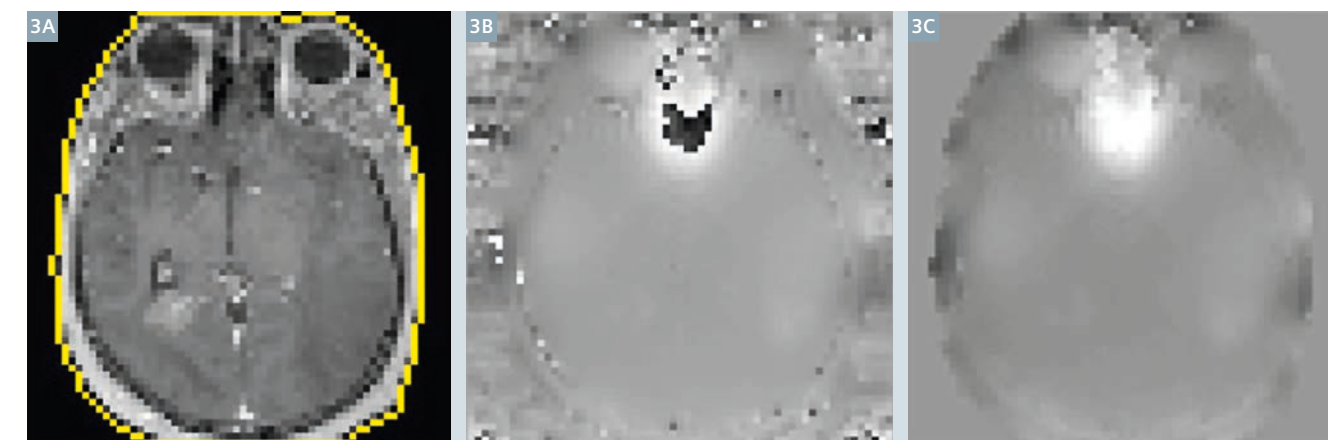
To support external beam radiotherapy, patients need to be scanned in positions and configurations that can be reproduced at treatment. In addition to necessitating a wide bore MRI scanner, an indexed flat table top insert was purchased from a company that specializes in radiation therapy immobilization systems (Civco, Kalona, IA, USA). A number of immobilization accessories were customized for use in the MRI environment, most notably a head and neck mask attachment system. To support high quality scanning of patients in treatment position without interfering with their configuration for treatment, a series of attachments to hold surface coils (primarily 18-channel body coils) relatively close to the patient without touching are used.

### Initial commissioning and tests

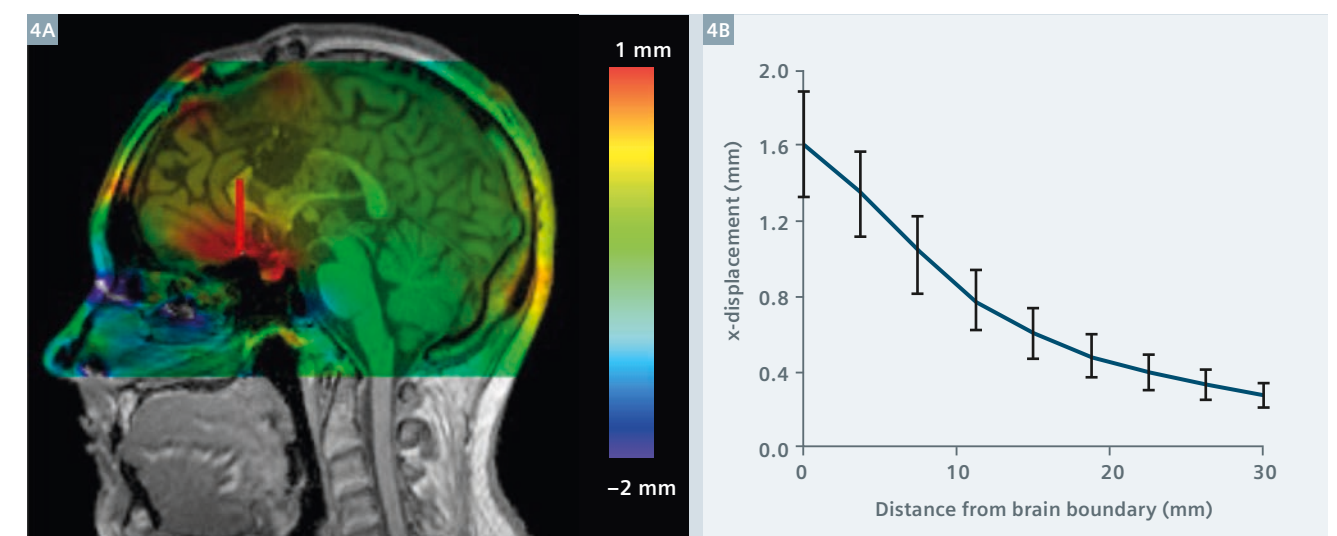
To commission the system, a number of tests were performed in addition to the standard processes for MRI acceptance and quality assurance. The laser system was calibrated to the scanner coordinates through imaging of a phantom with externally visible laser alignment markings and internal MRI-identifiable coordinates

indicating the nominal laser intersection, and end-to-end tests were performed on phantoms and volunteers to establish the accuracy of isocenter marking using MRI scans as a source of input.

To characterize system-level distortion, a custom phantom was developed to fill the bore of the magnet (with perimeter space reserved for testing the 18-channel body coil if desired). The resulting phantom was a roughly cylindrical section with a sampling volume measuring 46.5 cm at the base, with a height of 35 cm, and a thickness of 16.8 cm. This sampling volume was embedded with a three-dimensional array of interconnected spheres, separated by 7 mm center-to-center distances. The resulting system provided a uniform grid of 4689 points to sample the local distortion. The phantom was initially scanned using a 3D, T1-weighted, spoiled gradient echo imaging sequence (VIBE, TR 4.39 ms and TE 2.03 ms, bandwidth 445 Hz/pixel) to acquire a volume with field-of-view of  $500 \times 500 \times 170$  mm with a spatial resolution of  $0.98 \times 0.98 \times 1$  mm. Standard 3D shimming was used for scanning, and 3D distortion correction was applied to the images prior



3 T1-weighted image with external contour delineated as a mask (3A). The  $B_0$  inhomogeneity map acquired from this subject (3B) was unwrapped within the boundaries of the mask, yielding the resulting distortion map (3C). Reprinted with permission from Wang H, Balter J, Cao Y. Patient-induced susceptibility effect on geometric distortion of clinical brain MRI for radiation treatment planning on a 3T scanner. *Phys Med Biol* 58(3):465-77, 2013.



4 Colorwash of distortion-induced displacements through a sagittal plane of a subject (4A). Analysis of displacements along a line moving away from the sinus (red line in fig. 4A) shows the falloff of distortion due to susceptibility differences as a function of distance from the interface (4B). Reprinted with permission from Wang H, Balter J, Cao Y. Patient-induced susceptibility effect on geometric distortion of clinical brain MRI for radiation treatment planning on a 3T scanner. *Phys Med Biol* 58(3):465-77, 2013.

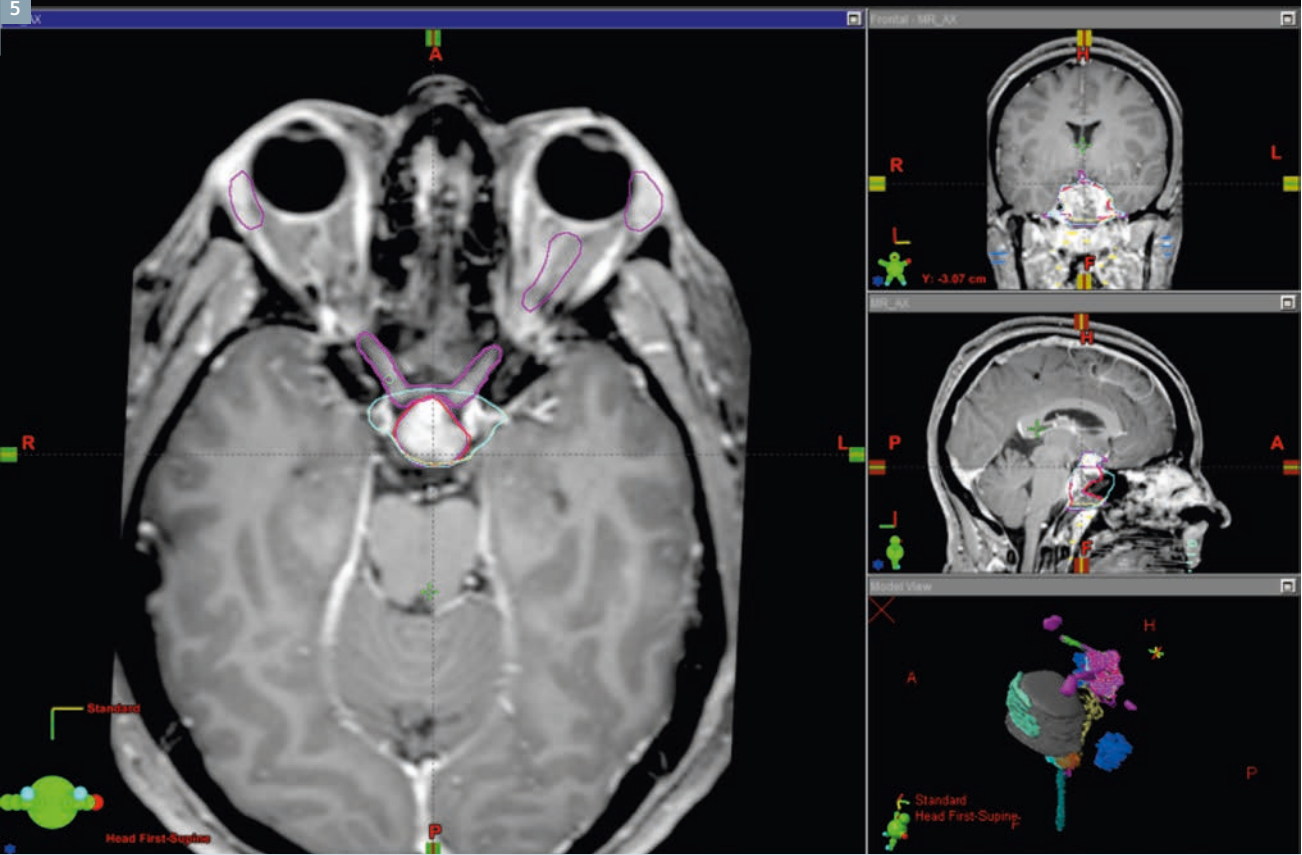
to analysis. For this initial test, the body coil integrated into the magnet was used. Automated analysis of the images localized the sphere centers, yielding a deformation vector field that described the influence of system-level distortion on the measured sphere locations. This initial test demonstrated the accuracy of coordinate mapping via this scanning protocol, with average 3D distortions of less than 1 mm at radii of up to 17 cm in planes through the bore center

as well as  $\pm 6$  cm along the bore length. Of note, scanning was performed using the syngo MR D11 software version. Future tests will be performed on the syngo MR D13 release.

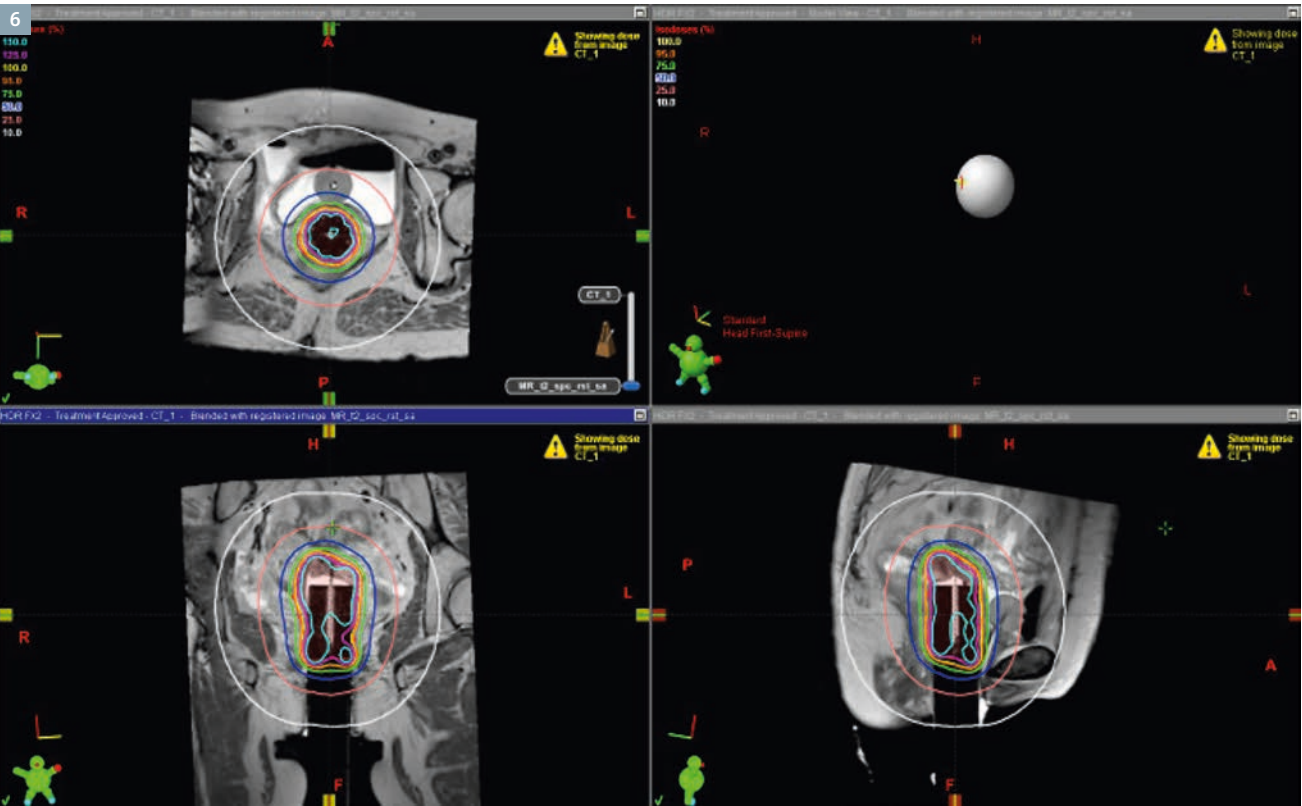
To begin to assess the impact of subject-induced susceptibility on distortions,  $B_0$  inhomogeneity maps were acquired during routine patient scanning and analyzed (for 19 patients) under an IRB-approved protocol.

These maps were acquired using a 2D, double-echo, spoiled gradient echo sequence (GRE field mapping TE<sub>1</sub> 4.92 ms, TE<sub>2</sub> 7.38 ms, TR 400 ms, flip angle 60 degrees, voxel size  $3.5 \times 3.5 \times 3.75$  mm), masked by the boundaries of the head acquired from T1-weighted images, and unwrapped using an algorithm from the Oxford Center for Functional Magnetic Resonance Imaging of the Brain [1]. The resulting maps showed homogeneity





5 Post-contrast T1-weighted images of a patient scanned in an immobilization mask using an anterior 18-channel body surface coil and a posterior 4-channel small soft coil and displayed in a radiation therapy treatment planning system (Eclipse, Varian, Palo Alto, CA, USA). Various delineated structures shown are used to guide optimization of intensity-modulated radiation therapy.



6 Display from a brachytherapy treatment planning system (Brachyvision, Varian, Palo Alto, CA, USA) showing orthogonal planes through cylindrical applicator implanted in a patient. Source locations (red dashes through the center of the applicator) are shown, as well as radiation isodose lines.

of 0.035 ppm or less over 88.5% of a 22 cm diameter sphere, and 0.1 ppm or less for 100% of this volume.

These inhomogeneity maps were applied to calculate distortions from a typical clinical brain imaging sequence (3D T1-weighted MPAGE sequence with TE 2.5 ms, Siemens TR 1900 ms, TI 900 ms, flip angle 9 degrees, voxel size  $1.35 \times 1.35 \times 0.9$  mm, frequency-encoding sampling rate of 180 Hz/pixel). On these images, 86.9% of the volume of the head was displaced less than 0.5 mm, 97.4% was displaced less than 1 mm, and 99.9% of voxels exhibited less than 2 mm displacement. The largest distortions occurred at interfaces with significant susceptibility differences, most notably those between the brain and either metal implants or (more significantly) adjacent air cavities. In the location with the largest displacement (interface with the sinus), the average displacement of 1.6 mm at the interface falls to below 1 mm approximately 7 mm away.

system is currently pending modification of part of the applicator for safety and image quality reasons, although patients undergoing other implants (e.g. cylinders) have had MRI scans to support treatment planning.

### Summary

We have implemented the initial phase of MRI-based radiation oncology simulation in our department, and have scanned over 300 patients since operations began just over one year ago. The system demonstrates sufficient geometric accuracy for supporting radiation oncology decisions for external beam radiation therapy, as well as brachytherapy. Work is ongoing in optimizing MRI scanning techniques for radiation oncology in various parts of the body and for various diseases. In addition to current and future work in optimizing MRI for use in routine radiation therapy,

a variety of research protocols are underway using this system. A major current focus is on using MRI without CT for external beam radiation therapy. Results of these efforts will be presented in future articles.

### References

- 1 Jenkinson M. Fast, automated, N-dimensional phase-unwrapping algorithm. *Magn Reson Med*. 2003 Jan;49(1):193-7.
- 2 Dimopoulos JC, Petrow P, Tanderup K, Petric P, Berger D, Kirisits C, Pedersen EM, van Limbergen E, Haie-Meder C, Pötter R. Recommendations from Gynaecological (GYN) GEC-ESTRO Working Group (IV): Basic principles and parameters for MR imaging within the frame of image based adaptive cervix cancer brachytherapy. *Radiother Oncol* 103(1):113-22, 2012.
- 3 Wang H, Balter J, Cao Y. Patient-induced susceptibility effect on geometric distortion of clinical brain MRI for radiation treatment planning on a 3T scanner. *Phys Med Biol* 58(3):465-77, 2013.

### Examples of clinical use

We have implemented a number of scanning protocols in our first year of operation. Routine scans are performed for patients with intracranial lesions of all forms, as well as for those with nasopharyngeal tumors, hepatocellular carcinoma, and certain spinal and pelvic lesions. Routine use of the system for MRI-based brachytherapy of patients with cervical cancer using a ring and tandem



### Contact

James M. Balter, Ph.D., FAAPM  
Professor and co-director,  
Physics division  
Department of Radiation Oncology  
University of Michigan  
Ann Arbor, MI  
USA  
Phone: +1(734)936-9486  
jbalter@umich.edu



# Development of MR-only Planning for Prostate Radiation Therapy Using Synthetic CT

Peter Greer, Ph.D.<sup>1</sup>; Jason Dowling, Ph.D.<sup>2</sup>; Peter Pichler, M.P.H.<sup>3</sup>; Jidi Sun, M.Sc.<sup>3</sup>; Haylea Richardson, B.Med.Rad.Sc.<sup>3</sup>; David Rivest-Henault, Ph.D.<sup>2</sup>; Soumya Ghose, Ph.D.<sup>2</sup>; Jarad Martin, M.D.<sup>1</sup>; Chris Wratten, FRANZCR<sup>1</sup>; Jameen Arm, MSc<sup>4</sup>; Leah Best, MSc<sup>4</sup>; Jim Denham, M.D.<sup>1</sup>; Peter Lau, FRANZCR<sup>4</sup>

<sup>1</sup> Calvary Mater Newcastle, Newcastle, New South Wales, Australia and University of Newcastle, Newcastle, New South Wales, Australia

<sup>2</sup> CSIRO, Australian e-Health Research Centre, Brisbane, Queensland, Australia

<sup>3</sup> Calvary Mater Newcastle, Newcastle, New South Wales, Australia

## Introduction

The department of Radiation Oncology at Calvary Mater Newcastle, treats approximately 1,800 new patients per year. When it comes to prostate treatments, MR scans are used in addition to CT for treatment planning. Having to undergo two scans however is a burden both to patients as well as the health system. We have looked into addressing this by replacing the CT by an MR-only<sup>1</sup> workflow when treating patients with prostate cancer.

## Description of the current treatment process

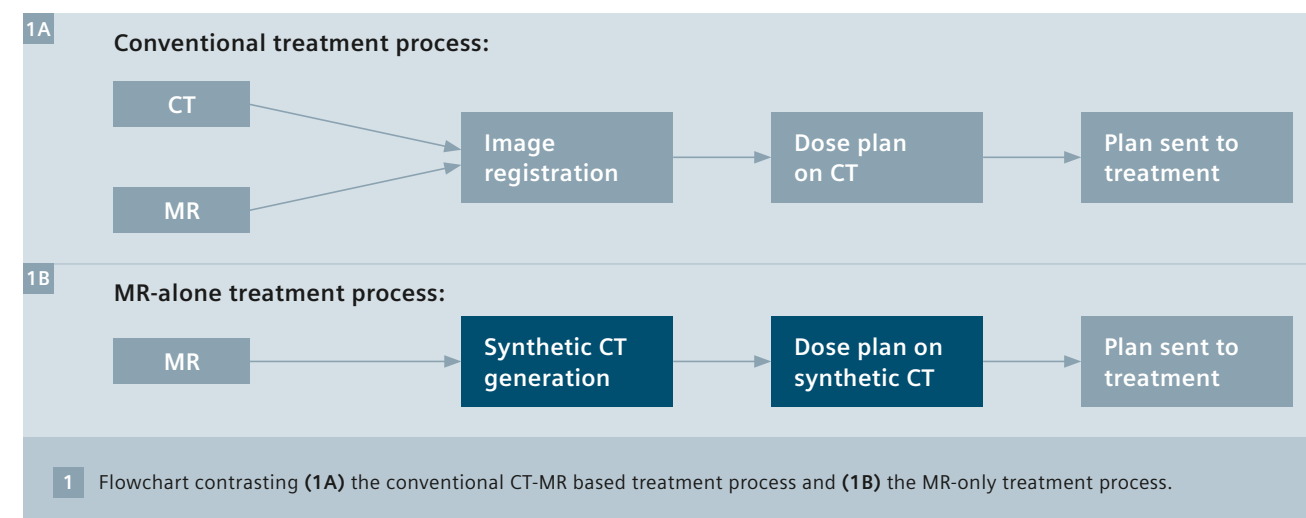
In the conventional CT based workflow the patient undergoes two imaging sessions, an MR imaging session and a CT imaging session. The MR dataset with its high soft

tissue contrast enables precise visualisation of the prostate target and adjacent rectum and bladder organs at risk, while the CT dataset provides electron density information for dose calculations. The two image sets are registered in the Varian Eclipse™ treatment planning system (TPS) and the anatomical target and normal tissue contours delineated on the MR scan are transferred to the CT scan. Dose calculation and beam definition are then performed on the CT scan. Virtual or digitally reconstructed radiographs (DRRs) are also generated from the CT scan which shows the location of implanted fiducial gold markers in the prostate relative to the beam isocenter. These are used as reference images to align the patient using orthogonal X-rays before treatment in one of our five Varian (Trilogy™ and TrueBeam™) linear accelerators.

## MR-only workflow<sup>1</sup>

The MR-only workflow differs in that the only imaging session is the MR and a synthetic CT scan is produced for dose calculations and DRR generation [1]. This workflow reduces the patient and health system burden and reduces systematic errors in treatment planning introduced by image registration uncertainties. This project is a collaboration between the clinical/academic site the Department of Radiation Oncology, Calvary Mater Newcastle and the Biomedical Imaging Research Group of the Commonwealth

<sup>1</sup> Radiotherapy Planning where MR data is the only imaging information is ongoing research. The concepts and information presented in this article are based on research and are not commercially available. Its future availability cannot be ensured.



Scientific and Industrial Research Organisation (CSIRO).

The major technical steps in the treatment process are setup and imaging of the patient in the 3T MAGNETOM Skyra suite, production of synthetic CT scans; contouring of relevant organs; beam definition and dose calculation in Eclipse; setup, image-guided positioning and treatment at the Linac.

To date 40 men with ages ranging from 58 to 78, undergoing prostate cancer radiation therapy treatment have been scanned under a research protocol. All prostate patients undergoing long fractionation treatment were eligible except that patients with hip prostheses were excluded due to distortions induced by metallic implants. Synthetic CT scans were produced for treatment planning comparisons to conventional CT based dose calculations.

Conventional MR scanning sequences are currently used for the MR-only workflow. Three sequences are used. The planning MR is a 3D, T2-weighted 1.6 mm isotropic voxel SPACE sequence with field-of-view (FOV) to cover the entire pelvis (ranging from 380-450 mm<sup>2</sup>). The prostate delineation sequence is a 2D axial T2-weighted sequence with FOV approximately 200 × 200 mm<sup>2</sup>. A further T1-weighted gradient echo sequence with flip angle 80 degrees is used to image the implanted pros-

tate fiducial markers (gold seeds 1 × 3 mm). These sequences were acquired in 12-15 minutes total with 340 s for the planning MR, 235 s for the small FOV T2 scan and 186 s for the T1 flip 80 scan. Patients were MR imaged prior to treatment as close as possible to the acquisition of the conventional planning CT scan so that dose comparisons on synthetic CT and conventional CT could be made. Although not necessary for treatment planning a further set of weekly MR scans was obtained for each patient to examine patient anatomical and dose variations. Therefore the data set consists of one MR session of three sequences for RT planning and seven MR scanning sessions of three sequences throughout the duration of treatment.

Seven field intensity modulated treatment delivery is used at our Center for prostate treatments. The treatments are delivered in 39 fractions of 2 Gy per fraction. Typical margins are 7 mm with 5 mm posteriorly.

## Simulation at the MR

The patient is positioned at MR in the treatment position. This is achieved with an MR compatible laser bridge for patient rotation alignment, a radiation therapy specific couch top and coil mounts (CIVCO, Rotterdam, The Netherlands) which

hold the coils away from the patient surface so they do not disturb the patient position. The 3T images are utilized for both delineation of the target and normal tissues using the MR patient model and for the production of the synthetic CT for dose calculation and DRRs for image-guidance at treatment.

The synthetic CT scans are created using an enhancement of our previous single atlas method [2] that combines multi-atlas deformable registration to the patient MR scan and local weighted voting to assign a CT value to each voxel of the MR planning scan. Firstly an atlas database is created in two steps:

1. A set of matching patient MR and CT planning scans are acquired;
2. The patient CT scan is deformably registered to the corresponding patient MR scan to form conjugate MR-CT pairs with matching geometry.

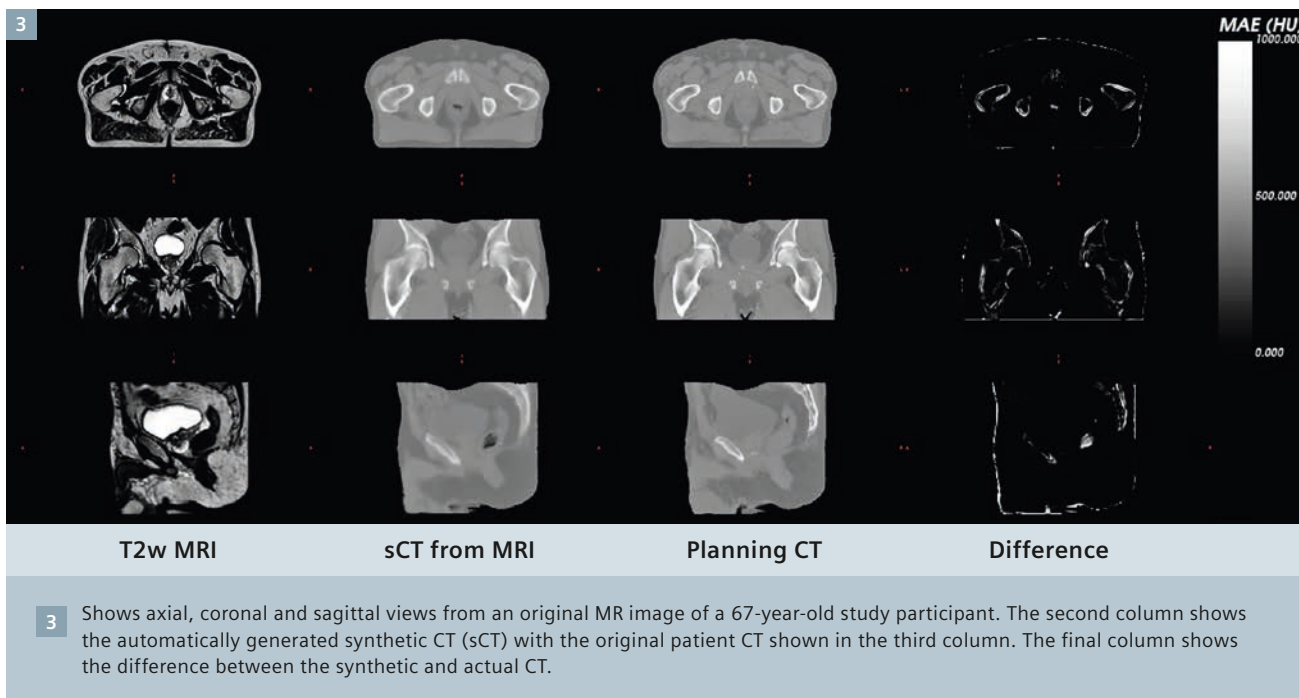
Then to create synthetic CT scans from a subsequent patient planning MR scan the following steps are used:

1. Each atlas MR scan is deformably registered to the patient planning MR scan;
2. For each small region of the patient planning MR, the intensity is compared to the same region in all the registered atlas MR scans;
3. Each atlas scan is assigned a weighting according to the similarity of the region values with the most similar having the highest weighting (all assigned weights sum to 1);
4. The CT values from the corresponding region of the conjugate CT atlas scans are added together using the previously determined weightings to provide the CT intensity value of that region of the synthetic CT scan. Methods to automatically segment both prostate and normal tissues are also being developed which will further increase treatment planning efficiency [3, 4]. The bone contours on the MR scans can be segmented very accurately with the deformable image registration method.



**2** Patient positioning for MR scanning showing the coil bridges.





## Treatment planning

The synthetic CT and MR images are imported to the Eclipse TPS with the AAA algorithm. The synthetic CT is first written to DICOM format with the header details written so that Eclipse interprets this as a CT scan for the patient. As the synthetic CT is created from the MR image data the scans are inherently registered. Target and normal tissue anatomy are delineated by the radiation oncologist on the MR scans. A treatment plan and dose calculation is then developed by the radiation therapist using the synthetic CT scan. The dose is then displayed for the radiation oncologist on the MR scan. The image guidance is performed using the Varian On-Board-Imager® and the treatment plan is delivered using the Varian Trilogy Linac.

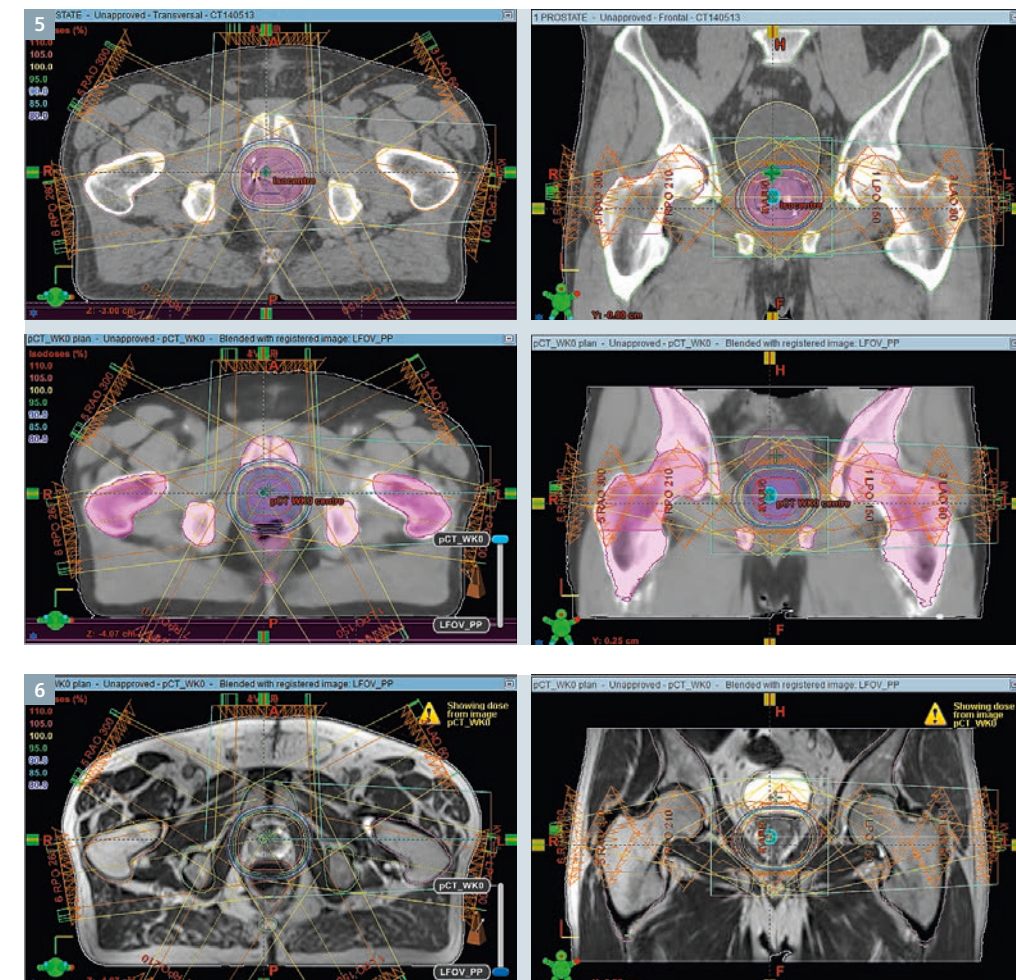
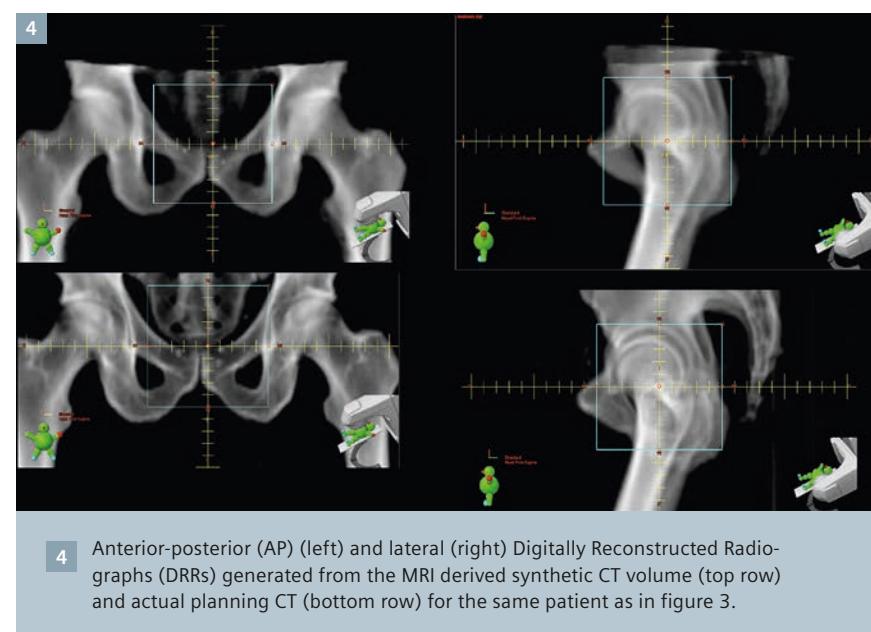
Doses calculated on the synthetic CT scans were compared to gold standard doses calculated on the conventional CT scan with an average difference of 0.3% on average. A major advantage of the technique is that it does not require specialized sequences such as ultra-short echo time sequences. Only the single 3D SPACE sequence is required for synthetic CT generation which reduces the potential for patient motion compared with multi-sequence

methods of generating synthetic CT that have been proposed [5, 6].

## Conclusion

This study has shown that synthetic CT scans can be generated from MR scans using conventional T2-weighted sequences and that dose calculations are comparable to conventional CT scan dose calculations. Investigations of MR image distortion were also performed using test phantoms. Distortions in the

region of the prostate were found to be sub-mm and distortions at the periphery were a maximum of 1.7 mm with the MAGNETOM Skyra 3D distortion correction applied. The MR-only workflow is efficient and only requires one imaging session for the patient. The next stage of our work is a prospective study where treatment will be performed using the MR-based treatment plan for a group of patients. MR-only prostate treatment planning is feasible and represents an improved process in radiation therapy planning.



## Acknowledgments

This work was supported by Cancer Council New South Wales research grant RG11-05, the Prostate Cancer Foundation of Australia (Movember Young Investigator Grant Y12011) and Cure Cancer Australia.

## References

- Greer P, Dowling J, Lambert J, Frapp J, Parker J, Denham J, et al. A magnetic resonance imaging-based workflow for planning radiation therapy for prostate cancer. *Med. J. Aust.* 2011;194:S24.
- Dowling JA, Lambert J, Parker J, Salvado O, Frapp J, Capp A, et al. An atlas-based electron density mapping method for magnetic resonance imaging (MRI)-alone treatment planning and adaptive MRI-based prostate radiation therapy. *Int. J. Radiat. Oncol. Biol. Phys.* 2012;83:e5–11.
- Dowling JA, Frapp J, Chandra S, Pluim JPW, Lambert J, Parker J, et al. Fast automatic multi-atlas segmentation of the prostate from 3D MR images. *Prostate Cancer Imaging. Image Analysis and Image-Guided Interventions.* Springer; 2011. p. 10–21.
- Chandra S, Dowling J, Shen K, Raniga P, Pluim J, Greer P, et al. Patient Specific Prostate Segmentation in 3D Magnetic Resonance Images. *IEEE Transactions on Medical Imaging.* 2012 Aug 2;31.
- Johansson A, Karlsson M and Nyholm T, CT substitute derived from MRI sequences with ultrashort echo time, *Med. Phys.* 2011;2708-2714
- Hsu, S-H, Cao Y, Huang K, Feng M, Balter JM, Investigation of a method for generating synthetic CTmodels from MRI scans of the head and neck for radiation therapy, *Phys. Med. Biol.* 2013;8419-8435.



## Contact

Peter Greer  
Principal Physicist  
Calvary Mater Newcastle  
Corner of Edith & Platt Streets  
Waratah, NSW, 2298 Australia  
Phone: +61 2 4014 3689  
peter.greer@newcastle.edu.au



## Contact

Jason Dowling  
Research Scientist  
CSIRO, Australian e-Health Research Centre  
Level 5 – UQ Health Sciences Building  
Royal Brisbane and Women's Hospital  
Herston, QLD, 4029 Australia  
Phone: +61 7 3253 3634  
Jason.Dowling@csiro.au



# Technical Aspects of MR-only Radiotherapy

Tufve Nyholm, Joakim Jonsson

Umeå University, Sweden

## Introduction

Magnetic resonance imaging (MRI) has emerged as a key component in modern radiotherapy. The superior soft tissue contrast compared to computed tomography (CT) allows for increased accuracy in the definition of both target and organs at risk [7] using commonplace sequences [29]. Functional imaging techniques, primarily diffusion-weighted imaging and dynamic contrast enhanced imaging, are currently studied as a means of identifying areas within a tumor that require a higher dose in dose-painting trials [41]. Several current studies also aim to evaluate the possibilities of early treatment response assessment using MRI [25], which could enable treatment adaptation. At present, the main rationale of integrating MRI into the radiotherapy workflow is the gain in accuracy in target volume definitions. For several major patient groups, MR imaging is preferable from a medical point of view, i.e. for tumor definition [5, 27, 30]. CT or CT equivalent information is still, however, required for the technical aspects of treatment planning such as:

- accurate dose calculations, which depend on knowledge of the attenuation properties of the tissue measured in a CT exam and
- generation of reference images which are used for patient positioning based on in-room X-ray imaging.

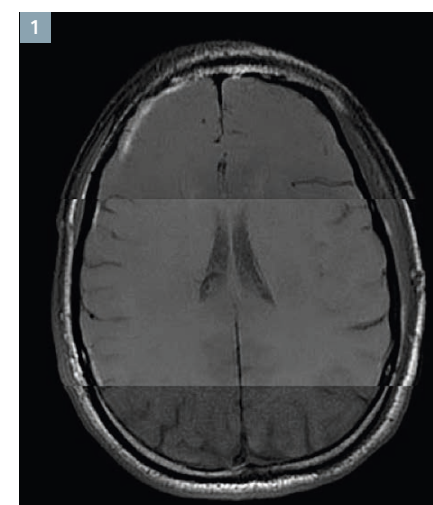
Therefore, it is common practice to acquire both CT and MR data and align these image series in the same coordinate system, or frame of reference, through image registration.

The MR data is used to define the target volume and the CT data to plan the treatment and serve as a reference for patient positioning. This workflow is, however, not optimal for several reasons. Besides the increase in cost and workload when using multiple imaging modalities, there is also an introduction of additional geometrical uncertainty due to the image registration.

Image registration is commonly performed at many clinics in order to align two image sets within a common frame of reference. Depending on the purpose of the image registration and the properties of the available image data, the registration can be performed in several ways. Mutual information rigid registration, based either on the full image volume or a smaller sub-volume, is available in most clinical treatment planning systems. For prostate cancer cases, where gold fiducial markers are commonly used, landmark registration methods can be employed in order to co-register MRI data to the planning CT. Manual registration, which is a robust but time-consuming method, is also an option. Regardless of method, image registration is a tricky business for several reasons. First off, for clinical cases we never know the correct alignment of two images, which makes it difficult to assess the uncertainties of a specific method. Phantom studies and purely digital experiments are unlikely to reflect the full complexity of the clinical case. Secondly, and related to the aforementioned problem, is the lack of robust quality measures for individual registrations. Finally, the task may actually be close to impossible,

regardless of registration method.

An example could be a prostate case without implanted fiducial markers. MRI is the imaging modality of choice for target definition, due to the greater soft tissue contrast. The prostate behaves much in the same way as other soft tissue tumors, i.e. its position in the body is not fixed and the spatial relation to surrounding bony anatomy may vary. This implies that a sub-volume based registration algorithm would be suitable in order to avoid any negative influence the surrounding anatomy may have on the registration. Although there are limited references regarding the matter, it is reasonable to assume that the limited soft tissue contrast in, and in close proximity to, the prostate gland in the CT image set would degrade the quality of a multi-modal sub-volume



1 Top 40 Hz/pixel, mid 100 Hz/pixel, bottom 400 Hz/pixel. Notice differences in signal-to-noise but especially geometrical differences.

registration. In other words, the reason that soft tissue registrations between MR and CT images will be associated with substantial uncertainties is exactly the same reason why we need MR image data to begin with; we lack sufficient anatomical information on soft tissue in the CT images. For the sake of balance, it should be said that for some indications, such as intracranial lesions, including larger volumes in the registration is not associated with any added uncertainty since the soft tissue is relatively fixed with respect to the bony anatomy. Even in those cases, however, image registration uncertainty is still a factor to consider. Ulin et al. [42] investigated the clinical variability of MR-CT registrations for one patient with an intracranial lesion for 45 clinics. The analysis revealed a standard deviation of 2.2 mm, which only accounts for the variability among the observers. There may still be a systematic component on top of this.

In summary, MR imaging has been shown to increase the geometrical accuracy in the definition of target volume. The challenge today is to make sure that we can radiate this target volume in an accurate and precise manner. This problem can be reduced into several sub-problems, e.g. control over geometrical distortions in the MR images; differences in the patient setup in the MR scanner compared to treatment; and registration uncertainties introduced when MR and CT data is placed in the same coordinate system. In this article we provide a brief overview of the current knowledge regarding geometrical distortions and patient setup in the radiotherapy context and describe the problems and proposed solutions for MR only radiotherapy.

## MR image distortions

Geometric distortions in MR images can be caused by the system itself, from nonlinearities in the magnetic gradients or inhomogeneities in the static magnetic field. Nonlinearities in the gradients can be characterized

and corrected using spherical harmonics expansions of the fields generated by the gradient coils and can be accurately corrected using software supplied by the MR vendors.

Distortions can also be caused by the imaged object in the form of chemical shift or magnetic susceptibility artefacts. Image distortions due to susceptibility effects and chemical shift in conventional MR imaging are inversely proportional to the gradient field strength, so that stronger gradients will minimize such distortions at a cost of more image noise. Phantom studies have shown the residual distortion for clinical sequences to be within 1 mm [18, 31]. Object-induced distortion effects have also been investigated in clinical data and the effect proved to be small for internal structures relevant for prostate treatments [28]. In general, anatomical imaging sequences using relatively high bandwidths reduce distortions caused by susceptibility effects and chemical shift to an acceptable level for radiotherapy [26, 40]. Methods using post-processing corrections [35] or special modes of acquisition [6] have also been studied.

Some MR protocols are more sensitive to geometric distortions, echo planar imaging being one example. Such sequences can display significant geometric distortions due to susceptibility effects, and must be handled with care when used for radiotherapy purposes.

## MR imaging using immobilization equipment

Planning CT scans are normally acquired using flat table tops to match the flat treatment couch used at the accelerator. The standard patient support is concave in most MRI scanners, although some have flat couches. The problem of concave patient supports is easily surmounted, either by manufacturing a flat table top insert at the hospital or by purchasing a commercial solution. Flat table tops are

necessary if patient immobilization is to be used at the MRI scanner.

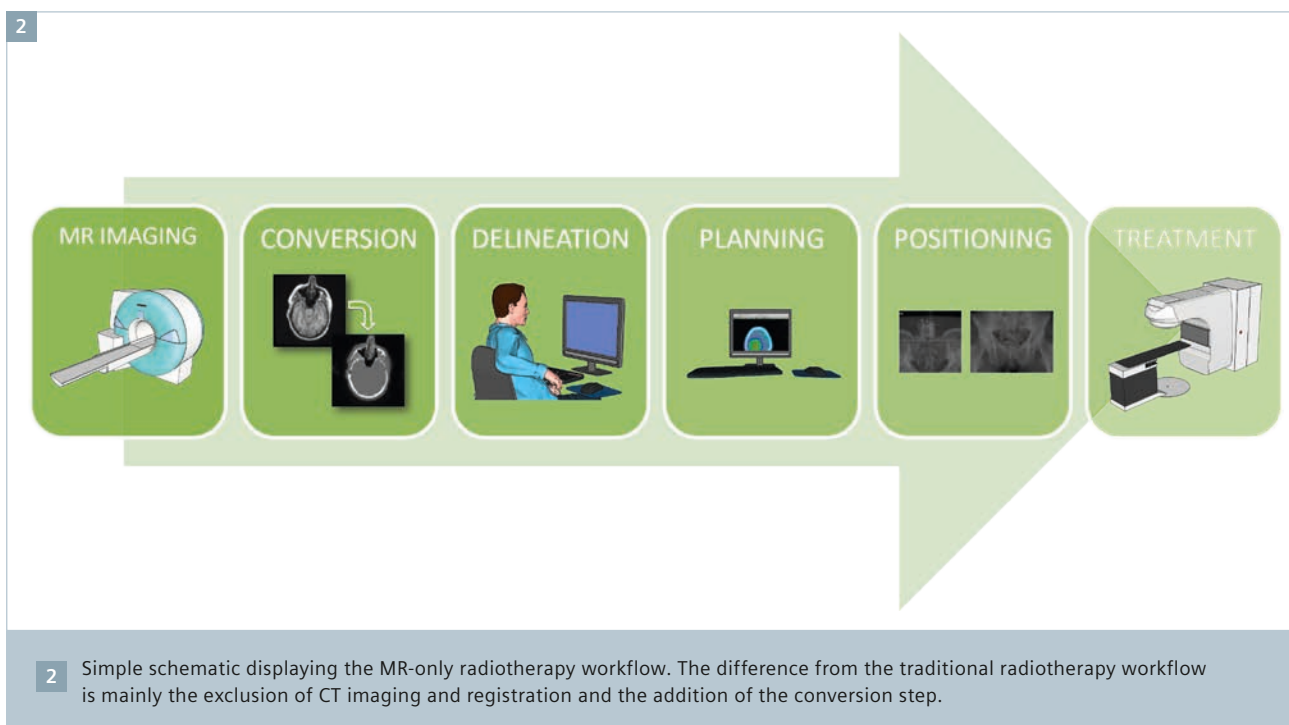
A more intricate problem is MRI compatibility of the immobilization equipment, both in material properties and size. MR safe materials must be used for base-plates, nuts, bolts and other fittings. A traditional plastic face mask for head and neck immobilization is normally constructed in MR safe materials; however, a standard MRI head coil will not be able to accommodate it. By using surface coils (i.e. flex coils) instead, imaging of the immobilized head and neck is possible, although a dedicated head coil still provide higher quality images [10]. When using surface coils for radiotherapy planning, care must be taken not to place the coils directly on the skin of the patient since the external anatomy may be distorted. Instead, the coils should be placed either hanging from a frame or on top of a holder close to the patient surface, without touching it. Nowadays, MRI compatible immobilization equipment and coil holders are commercially available.

## MR-only radiotherapy<sup>1</sup>

In this article, we define MR-only radiotherapy as external beam radiotherapy where MR data is the only imaging information that is used for the planning and preparation of the treatment. Arguments for an MR-only workflow commonly include the avoidance of image registration in the planning stage of the treatment [1, 4, 8, 15, 18, 19, 20, 23, 31, 33, 39], reduced costs due to less imaging or a simplified workflow [1, 4, 8, 24, 39], and reduced exposure to unspecifically aimed radiation [4, 18, 39].

<sup>1</sup> Radiotherapy Planning where MR data is the only imaging information is ongoing research. The concepts and information presented in this article are based on research and are not commercially available. Its future availability cannot be ensured.





Current methods of accurate dose calculations rely heavily on CT (or CT equivalent) information due to the relationship between Hounsfield units and electron density, and will probably continue to do so for the foreseeable future. Therefore, a reliable conversion method from MR information to CT equivalent information will be necessary for an MR-only workflow in radiotherapy. Several methods have been investigated by multiple research teams.

### Manual bulk density assignment

A method that has been researched extensively is segmentation, i.e. dividing the image into classes with different attenuation properties. The simplest form of segmentation is to only use one tissue class and assign a bulk density to the entire patient, typically that of water or a mixture of adipose tissue and muscle. Even though this is an extremely simplified version of reality, it yields acceptable dosimetric results. Typical dosimetric differences from inhomogeneity corrected CT based dose calculations using this approach have been reported to

be within 2-3% for prostate and intracranial target volumes [9, 17, 22, 23, 32, 33, 38]. A significant problem with this approach is that the traditional method of patient positioning at treatment depends on anatomical reference images that visualize bony anatomy. To overcome this issue, the number of tissue classes can be increased to include e.g. bone, soft tissue, lung tissue and air, and assign each tissue class an appropriate bulk density. In addition to making the creation of anatomical reference images possible, this also increases the dosimetric accuracy to around 1% for intracranial targets volumes [17, 22, 38] and between 1-2% for prostate treatments [17, 23].

Although the dosimetric results are relatively accurate, the method of manual density assignment has problems – the method relies on the precision of the operator that defines the anatomy in the MR images. This is of limited importance in the dosimetric aspect, but may have substantial impact on the subsequently generated positioning references. Also, the method is so labor intensive and time consum-

ing that it is not feasible for widespread clinical implementation. In order to accomplish such a development, automated conversion methods from MR to s-CT data are needed.

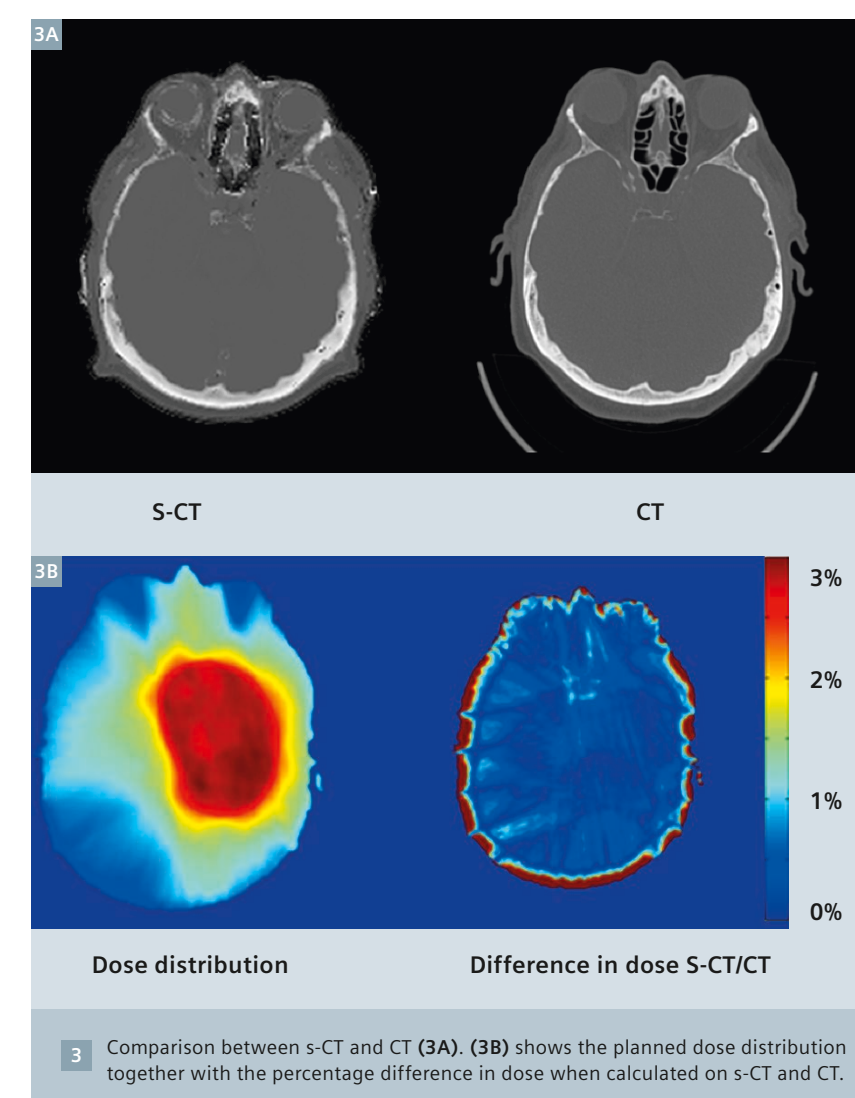
### Atlas methods

One method for automatically generating s-CT data is the combined MR-label image atlas. By deformably registering the atlas MR image to a new patient MR image and applying the resulting deformation field to the corresponding label image, a new image can be created based on the data in the label image. The label image can contain any information, e.g. CT or attenuation data. This approach has been used for attenuation correction applications in PET/MRI [37] as well as for dose calculation purposes in radiotherapy [8]. Atlas methods do not normally rely on tissue segmentation; instead, the full complexity atlas label image is warped onto the patient shape. Dosimetric results indicate accuracy comparable to bulk density assignment; for the radiotherapy application, Dowling et al [8] reported point dose differences between atlas label image and CT based calculations of about

2%. Atlas based methods are normally sensitive to atypical anatomy; e.g. in the study by Dowling et al., 2 out of 39 patients had to be excluded for this reason. Although atlas based methods are fairly robust and automatic, an argument can be made that the deformable image registration is associated with a considerable geometric uncertainty. This uncertainty is introduced into the treatment if the deformed label image is used to create the positioning reference image and not solely for dose calculations.

### Direct conversion

With the advent of ultra-short echo time imaging (UTE), interest has increased for direct conversion of MR image intensities to Hounsfield units. Since cortical bone appears as a signal void in traditional MR imaging, it has been impossible to distinguish it from air. UTE imaging samples the signal during the free induction decay, before the signal from cortical bone and other tissues with short T2 relaxation times has vanished [36], making it possible to discriminate such tissues from air. Even though UTE images render signal from bone, it is not presently possible to find any single MR sequence which is directly convertible to Hounsfield units – more information is necessary. Several researchers have suggested using UTE sequences with several different echo-times to segment soft-tissue, air and bone [2, 3, 21]. This technique is fully automatic and preserves the geometric integrity of the input image. UTE images suffer from the same system related distortions as traditional MR sequences; however, the fast radial sampling makes it less sensitive to common object related distortions such as chemical shift and susceptibility effects. An alternative to the previously mentioned segmentation approach is to build a statistical model that relates MR voxel intensities to Hounsfield units [12, 34]. Such an approach yields an s-CT image with a continuous Hounsfield unit distribution, as well as making it possible to estimate the uncertainties in the conversion [13]. Recent studies



compared dose calculations on s-CT data with CT data, and found statistically insignificant dose differences of less than  $\pm 0.5\%$  for intracranial targets [14, 16].

It is also possible to combine segmentation methods with direct conversion. A recent study [19] investigated the accuracy of a conversion method where the pelvic bone structures were first delineated manually. These delineations then served as input for a direct conversion method which could successfully convert the image intensities from standard MRI sequences to Hounsfield units. When the entire remaining anatomy was set to a bulk density, all points within the prostate PTV were within  $\pm 1.3\%$  of

the dose calculated on the standard CT input data.

The atlas registration approach can also produce segmentations that can serve as input for a later stage direct conversion. Hoffman et al. [11], which employed this approach for attenuation correction of PET/MR images, demonstrated that the method could accurately predict the attenuation map of a patient from MR input data. No systematic differences were found between PET images corrected with s-CT data and actual CT data. These combined methods ease the demand on the local accuracy of the segmentation, since the final conversion is performed using direct voxel wise conversion.



## Summary

Radiotherapy is a local treatment modality that is highly dependent on image guidance. Over the last decade there has been an increased clinical use of both MRI and PET to enable accurate delineation of the target volume. However, the radiotherapy workflow does still depend on CT information as the treatment planning softwares require attenuation data to be able to perform accurate dose calculation and to generate reference images for positioning. It has been shown that it is possible to generate CT equivalent information based on MR data, and with this technology it will be possible to abandon the CT in the future for those diagnoses where MR is the modality of choice for target delineation. Imaging in treatment position and risk of geometrical distortions are two other areas that need to be addressed when introducing an MR scanner in the radiotherapy environment.



## Contact

Tufve Nyholm  
Department of Radiation Sciences  
Umeå University  
Umeå  
Sweden  
Phone: +46 90 785 8432  
tufve.nyholm@umu.se

## References

- Beavis, A W, P Gibbs, R A Dealey, and V J Whitton. 1998. "Radiotherapy Treatment Planning of Brain Tumours Using MRI Alone." *The British Journal of Radiology* 71 (845): 544–48.
- Berker, Yannick, Jochen Franke, André Salomon, Moritz Palmowski, Henk C W Donker, Yavuz Temur, Felix M Mottaghy, et al. 2012. "MRI-Based Attenuation Correction for Hybrid PET/MRI Systems: A 4-Class Tissue Segmentation Technique Using a Combined Ultrashort-Echo-time/ Dixon MRI Sequence." *Journal of Nuclear Medicine* 53 (5): 796–804. doi:10.2967/jnumed.111.092577.
- Catana, Ciprian, Andre van der Kouwe, Thomas Benner, Christian J Michel, Michael Hamm, Matthias Fenchel, Bruce Fischl, Bruce Rosen, Matthias Schmand, and A Gregory Sorensen. 2010. "Toward Implementing an MRI-Based PET Attenuation-Correction Method for Neurologic Studies on the MR-PET Brain Prototype." *Journal of Nuclear Medicine* 51 (9): 1431–38. doi:10.2967/jnumed.109.069112.
- Chen, Lili, Robert a Price, Lu Wang, Jinsheng Li, Lihong Qin, Shawn McNeeley, C-M Charlie Ma, Gary M Freedman, and Alan Pollack. 2004. "MRI-Based Treatment Planning for Radiotherapy: Dosimetric Verification for Prostate IMRT." *Int J Radiat Oncol Biol Phys* 60 (2): 636–47. doi:10.1016/j.ijrobp.2004.05.068.
- Chung, Na Na, Lai Lei Ting, Wei Chung Hsu, Louis Tak Lui, and Po Ming Wang. 2004. "Impact of Magnetic Resonance Imaging versus CT on Nasopharyngeal Carcinoma: Primary Tumor Target Delineation for Radiotherapy." *Head & Neck* 26 (3): 241–46. doi:10.1002/hed.10378.
- Crijns, S P M, C J G Bakker, P R Seevinck, H de Leeuw, J J W Lagendijk, and B W Raaymakers. 2012. "Towards Inherently Distortion-Free MR Images for Image-Guided Radiotherapy on an MRI Accelerator." *Physics in Medicine and Biology* 57 (5): 1349–58. doi:10.1088/0031-9155/57/5/1349.
- Dirix, Piet, Karin Haustermans, and Vincent Vandecaveye. 2014. "The Value of Magnetic Resonance Imaging for Radiotherapy Planning." *Seminars in Radiation Oncology* 24 (3). Elsevier: 151–59. doi:10.1016/j.semradonc.2014.02.003.
- Dowling, Jason A, Jonathan Lambert, Joel Parker, Olivier Salvado, Jurgen Fripp, Anne Capp, Chris Wratten, James W Denham, and Peter B Greer. 2012. "An Atlas-Based Electron Density Mapping Method for Magnetic Resonance Imaging (MRI)-Alone Treatment Planning and Adaptive MRI-Based Prostate Radiation Therapy." *Int J Radiat Oncol Biol Phys* 83 (1). Elsevier Inc: e5–11. doi:10.1016/j.ijrobp.2011.11.056.
- Eilertsen, Karsten, Line Nilsen Tor Arne Vestad, Oliver Geier, and Arne Skretting. 2008. "A Simulation of MRI Based Dose Calculations on the Basis of Radiotherapy Planning CT Images." *Acta Oncologica* 47 (7): 1294–1302. doi:10.1080/02841860802256426.
- Hanvey, S, M Glegg, and J Foster. 2009. "Magnetic Resonance Imaging for Radiotherapy Planning of Brain Cancer Patients Using Immobilization and Surface Coils." *Physics in Medicine and Biology* 54 (18): 5381–94. doi:10.1088/0031-9155/54/18/002.
- Hofmann, Matthias, Florian Steinke, Verena Scheel, Guillaume Charpiat, Jason Farquhar, Philip Aschoff, Michael Brady, Bernhard Schölkopf, and Bernd J Pichler. 2008. "MRI-Based Attenuation Correction for PET/MRI: A Novel Approach Combining Pattern Recognition and Atlas Registration." *Journal of Nuclear Medicine* 49 (11): 1875–83. doi:10.2967/jnumed.107.049353.
- Johansson, Adam, Mikael Karlsson, and Tufve Nyholm. 2011. "CT Substitute Derived from MRI Sequences with Ultrashort Echo Time." *Medical Physics* 38 (5): 2708. doi:10.1118/1.3578928.
- Johansson, Adam, Yu Yun, Thomas Askund, Mikael Karlsson, and Tufve Nyholm. 2012. "Voxel-Wise Uncertainty in CT Substitute Derived from MRI." *Medical Physics* 39 (6): 3283–90. doi:10.1118/1.4711807.
- Jonsson, Joakim H, Mohammad M Akhtari, Magnus G Karlsson, Adam Johansson, Thomas Askund, and Tufve Nyholm. 2015. "Accuracy of Inverse Treatment Planning on Substitute CT Images Derived from MR Data for Brain Lesions." *Radiation Oncology (London, England)* 10 (1): 13. doi:10.1186/s13014-014-0308-1.
- Jonsson, Joakim H, Anders Garpebring, Magnus G Karlsson, and Tufve Nyholm. 2012. "Internal Fiducial Markers and Susceptibility Effects in MRI-Simulation and Measurement of Spatial Accuracy." *Int J Radiat Oncol Biol Phys* 82 (5): 1612–18. doi:10.1016/j.ijrobp.2011.01.046.
- Jonsson, Joakim H, Adam Johansson, Karin Söderström, Thomas Askund, and Tufve Nyholm. 2013. "Treatment Planning of Intracranial Targets on MRI Derived Substitute CT Data." *Radiotherapy and Oncology* 108: 118–22.
- Jonsson, Joakim H, Magnus G Karlsson, Mikael Karlsson, and Tufve Nyholm. 2010. "Treatment Planning Using MRI Data: An Analysis of the Dose Calculation Accuracy for Different Treatment Regions." *Radiation Oncology* 5 (1): 62. doi:10.1186/1748-717X-5-62.
- Kapanen, Mika, Juhani Collan, Annette Beule, Tiina Seppälä, Kauko Saarilahti, and Mikko Tenhunen. 2013. "Commissioning of MRI-Only Based Treatment Planning Procedure for External Beam Radiotherapy of Prostate." *Magnetic Resonance in Medicine* 70 (1): 127–35. doi:10.1002/mrm.24459.
- Kapanen, Mika, and Mikko Tenhunen. 2013. "T1/T2\*-Weighted MRI Provides Clinically Relevant Pseudo-CT Density Data for the Pelvic Bones in MRI-Only Based Radiotherapy Treatment Planning." *Acta Oncologica (Stockholm, Sweden)* 52 (3): 612–18. doi:10.3109/0284186X.2012.692883.
- Karlsson, Mikael, Magnus G Karlsson, Tufve Nyholm, Christopher Amies, and Björn Zackrisson. 2009. "Dedicated Magnetic Resonance Imaging in the Radiotherapy Clinic." *Int J Radiat Oncol Biol Phys* 74 (2): 644–51. doi:10.1016/j.ijrobp.2009.01.065.
- Keereman, Vincent, Yves Fierens, Tom Broux, Yves De Deene, Max Lonnew, and Stefaan Vandenberghe. 2010. "MRI-Based Attenuation Correction for PET/MRI Using Ultrashort Echo Time Sequences." *Journal of Nuclear Medicine* 51 (5): 812–18. doi:10.2967/jnumed.109.065425.
- Kristensen, Brian Holch, Finn Jørgen Laursen, Vibeke Løgager, Poul Flemming Geertsen, and Anders Krarup-Hansen. 2008. "Dosimetric and Geometric Evaluation of an Open Low-Field Magnetic Resonance Simulator for Radiotherapy Treatment Planning of Brain Tumours." *Radiotherapy and Oncology* 87 (1): 100–109. doi:10.1016/j.radonc.2008.01.014.
- Lambert, Jonathan, Peter B Greer, Fred Menk, Jackie Patterson, Joel Parker, Kara Dahl, Sanjiv Gupta, et al. 2011. "MRI-Guided Prostate Radiation Therapy Planning: Investigation of Dosimetric Accuracy of MRI-Based Dose Planning." *Radiotherapy and Oncology : Journal of the European Society for Therapeutic Radiology and Oncology* 98 (3). Elsevier Ireland Ltd: 330–34. doi:10.1016/j.radonc.2011.01.012.
- Lee, Young K, Marc Bollet, Geoffrey Charles-Edwards, Maggie A Flower, Martin O Leach, Helen McNair, Elizabeth Moore, Carl Rowbottom, and Steve Webb. 2003. "Radiotherapy Treatment Planning of Prostate Cancer Using Magnetic Resonance Imaging Alone." *Radiotherapy and Oncology* 66 (2): 203–16. doi:10.1016/S0. doi:10.1088/0031-9155/57/5/1349.
- Li, Sonia P, and Anwar R Padhani. 2012. "Tumor Response Assessments with Diffusion and Perfusion MRI." *Journal of Magnetic Resonance Imaging* 35 (4): 745–63. doi:10.1002/jmri.22838.
- Liney, Gary P, and Marinus A Moerland. 2014. "Magnetic Resonance Imaging Acquisition Techniques for Radiotherapy Planning." *Seminars in Radiation Oncology* 24 (3). Elsevier: 160–68. doi:10.1016/j.semradonc.2014.02.014.
- Milosevic, M, S Voruganti, R Blend, H Alasti, P Warde, M McLean, P Catton, C Catton, and M Gospodarowicz. 1998. "Magnetic Resonance Imaging (MRI) for Localization of the Prostatic Apex: Comparison to Computed Tomography (CT) and Urethrography." *Radiotherapy and Oncology* 47 (3): 277–84.
- Pasquier, D, N Betrouni, M Vermandel, T Lacornerie, E Lartigau, and J Rousseau. 2006. "MRI Alone Simulation for Conformal Radiation Therapy of Prostate Cancer: Technical Aspects." *IEEE EMBS, January*, 160–63. doi:10.1109/IEMBS.2006.260341.
- Paulson, Eric S., Beth Erickson, Chris Schultz, and X. Allen Li. 2015. "Comprehensive MRI Simulation Methodology Using a Dedicated MRI Scanner in Radiation Oncology for External Beam Radiation Treatment Planning." *Medical Physics* 42 (1): 28–39. doi:10.1118/1.4896096.
- Prabhakar, R, K P Hareesh, T Ganesh, R C Joshi, P K Julka, and G K Rath. 2007. "Comparison of Computed Tomography and Magnetic Resonance Based Target Volume in Brain Tumors." *Journal of Cancer Research and Therapeutics* 3 (2): 121–23.
- Prabhakar, R, P K Julka, T Ganesh, a Munshi, R C Joshi, and G K Rath. 2007a. "Feasibility of Using MRI Alone for 3D Radiation Treatment Planning in Brain Tumors." *Japanese Journal of Clinical Oncology* 37 (6): 405–11. doi:10.1093/jjco/hym050.
- Prabhakar, R, P K Julka, T Ganesh, A Munshi, R C Joshi, and G K Rath. 2007b. "Feasibility of Using MRI Alone for 3D Radiation Treatment Planning in Brain Tumors." *Japanese Journal of Clinical Oncology* 37 (6): 405–11. doi:10.1093/jjco/hym050.
- Ramsey, C R, and A L Oliver. 1998. "Magnetic Resonance Imaging Based Digitally Reconstructed Radiographs, Virtual Simulation, and Three-Dimensional Treatment Planning for Brain Neoplasms." *Medical Physics* 25 (10): 1928–34.
- Rank, Christopher M, Christoph Tremmel, Nora Hünemohr, Armin M Nagel, Oliver Jäkel, and Steffen Greilich. 2013. "MRI-Based Treatment Plan Simulation and Adaptation for Ion Radiotherapy Using a Classification-Based Approach." *Radiation Oncology* 8 (1): 51. doi:10.1186/1748-717X-8-51.
- Reinsberg, Stefan a, Simon J Doran, Elizabeth M Charles-Edwards, and Martin O Leach. 2005. "A Complete Distortion Correction for MR Images: II. Rectification of Static-Field Inhomogeneities by Similarity-Based Profile Mapping." *Physics in Medicine and Biology* 50 (11): 2651–61. doi:10.1088/0031-9155/50/11/014.
- Robson, Matthew D, Peter D Gatehouse, Mark Bydder, and Graeme M Bydder. 2003. "Magnetic Resonance: An Introduction to Ultrashort TE (UTE) Imaging." *Journal of Computer Assisted Tomography* 27 (6): 825–46.
- Schreibmann, Eduard, Jonathon a. Nye, David M. Schuster, Diego R. Martin, John Votaw, and Tim Fox. 2010. "MR-Based Attenuation Correction for Hybrid PET-MR

Brain Imaging Systems Using Deformable Image Registration." *Medical Physics* 37 (5): 2101–9. doi:10.1118/1.3377774.

38 Stancescu, T, H-S Jans, N Pervez, P Stavrev, and B G Fallone. 2008. "A Study on the Magnetic Resonance Imaging (MRI)-Based Radiation Treatment Planning of Intracranial Lesions." *Physics in Medicine and Biology* 53 (13): 3579–93. doi:10.1088/0031-9155/53/13/013.

39 Stancescu, Teodor, Jans Hans-sonke, Pavel Stavrev, and B Gino Fallone. 2006. "3T MR-Based Treatment Planning for Radiotherapy of Brain Lesions." *Radiology and Oncology* 40 (2): 125–32.

40 Walker, Amy, Gary Liney, Peter Metcalfe, and Lois Holloway. 2014. "MRI Distortion: Considerations for MRI Based Radiotherapy Treatment Planning." *Australasian Physical & Engineering Sciences in Medicine / Supported by the Australasian College of Physical Scientists in Medicine and the Australasian Association of Physical Sciences in Medicine*, February. doi:10.1007/s13246-014-0252-2.

41 Van der Heide, Uulke A, Antonetta C Houweling, Greetje Groenendaal, Regina G H Beets-Tan, and Philippe Lambin. 2012. "Functional MRI for Radiotherapy Dose Painting." *Magnetic Resonance Imaging* 30 (9). Elsevier Inc.: 1216–23. doi:10.1016/j.mri.2012.04.010.

42 Kenneth Ulin, Marcia Urie, Joel Cherlow. 2010. "Results of a Multi-Institutional Benchmark Test for Cranial CT/MR Image Registration" *Int. J. Radiation Oncology Biol. Phys.* 77 (5): 1584-1589.



# 4D-MRI: Future of Radiotherapy of Moving Targets?

Kinga Barbara Bernatowicz; Rosalind Lucy Perrin; Marta Peroni; Damien Charles Weber; Antony John Lomax

Center for Proton Therapy (CPT), Paul Scherrer Institut, Villigen PSI, Switzerland

## Background

4D-CT imaging is widely used in radiotherapy planning of moving tumors to account for motion, and to provide the physical properties of tissue for dose calculations, e.g. electron density for conventional radiation therapy or proton stopping power for proton therapy. However, it is limited to representing only a single, averaged breathing cycle, often contains imaging artifacts, and contributes a substantial dose exposure for the patient. To over-

come these issues, a 4D-MRI imaging protocol applied to evaluating respiratory motion of the liver was proposed by von Siebenthal et al. [1].

This approach is capable of resolving irregular respiratory motion, with the added benefit of delivering no imaging dose to the patient. Unfortunately, whilst being a promising technique, MR imaging alone does not provide the physical properties of tissue required for accurate dose calculations. However, by combining the motion information pro-

vided by 4D-MRI, with the density data provided by single phase CT data, the advantages of motion imaging with 4D-MRI can now be applied to radiotherapy applications.

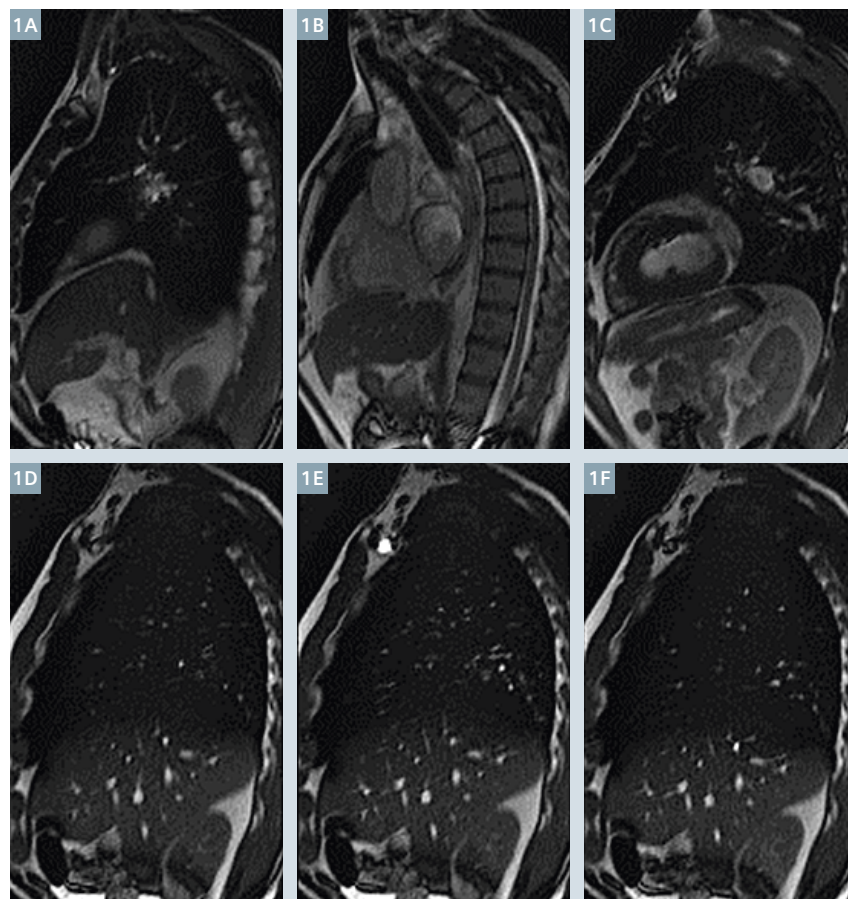
## 4D-MRI acquisition

The 4D-MRI protocol relies on the interleaved acquisition of a 'navigator' and different image slices in the sagittal plane (Fig. 1). The navigator is fixed at a single position throughout the acquisition time, and describes the motion state of the volume of interest at any instant during the acquisition. The actual 2D image slice is then scanned through the planned field-of-view (FOV).

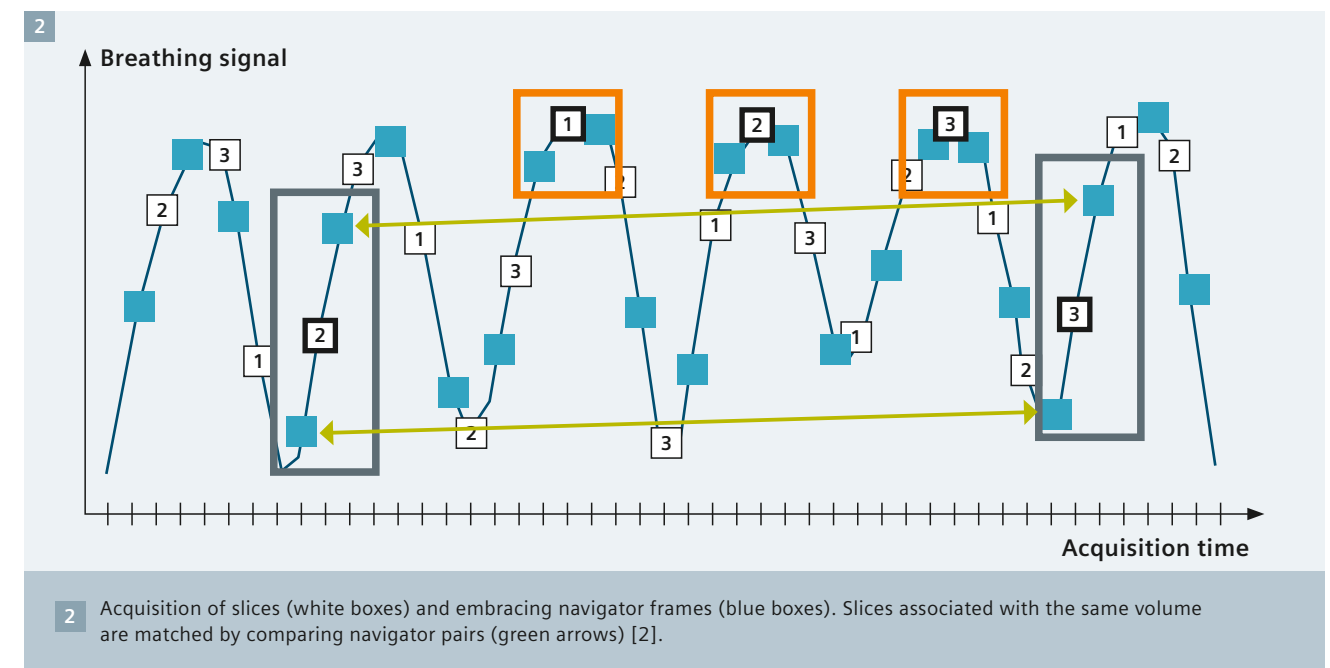
This experimental sequence\* does not make any assumptions about the breathing amplitude, its regularity, or the number of reconstructed phases. In contrast, commonly used methods for 4D imaging use a one-dimensional respiratory signal for sorting the 2D images, whereas 4D-MRI images can be retrospectively sorted based directly on the acquired navigator frames. The correspondence of the imaging slices is then established by comparing the two temporally embracing navigator frames (see Fig. 2). If these navigator frames are similar, the image slices can be stacked into a (3D) volume with the same time stamp and therefore, a complete 4D image data set with the same temporal resolution as the navigator frames can be reconstructed.

This approach has now been implemented on a 1.5T MAGNETOM Aera MR system (Siemens Healthcare, Erlangen, Germany) using an experimental version of the balanced steady state

\*Work in progress, the product is still under development and not commercially available yet. Its future availability cannot be ensured.



1 Sagittal slices through the thorax and upper abdomen, showing image slices (1A–C) and navigator slices (1D–F) acquired with the experimental 4D-MRI protocol\*.



free precession sequence (TrueFISP)\*. Images are acquired in batches of 3-5 minute duration, with up to one hour of total acquisition time and with image slice thicknesses of 4 to 6 mm. Recent advances in the field are now looking at the simultaneous acquisition of navigator and data slices, with use of other advanced sequences, for example CAIPRINHA [3].

## Applications

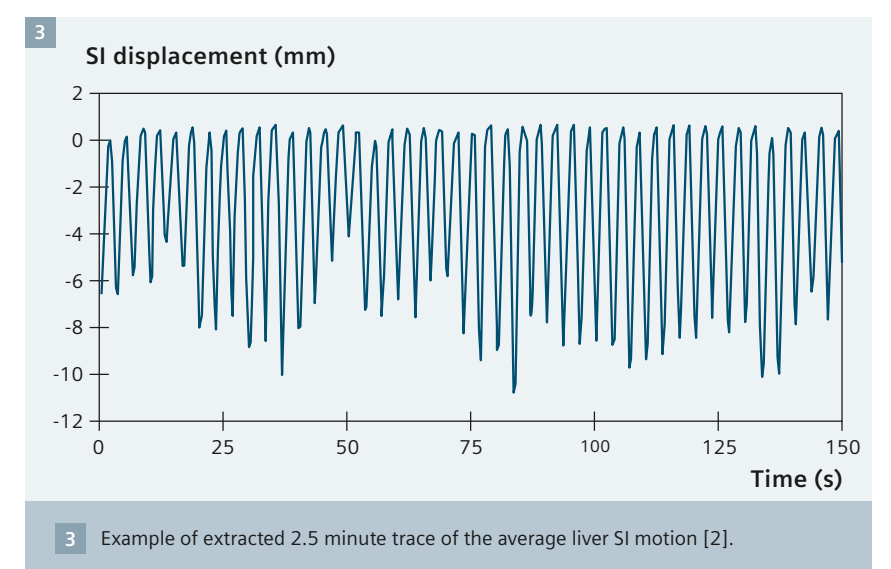
### • Intra- and inter-fraction motion studies

Since MRI involves no radiation dose to patients or volunteers, 4D-MRI protocols allow for repeated studies on the same subject and/or for longer time period acquisitions in order to capture breathing variability (Fig. 3). Motion deformation fields can also be extracted using deformable image registration.

### • Mapping motion from MRI-CT

The 4D-CT (MRI) method has now been developed within our group for simulating many 4D-CT data sets from a single, static reference CT and a data-base of motion deformation fields extracted from 4D-MRI studies

\*Work in progress, the product is still under development and not commercially available yet. Its future availability cannot be ensured.

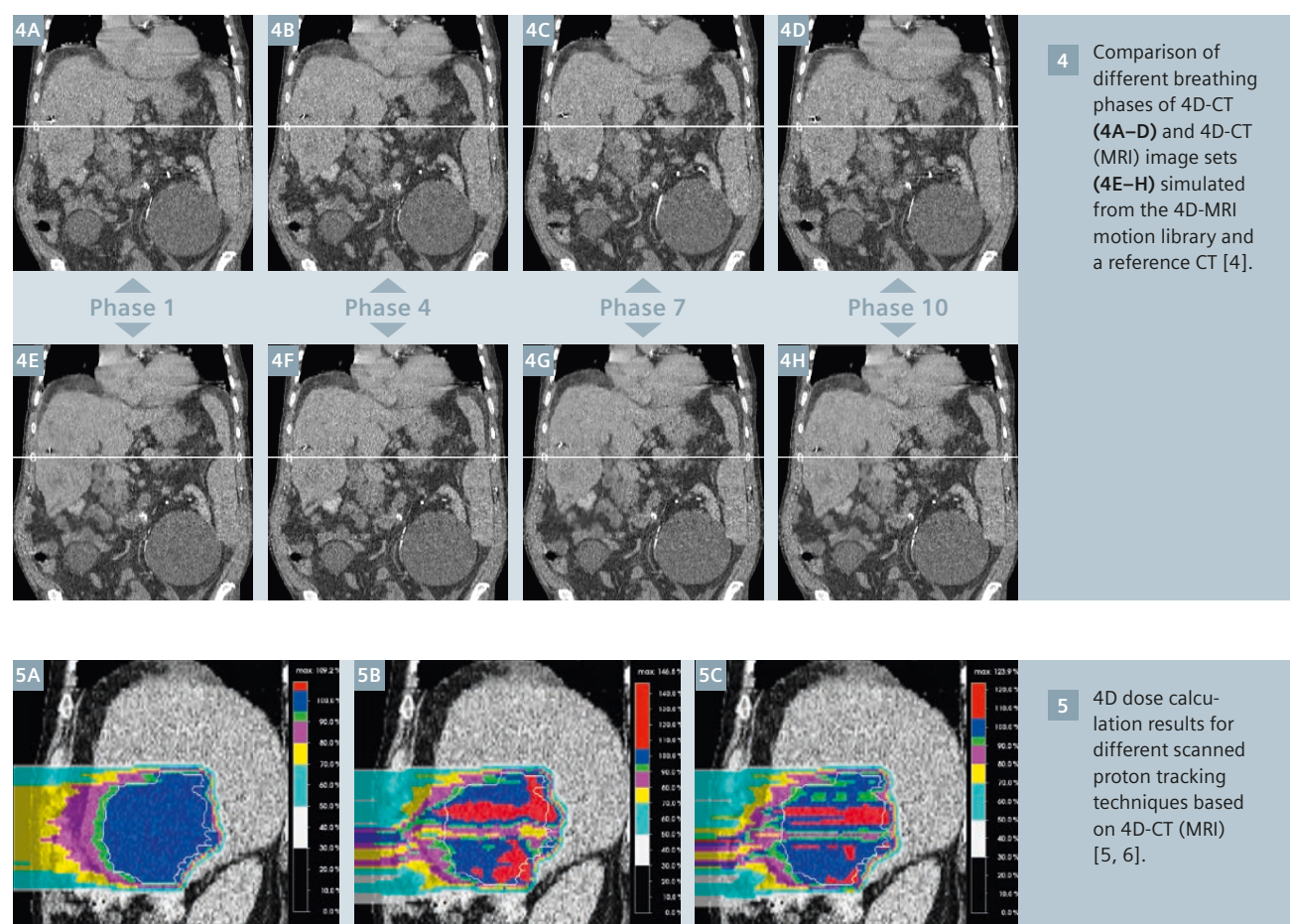


[4]. The mapping of motion information from 4D-MRI onto CT images is thereby achieved using subject-specific or population-based models, based on the establishment of mechanical correspondences between structures of interest (e.g. the liver). The resulting 4D-CT (MRI) images are of good quality when compared to 4D-CT (Fig. 4), and now represent the tissue properties necessary for dose calculations, whilst incorporating the motion information provided by 4D-MRI.

### • 4D dose calculations in radiotherapy

Including the realistic, variable respiratory motion in provided by 4D-CT (MRI) data into 4D dose calculations, opens the door to novel future applications. Based on such data sets, advanced imaging and delivery methods, such as beam tracking (Fig. 5), can now be evaluated and comprehensive 4D planning studies and robustness evaluations performed.





## Summary

4D-MRI, combined with CT data to produce 4D-CT (MRI) data sets, is a powerful new technique for imaging and modeling motion for radiotherapy applications. It allows for accurate modeling of motion variability, an important limitation of current 4D-CT techniques, and will allow in the future for the acquisition of patient specific motion libraries for advanced motion mitigation techniques such as tracking and re-tracking [5, 6].

## References

- 1 von Siebenthal M, Székely G, Gamper U, Boesiger P, Lomax A, Cattin P., 4D MR imaging of respiratory organ motion and its variability., *Phys Med Biol.* 2007 Mar 21;52(6):1547-64. Epub 2007 Feb 16.
- 2 PhD Thesis, von Siebenthal, M. 2008, [http://www.vision.ee.ethz.ch/~organmot/chapter\\_publications.shtml](http://www.vision.ee.ethz.ch/~organmot/chapter_publications.shtml)
- 3 Celicanin Z, Bieri O, Preiswerk F, Cattin P, Scheffler K, Santini F., Simultaneous acquisition of image and navigator slices using CAIPIRINHA for 4D MRI., *Magn Reson Med.* 2014 Feb 24. doi: 10.1002/mrm.25134. [Epub ahead of print].
- 4 Boye D, Lomax T, Knopf A., Mapping motion from 4D-MRI to 3D-CT for use in 4D dose calculations: a technical feasibility study. *Med Phys.* 2013 Jun;40(6):061702. doi: 10.1118/1.4801914.
- 5 Zhang Y., Knopf A, Tanner C, Boye D, Lomax AJ., Deformable motion reconstruction for scanned proton beam therapy using on-line x-ray imaging., *Phys Med Biol.* 2013 Dec 21;58(24):8621-45. doi: 10.1088/0031-9155/58/24/8621. Epub 2013 Nov 21.
- 6 Zhang Y, Knopf A, Tanner C, Lomax AJ., Online image guided tumour tracking with scanned proton beams: a comprehensive simulation study., *Phys Med Biol.* 2014 Nov 24;59(24):7793-7817. doi:10.1088/0031-9155/59/24/7793.

## Contact

Kinga Barbara Bernatowicz  
Paul Scherrer Institute  
5323 Villigen PSI  
Switzerland  
[kinga.bernatowicz@psi.ch](mailto:kinga.bernatowicz@psi.ch)

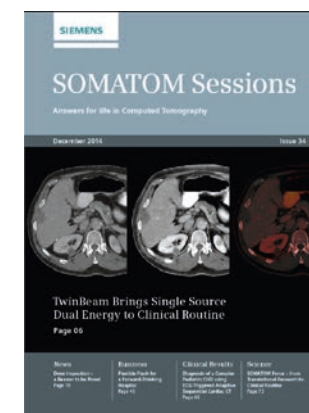
# Siemens Healthcare Publications

Our publications offer the latest information and background for every healthcare field. From the hospital director to the radiological assistant – here, you can quickly find information relevant to your needs.



## Medical Solutions

Innovations and trends in healthcare. The magazine is designed especially for members of hospital management, administration personnel, and heads of medical departments.



## SOMATOM Sessions

Everything from the world of computed tomography.



## AXIOM Innovations

Everything from the world of interventional radiology, cardiology, and surgery.



## MAGNETOM Flash

Everything from the world of magnetic resonance imaging.

## MAGNETOM Flash – Imprint

© 2015 by Siemens AG,  
Berlin and Munich,  
All Rights Reserved

## Publisher:

**Siemens AG**  
Medical Solutions  
Business Unit Magnetic Resonance,  
Karl-Schall-Straße 6, D-91052 Erlangen,  
Germany

**Editor-in-chief:** Antje Hellwich  
([antje.hellwich@siemens.com](mailto:antje.hellwich@siemens.com))

**Editorial Board:** Wellesley Were;  
Ralph Strecker; Sven Zühlsdorff, Ph.D.;  
Gary R. McNeal, MS (BME);  
Peter Kreisler, Ph.D.

**Production:** Norbert Moser, Siemens AG,  
Medical Solutions

**Layout:** Agentur Baumgärtner,  
Friedrichstraße 4, D-90762 Fürth, Germany

**Printer:** Rotaplan Offset Kammann Druck GmbH,  
Hofer Straße 1,  
D - 93057 Regensburg, Germany

Note in accordance with § 33 Para.1 of the German Federal Data Protection Law: Despatch is made using an address file which is maintained with the aid of an automated data processing system.

MAGNETOM Flash is sent free of charge to Siemens MR customers, qualified physicians, technologists, physicists and radiology departments throughout the world. It includes reports in the English language on magnetic resonance: diagnostic and therapeutic methods and their application as well as results and experience gained with corresponding systems and solutions. It introduces from case to case new principles and procedures and discusses their clinical potential. The statements and views of the authors in the individual contributions do not necessarily reflect the opinion of the publisher.

The information presented in these articles and case reports is for illustration only and is not intended to be relied upon by the reader for instruction as to the practice of medicine. Any health care practitioner reading this information is reminded that they must use their own learning, training and expertise in dealing with their individual patients. This material does not substitute for that duty and is not intended by Siemens Medical Solutions to be used for any purpose in that regard. The drugs and doses mentioned herein are consistent with the approval labeling for uses and/or indications for that duty and is not intended by Siemens Medical Solutions to be used for any purpose in that regard. The drugs and doses mentioned herein are consistent with the approval labeling for uses and/or indications for that duty and is not intended by Siemens Medical Solutions to be used for any purpose in that regard. The treating physician bears the sole responsibility for the diagnosis and treatment of patients, including drugs and

doses prescribed in connection with such use. The Operating Instructions must always be strictly followed when operating the MR system. The sources for the technical data are the corresponding data sheets. Results may vary.

Partial reproduction in printed form of individual contributions is permitted, provided the customary bibliographical data such as author's name and title of the contribution as well as year, issue number and pages of MAGNETOM Flash are named, but the editors request that two copies be sent to them. The written consent of the authors and publisher is required for the complete reprinting of an article.

We welcome your questions and comments about the editorial content of MAGNETOM Flash. Please contact us at [magnetomworld.med@siemens.com](mailto:magnetomworld.med@siemens.com).

Manuscripts as well as suggestions, proposals and information are always welcome; they are carefully examined and submitted to the editorial board for attention. MAGNETOM Flash is not responsible for loss, damage, or any other injury to unsolicited manuscripts or other materials. We reserve the right to edit for clarity, accuracy, and space. Include your name, address, and phone number and send to the editors, address above.



On account of certain regional limitations of sales rights and service availability, we cannot guarantee that all products included in this brochure are available through the Siemens sales organization worldwide. Availability and packaging may vary by country and is subject to change without prior notice. Some/All of the features and products described herein may not be available in the United States.

The information in this document contains general technical descriptions of specifications and options as well as standard and optional features which do not always have to be present in individual cases, and which

may not be commercially available in all countries. Due to regulatory reasons their future availability cannot be guaranteed. Please contact your local Siemens organization for further details.

Siemens reserves the right to modify the design, packaging, specifications, and options described herein without prior notice. Please contact your local Siemens sales representative for the most current information.

Note: Any technical data contained in this document may vary within defined tolerances. Original images always lose a certain amount of detail when reproduced.

\*MAGNETOM 7T is still under development and not commercially available yet. Its future availability cannot be ensured. This research system is not cleared, approved or licensed in any jurisdiction for patient examinations. This research system is not labelled according to applicable medical device law and therefore may only be used for volunteer or patient examinations in the context of clinical studies according to applicable law.

Not for distribution in the US

#### Global Business Unit

Siemens AG  
Medical Solutions  
Magnetic Resonance  
Henkestraße 127  
DE-91052 Erlangen  
Germany  
Phone: +49 9131 84-0  
[www.siemens.com/healthcare](http://www.siemens.com/healthcare)

#### Local Contact Information

##### Asia/Pacific:

Siemens Medical Solutions  
Asia Pacific Headquarters  
The Siemens Center  
60 MacPherson Road  
Singapore 348615  
Phone: +65 6490 6000

##### Canada:

Siemens Canada Limited  
Healthcare  
1550 Appleby Lane  
Burlington, ON L7L 6X7, Canada  
Phone +1 905 315-6868

#### Europe/Africa/Middle East:

Siemens AG, Healthcare  
Henkestraße 127  
91052 Erlangen, Germany  
Phone: +49 9131 84-0

##### Latin America:

Siemens S.A., Medical Solutions  
Avenida de Pte. Julio A. Roca No 516, Piso  
C1067 ABN Buenos Aires, Argentina  
Phone: +54 11 4340-8400

##### USA:

Siemens Medical Solutions USA, Inc.  
51 Valley Stream Parkway  
Malvern, PA 19355-1406, USA  
Phone: +1 888 826-9702

#### Global Siemens Headquarters

Siemens AG  
Wittelsbacherplatz 2  
80333 Muenchen  
Germany

#### Global Siemens Healthcare Headquarters

Siemens AG  
Healthcare  
Henkestraße 127  
91052 Erlangen  
Germany  
Phone: +49 9131 84-0  
[www.siemens.com/healthcare](http://www.siemens.com/healthcare)